Nitrogen Cycle Electrocatalysis

Victor Rosca,[†] Matteo Duca, Matheus T. de Groot,[‡] and Marc T. M. Koper*

Leiden Institute of Chemistry, Leiden University, PO Box 9502, 2300 RA Leiden, The Netherlands

Received December 12, 2008

Contents

1. Introduction 2209
2. Ammonia Oxidation 2212
2.1. Ammonia Oxidation on Platinum 2212
2.2. Ammonia Oxidation on Other Metal and Alloy Electrodes 2215
2.3. Comparison to Enzymatic Ammonia Oxidation 2215
3. Hydrazine Oxidation 2215
3.1. Hydrazine Oxidation on Pt Electrodes in Acidic and Alkaline Media 2215
3.2. Hydrazine Oxidation on Other Metal Electrodes 2217
3.3. Hydrazine Oxidation on Functionalized Electrodes 2217
3.4. Hydrazine Oxidation by Enzymes 2218
4. Hydroxylamine Oxidation and Reduction 2218
4.1. Reactions of Hydroxylamine: Equilibrium Considerations 2218
4.2. Hydroxylamine Oxidation and Reduction on Platinum 2219
4.3. Hydroxylamine Reduction and Oxidation at Other Electrodes 2220
4.4. Comparison to Hydroxylamine Oxidoreductase 2220
5. Nitrogen Reduction 2221
6. Nitrous Oxide Reduction 2221
6.1. Nitrous Oxide Reduction on Transition-Metal Electrodes 2221
6.2. Comparison to Nitrous Oxide Reduction by Enzymes 2221
7. Nitric Oxide Reduction and Oxidation 2222
7.1. Reactions of Nitric Oxide: Equilibrium Considerations 2222
7.2. Nitric Oxide Reduction on Platinum 2222
7.2.1. Nitric Oxide Reductive Stripping 2222
7.2.2. Continuous Nitric Oxide Reduction on Platinum 2225
7.3. Nitric Oxide Reduction on Other Metals 2225
7.3.1. Nitric Oxide Reductive Stripping 2225
7.3.2. Continuous Nitric Oxide Reduction on Transition Metal Electrodes 2226
7.4. Nitric Oxide Reduction on Functionalized Electrodes 2226
7.5. Nitric Oxide Oxidation 2228
7.5.1. Nitric Oxide Oxidative Stripping on Platinum 2228
7.5.2. Continuous Nitric Oxide Oxidation 2228
7.5.3. Nitric Oxide Oxidation on Functionalized Electrodes 2228
7.6. Comparison to Nitric Oxide Reduction by Enzymes 2228
8. Nitrite and Nitrous Acid Reduction and Oxidation 2229
8.1. Reactions of Nitrite and Nitrous Acid: Thermodynamic Considerations 2229
8.2. Nitrite and Nitrous Acid Reduction 2230
8.2.1. Nitrite Reduction on Platinum Electrodes 2230
8.2.2. Nitrite Reduction on Other Metal Electrodes 2231
8.2.3. Nitrite Reduction on Functionalized Electrodes 2232
8.3. Nitrite Oxidation 2232
8.3.1. Nitrite Oxidation on Metal Electrodes 2232
8.3.2. Nitrite Oxidation on Functionalized Electrodes 2232
8.4. Comparison to Nitrite Reduction by Enzymes 2232
9. Nitrate Reduction 2233
9.1. Reactions of Nitrate: Equilibrium and General Considerations 2233
9.2. Nitrate Reduction in Acidic Solution at Low Nitrate Concentration 2233
9.2.1. Nitrate Reduction at Platinum Electrodes 2233
9.2.2. Nitrate Reduction at Other Metal Electrodes 2235
9.2.3. Nitrate Reduction at Bimetallic Electrodes 2236
9.3. Nitrate Reduction at Platinum in Highly Acidic Solution at High Nitrate Concentration 2238
9.4. Nitrate Reduction in Alkaline Media 2239
9.5. Nitrate Reduction at Functionalized Electrodes 2240
9.6. Nitrate Reduction by Enzymes 2240
10. Concluding Remarks 2240
11. Acknowledgments 2240
12. References 2241

* Corresponding author. E-mail: m.koper@chem.leidenuniv.nl.
[†] Present address: Energy research Centre of The Netherlands (ECN), P.O. Box 1, 1755 ZG Petten, The Netherlands.
[‡] Present address: Research, Development & Innovation, AkzoNobel Chemicals bv, Velperweg 76, P.O. Box 9300, 6800 SB Arnhem, The Netherlands.

1. Introduction

After carbon, hydrogen, and oxygen, nitrogen is the next most abundant element in the human body. Inorganic and organic compounds of nitrogen feature prominently in many biological and environmental, as well as industrial, processes. In nature, the inorganic compounds of nitrogen are controlled by a reaction cycle called the nitrogen cycle (Figure 1).[1] The denitrification pathway in this cycle, that is, the conversion of nitrate to dinitrogen, is employed by certain bacteria to produce ATP anaerobically and gain energy for cell growth. All organisms use ammonia as one of the starting building blocks for the synthesis of amino acids, nucleotides, and many other important biological compounds. Nitric oxide is

10.1021/cr8003696 CCC: $71.50
Published on Web 05/13/2009

Victor Rosca received his degree in chemistry and chemical technology from the State University of Moldova in 1998. In the same year, he joined the electrochemistry group of Professor I. C. Popescu at the University of Cluj-Napoca, Romania, as a research assistant to study mediated (bio)electrocatalysis for analytical applications. In 2002, he moved to the Laboratory of Inorganic Chemistry and Catalysis, Eindhoven University of Technology, The Netherlands, where he investigated the mechanism and structure sensitivity of electrocatalytic reactions of inorganic nitrogen compounds in the group of Marc Koper. He defended his Ph.D. thesis in 2006. He then moved to the Leiden Institute of Chemistry, Leiden University, as postdoctoral research associate in the Koper group to study the mechanism of electrocatalytic reactions of small molecules at metal−liquid interfaces using in situ infrared and surface-enhanced Raman spectroscopy. Since 2007, he has been a research scientist at the Energy Research Centre of The Netherlands (ECN), and he works on the development of polymer electrolyte fuel cells. His research interests include in situ and ex situ characterization of membrane electrode assemblies.

Matteo Duca was born in Bergamo, Italy, in 1983. He obtained his B.Sc. in Chemistry in 2005 from the University of Milano, Italy, working in the field of Molecular Electrochemistry with Prof. Patrizia R. Mussini. In 2007, he received his M.Sc. at the same university under the supervision of Prof. Sergio Trasatti, doing research on the electrocatalysis of hydrogen evolution on noble metal modified nickel cathodes. In 2008, he moved to Leiden University to join the group of Prof. Marc Koper for a Ph.D. project. Currently, he is investigating the electrochemical reactivity of nitrate and nitrite, with a view to determining the intermediates and steering the reaction's selectivity to benign products.

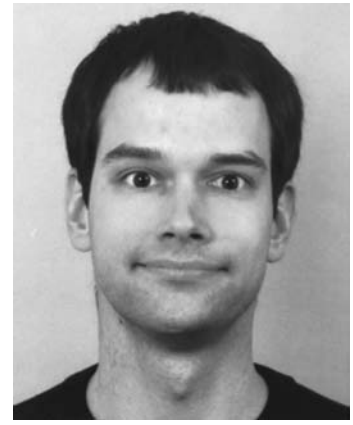

Thijs de Groot was born on August 12th, 1979, and grew up in Helmond, The Netherlands. He received his M.Sc. degree in chemical engineering from Eindhoven University of Technology in 2002. In his thesis project, he investigated the reduction of nitrate on platinum. After that he continued as a Ph.D. student with Marc Koper at the same university. He investigated the electrochemistry of immobilized hemes and heme proteins with a focus on nitrogen chemistry. He obtained his degree in 2007, after which he joined the Process and Product Technology group of AkzoNobel as a researcher, where he investigates electrochemical (membrane) processes and solid−liquid separation.

Marc Koper (1967) grew up in Soest, The Netherlands, and received his M.Sc. degree in chemistry from Utrecht University in 1991. He obtained his Ph.D. degree (cum laude) with J. H. Sluyters on the topic of electrochemical oscillations and chaos from Utrecht University in 1994. After a postdoctoral stay with W. Schmickler at the University of Ulm supported by a Marie Curie fellowship, he joined the faculty of the Department of Chemistry and Chemical Engineering of Eindhoven University of Technology in 1997 as a Fellow of the Royal Netherlands Academy of Arts and Sciences. In 2005, he became Full Professor of Fundamental Surface Science at Leiden University (The Netherlands), where his group studies fundamental aspects of electrocatalytic reactions using a range of experimental and theoretical techniques.

a key and compulsory intermediate in bacterial denitrification and an important biological messenger molecule in a variety of processes. Several compounds from the nitrogen cycle, such as ammonia, hydroxylamine, nitric acid, hydrazine, nitrous oxide, and ammonium nitrate, are also of notable economical importance and are produced in large amounts by the chemical industry. Emission control of NO_x is another important area of nitrogen chemistry, in which (gas-phase) heterogeneous catalysis plays an essential role. Ammonium nitrate is commonly used as an explosive and in agriculture as a nitrogen-rich fertilizer. However, high concentrations of nitrate in groundwater pose a serious threat to human health, and as a consequence, groundwater remediation from nitrate has become a topic of great environmental concern.[2]

Catalysis plays an important role in practically all of the conversions featured in the nitrogen cycle. Many of these conversions take place in an aqueous environment at room temperature, a statement that certainly applies to the enzymology of the nitrogen cycle (for reviews on various aspects of nitrogen cycle enzymology, see refs 3−5). Because of the importance of the nitrogen cycle and some of its intermediates, the detection of compounds such as nitric oxide, nitrite, and nitrate represents an active field in electroanalytical chemistry,[6,7] for which a detailed knowledge of the electrochemistry of these compounds is indispensable.

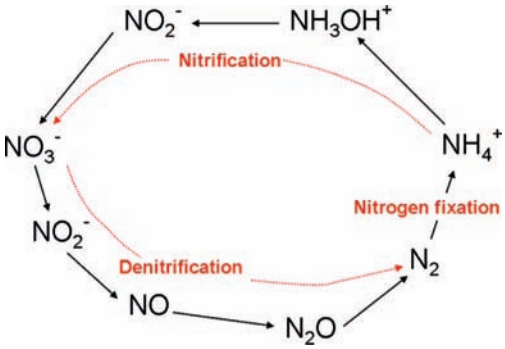

Figure 1. Simplified scheme of the "classical" nitrogen cycle. For more recent versions, see ref 1.

Outside the area of enzymology, typical examples of nitrogen cycle (electro)catalysis in the liquid phase include the Pt-catalyzed reduction of nitric oxide to hydroxylamine to finally provide caprolactam[8−10] (a process employed by BASF), the Pt−Pd catalyzed conversion of nitrate to hydroxylamine[9,11] (part of the so-called HPO (hydroxylamine phosphate oxime) process employed by DSM), ammonia oxidation at Pt or Ir electrodes for application in low-temperature fuel cells,[12,13] and the heterogeneously catalyzed reduction of nitrate to dinitrogen for groundwater remediation.[14] The latter process has been proposed as an alternative for the bacterial treatment of ground- and wastewater,[14,15] which is a costly and cumbersome process, and is currently an area of intense research in catalysis. In all of the above-mentioned cases, it is of prime importance to understand the underlying electrochemistry and electrocatalysis of the reaction, because these reactions take place at a polarized catalyst−solution interface. Interestingly, for practically all reactions in the nitrogen cycle, both "natural" catalysts, that is, enzymes, and man-made catalysts exist, the latter typically based on transition metals. As a consequence, comparing the activity, selectivity, and mechanistic pathways of enzymes vs man-made catalysts for reactions in the nitrogen cycle is an intriguing subject of fundamental interest.

The general complexity of nitrogen chemistry may be predicted straightforwardly from the observation that the formal oxidation states of nitrogen range from −3 to +5 and that stable compounds exist for all oxidation states. Standard electrode potentials for the long list of conceivable half-reactions have been calculated from their thermodynamic properties and have been collected by Maloy in the book by Bard, Parsons, and Jordan[16] and in the review on nitrogen electrochemistry by Plieth.[17] We refer the reader to these literature sources for extensive tabulations. A useful graphical representation of the standard potentials are so-called oxidation state diagrams, which plot the volt equivalent (VE, defined as the standard potential times the nitrogen oxidation state) of the half-reaction of a particular nitrogen compound to nitrogen (N_2) versus its oxidation state. Figure 2 shows such a diagram for the most important compounds in the nitrogen cycle in acidic solution (the diagram for alkaline media is quite similar, with corrections for the pK_a of some of the compounds[17]). This diagram illustrates that, under standard conditions, dinitrogen and ammonia are the most stable forms of nitrogen. For instance, in the reduction of nitrate, thermodynamically speaking, dinitrogen (and ammonia) should be the thermodynamically preferred end product(s). However, these plots tell us essentially nothing about the rate at which these conversions would take place,

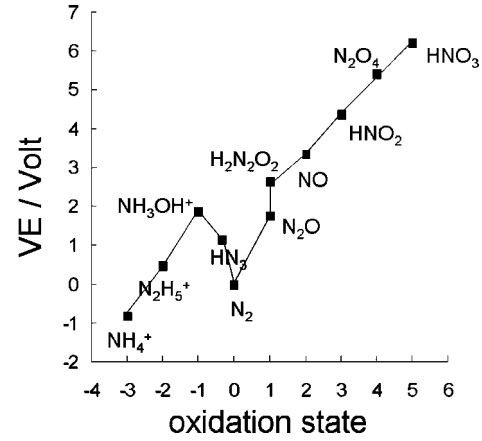

Figure 2. Oxidation state diagram of inorganic nitrogen compounds in acidic solution. VE is the "volt equivalent", that is, the standard potential for the conversion to N_2 times the nitrogen oxidation state of the species under consideration. (Note that HN_3 refers to azide).

and in fact few catalysts exist today that are able to convert nitrate to dinitrogen with 100% selectivity. By contrast, ammonia and nitrous oxide are preferred final products in nitrate reduction that may be formed with 100% selectivity depending on the electrocatalyst material, pH, and electrode potential. This simple observation illustrates the importance of kinetic considerations and catalysis in understanding and ultimately controlling nitrogen cycle electrochemistry.

The aim of this review is essentially threefold. First of all, we will attempt to summarize our current understanding of the mechanistic aspects of some of the most relevant electrocatalytic conversions in the nitrogen cycle (for previous reviews, see the extensive chapter by Plieth[17] and the shorter review on the electrochemistry of nitrogen oxides and oxyanions by Inzelt and Horányi[18]). Although this review cites no less than 374 scientific papers from the literature, the mere observation that this number is lower than the number of references in the 1978 review by Plieth illustrates the fact that we have been selective. Our discussions will be restricted to (bi)metallic electrode materials and functionalized electrode surfaces that are active for a particular reaction in the nitrogen cycle. Furthermore, we will only review those studies that provide a clear electrocatalytic insight, as opposed to electroanalytical insight. Because platinum turns out to be a good catalyst for many of the redox reactions featuring in the nitrogen cycle, many of our discussions will pertain to platinum. By functionalized electrode surfaces, we mean electrode surfaces modified by catalytically active compounds, typically organometallic coordination complexes or macrocycles, which may or may not have been inspired by active sites in enzymes involved in the nitrogen cycle. Our second aim is to discuss the various reactions and their mechanisms in relation to each other and to point out dominant pathways and intermediates that recur across the nitrogen cycle. Finally, our third aim is to succinctly compare the "electrochemical" mechanisms to the "enzymatic" mechanisms that have been suggested in the literature. It is hoped that this integral approach will spur more fundamental mechanistic studies of these important reactions in electrocatalysis.

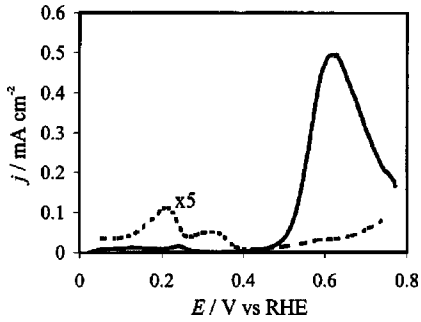

Figure 3. Voltammogram of platinum in the presence (solid line) and absence (dotted line) of 0.1 M NH_3 in 1 M KOH, scan rate 20 mV s^{-1}. The current of the blank voltammogram has been multiplied by a factor of 5 for clarity. Reproduced with permission from ref 30. Copyright 2001 Elsevier.

2. Ammonia Oxidation

2.1. Ammonia Oxidation on Platinum

The electrochemical oxidation of ammonia on transition metal surfaces has received considerable attention, particularly in connection with the possibility of using ammonia in fuel cells.[19−22] Furthermore, an adequate knowledge of ammonia electrochemistry is important for application in environmental (electro)catalysis[23,24] and in the electrochemical detection of ammonia.[25,26]

Ammonia may be oxidized to a variety of different products in the nitrogen cycle. Thermodynamically speaking, the most favorable reaction should be oxidation to N_2, which has a standard equilibrium potential of −0.057 V vs NHE (or −0.148 V vs RHE in alkaline media). Most electrochemical studies on ammonia oxidation have used platinum as an electrode material, and this will be the topic of this section. In section 2.2, we will briefly discuss results on other metals and alloys. A second important observation is the lack of any significant activity for ammonia oxidation in acidic solution. Halseid et al.[27] have recently published a study of ammonia oxidation, or rather ammonium oxidation on polycrystalline platinum in acidic media. They observed a small oxidation activity, and the formation of N_2 and NO using differential electrochemical mass spectrometry (DEMS). Ammonium also appears to affect the oxide formation on platinum, presumably through the formation of strongly bound species such as N(ads). Overall, however, the oxidation currents are very low, presenting only small but detectable changes from Pt blank cyclic voltammetry. Therefore, the remainder of this section is devoted to the discussion of ammonia oxidation in alkaline solution, where a much higher catalytic activity is observed.[12,13,28−30]

From ultrahigh vacuum (UHV) studies, it is known that ammonia interacts weakly with platinum surfaces, showing predominantly molecular adsorption at ambient temperatures, largely independent of the surface structure.[31−34] Dehydrogenation of ammonia (and further oxidation to NO) requires high temperatures (typically over 500 K) and the presence of co-adsorbed oxygen.[32,34,35]

With this in mind, the appreciable activity of platinum in ammonia electrooxidation in alkaline media at room temperature is quite a remarkable phenomenon. Figure 3 shows the voltammetric curve for ammonia oxidation on platinum in alkaline solution. It is observed that ammonia starts to be oxidized at ca. 0.45 V, in the so-called double-layer region of platinum, and goes through a maximum activity at around 0.6 V. De Vooys et al.[30] observed that at fixed potential, the current reaches steady-state values for potentials below 0.57 V, whereas at higher potentials, the electrode deactivates with time.

In early studies on polycrystalline platinum and other transition metal surfaces, ammonia oxidation in alkaline media was commonly viewed as a stepwise electrocatalytic dehydrogenation process, resulting in the formation of NH_x adsorbed species ($x = 1,2$) and ultimately in the formation of adsorbed atomic nitrogen:[12,23,36]

$$NH_3 \leftrightarrows NH_{3,ads} \quad \text{equilibrium} \tag{1}$$

$$NH_{3,ads} + HO^- \rightarrow NH_{2,ads} + e^- + H_2O \tag{2}$$

$$NH_{2,ads} + HO^- \rightarrow NH_{ads} + e^- + H_2O \quad \text{(rds)} \tag{3}$$

$$NH_{ads} + HO^- \rightarrow N_{ads} + e^- + H_2O \tag{4}$$

$$NH_{x,ads} + NH_{y,ads} + (x + y)\,HO^- \rightarrow N_2 + (x + y)H_2O + (x + y)e^- \tag{5}$$

On the basis of the experimentally observed Tafel slope (39 mV $decade^{-1}$) and a presumed Langmuir adsorption isotherm for ammonia adsorption, Oswin and Solomon suggested that the transformation NH_2(ads) → NH(ads) is the rate-determining step at moderately oxidative potentials.[12] It was assumed that molecular nitrogen was formed by the recombination of two nitrogen adatoms (reaction 5, $x = y = 0$). This step was expected to be the rate-determining step at high overpotentials.

In a later detailed mechanistic study, Gerischer and Mauerer[13] suggested that, similar to the role of oxygen (or hydroxyl) in ammonia dehydrogenation under UHV conditions, a (partially) discharged surface-bonded hydroxyl plays an important role in ammonia dehydrogenation under electrochemical conditions. The dimerization of NH_x ($x = 1,2$) fragments and the subsequent dehydrogenation of the resulting dimer was proposed as the most plausible scenario for the formation of molecular nitrogen, whereas atomic nitrogen was assumed to act as a catalyst poison. The authors performed an ex situ analysis indicating the formation of atomic nitrogen. Specifically, a platinized platinum electrode was polarized until its activity for ammonia oxidation dropped to zero. Then the electrode was removed from the electrochemical cell, dried, and heated to 400−600 °C, and a gas chromatographic analysis of the resulting gas mixture was performed. The gas chromatographic analysis of the resulting mixture indicated formation of predominantly dinitrogen, whereas the hydrogen content was negligible.

More recent studies, which combined electrochemistry with differential electrochemical mass spectrometry (DEMS), provided further details on the ammonia oxidation on polycrystalline platinum, essentially confirming the Gerischer−Mauerer mechanism.[28−30] Wasmus et al.[28] showed the formation of N_2 below potentials of 0.8 V, and the formation of oxygenated nitrogen species such as NO and N_2O above 0.8 V. This suggests that surface oxide formation is necessary for the formation of NO_x species from ammonia. Figure 4 shows results of an experiment by De Vooys et al.[30] combining voltammetry and DEMS, strongly suggesting that the intermediate leading to N_2 formation is an NH_x(ads) species and that N(ads) indeed serves as a poison. In the experiment, the ammonia adsorbate NH_x(ads) (where x could

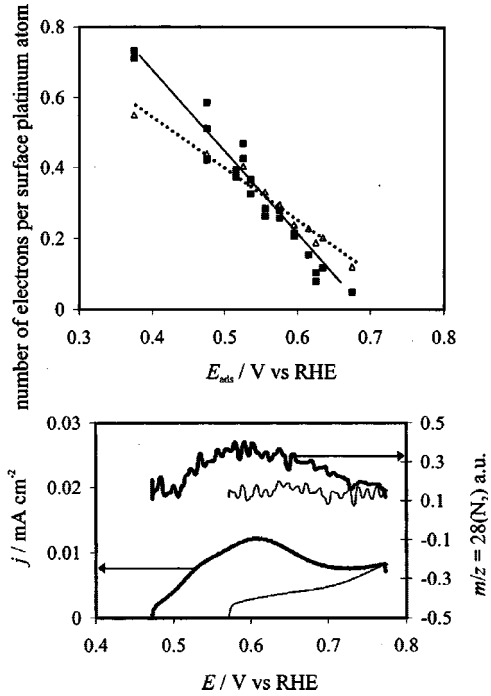

Figure 4. (a) Charge of the oxidation of the ammonia adsorbate in number of electrons per Pt surface atom formed at E_{ads} to 0.77 V on platinum; filled squares with solid line correspond to ammonia adsorbate; open triangles with dashed line correspond to the charge obtained in a blank 1 M KOH electrolyte without ammonia. (b) DEMS on ammonia adsorbate oxidation, $E_{ads} = 0.47$ (thick line) and 0.57 V (thin line) on platinum. Reproduced with permission from ref 30. Copyright 2001 Elsevier.

vary from 0 to 3) was formed at the adsorption potential E_{ads} in the presence of ammonia in the electrolyte, and then transferred to a cell containing the same electrolyte without ammonia. Next, the adsorbate was oxidized in a potential sweep to 0.77 V, that is, just below the potential of Pt surface oxidation. The top panel shows the charge obtained from this potential sweep (solid line with filled squares) compared with the charge obtained if there was no ammonia in solution (blank experiment; dashed line with open triangles). The experiment clearly shows that for $E_{ads} < 0.56$ V, an ammonia adsorbate is formed that can be further oxidized and, hence, yields a higher charge than the blank experiment. For $E_{ads} > 0.56$ V, the ammonia adsorbate cannot be oxidized; note that the adsorbate was oxidized up to 0.77 V, below the formation of platinum surface oxides and that no nitrogen oxides were formed in the adsorbate oxidation experiment as was confirmed by DEMS. This experiment strongly suggests that below 0.56 V NH_x(ads) species are formed on the surface, which can be further oxidized and dehydrogenated, and above 0.56 V only N(ads) is formed, which serves as a surface poison and cannot be oxidized further if the final oxidation potential remains below 0.77 V. This is consistent with N(ads) being the catalyst poison. The lower panel in Figure 4 shows two DEMS experiments following gas formation during the oxidation of the ammonia adsorbate formed at two different potentials. For an NH_x(ads) adsorbate formed below 0.56 V (bold solid line), the formation of N_2 is observed during its oxidation; for a N(ads) adsorbate formed above 0.56 V (thin solid line), no gas formation is observed. This is again consistent with the idea that the precursor for N_2 formation is NH_x(ads) and not N(ads).

In a subsequent in situ surface-enhanced Raman spectroscopy (SERS) study, de Vooys et al.[37] demonstrated the formation of atomic nitrogen during ammonia oxidation on palladium, which is a poor electrocatalyst for the formation of N_2 (see section 2.2). This result again suggests the poisoning role of N(ads) in the Gerischer−Mauerer mechanism. More recently, Vidal-Iglesias et al.[38] presented SERS experiments on ammonia oxidation on Pt. They observed spectral bands near 1340 and 2000 cm^{-1}, which would strongly suggest the formation of the azide ion, N_3^-. They ascribe the formation of azide to the reaction between NH_3 and a N_2H_x intermediate formed during the reaction, most likely hydrazine, N_2H_4, a reaction known to occur in alkaline media. More evidence for the possible involvement of hydrazine in the mechanism will be discussed in more detail below in relation to the mechanism of ammonia oxidation on a Pt(100) electrode.

Endo et al.[39] used the rotating ring-disk electrode (RRDE) technique to study ammonia oxidation on Pt and could detect some dissolved intermediates, both oxidizable and reducible ones. They also observed an anomalous decrease of the ammonia oxidation rate with increasing disk rotation rate. This suggests that oxidizable intermediates escape from the disk at higher rotation rate, such that the total current at the disk, which is not mass-transport limited, decreases. The reducible species observed at the ring for disk potentials higher than 0.8 V (vs RHE) are most likely NO_x species. The small oxidation current observed at the ring below 0.8 V should most likely be ascribed to hydrazine N_2H_4 or hydroxylamine, the latter formed in a reaction such as $NH_2(ads) + OH^- \rightarrow NH_2OH + e^-$.

Studies of ammonia oxidation on single-crystal platinum electrodes have provided more detailed insight into the mechanism. Gao et al.[40] reported mass spectrometry measurements of ammonia oxidation on Pt(100) and demonstrated a high activity of this surface. These authors also observed the production of molecular nitrogen between ca. 0.6 and 0.9 V. More recently, Vidal-Iglesias et al.[41] reported a voltammetric study of ammonia oxidation on Pt(111), Pt(110), and Pt(100), demonstrating that Pt(100) was by far the most active Pt surface for ammonia oxidation, exhibiting catalytic activity at potentials as low as 0.5 V, whereas Pt(111) and Pt(110) show very little activity in the potential range up to ca. 0.9 V. In a subsequent paper, Vidal-Iglesias et al.[42] concluded that the activity for ammonia oxidation was sensitive to the width of the (100) terrace and to some extent to the orientation of the step, although the Pt(100) surface remains the most active catalyst. The same authors also reported results of a DEMS study of ammonia oxidation on Pt(111), Pt(110), and Pt(100) using labeled ammonia (^{15}N).[43] The Pt(100) surface showed a very high activity and selectivity (up to ca. 0.7 V vs RHE) in ammonia oxidation to dinitrogen. At potentials more positive than ca. 0.7 V, nitrous oxide and nitric oxide become dominant products at this surface. For a cyclic voltammogram with an upper potential limit of ca. 1.5 V, a strong deactivation of the surface was observed. This effect must be related to both poisoning of the electrocatalyst surface by strongly adsorbed species, for example, atomic nitrogen or oxygen-containing species, and loss of surface order as a result of the surface oxidation and associated atomic roughening. Pt(111) and Pt(110) were shown to be much poorer electrocatalysts for ammonia oxidation in general and to dinitrogen in particular.

Motivated by the exceptional catalytic properties of the Pt(100) surface for ammonia oxidation, Vidal-Iglesias et al.[44] synthesized Pt nanoparticles with different (100) preferen-

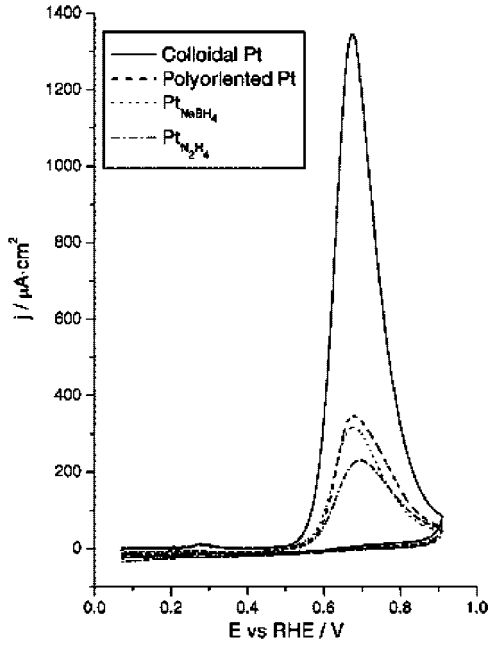

Figure 5. Ammonia oxidation on hydrazine−Pt, borohydride−Pt, and colloidal Pt nanoparticles and polyoriented platinum in 0.2 M NaOH and 0.1 M NH_3. Scan rate 10 mV s^{-1}. Reproduced with permission from ref 44. Copyright 2004 Elsevier.

tially oriented surface structures. The oxidation current density appeared very sensitive to the existence of Pt(100) domains. Figure 5 compares the voltammetry of four different Pt catalysts: polyoriented Pt, Pt nanoparticles obtained using hydrazine or borohydride as a reducing agent, and "colloidal Pt" obtained by a method described in ref 45, which is known to give rise to "cubic" nanoparticles with large Pt(100) domains. The latter catalyst is clearly superior to the other catalysts, proving the importance of the shape of the nanocatalyst particles in general and the importance of Pt(100) domains for ammonia oxidation in particular.

With the aim to further understand the origin of the structure sensitivity of ammonia oxidation on platinum, Rosca and Koper[46] have compared in detail the mechanism of ammonia oxidation on Pt(111) and Pt(100) in alkaline media. In agreement with the work from the Alicante group,[41,42] Pt(111) showed very little activity for ammonia oxidation (see the inset of Figure 6). The oxidative adsorption of ammonia on Pt(111) starts at potentials corresponding to the double-layer region, resulting in the formation of adsorbed species. Therefore, the first dehydrogenation steps do not seem to require the participation of co-adsorbed OH species, at variance with the Gerischer−Mauerer mechanism. The NH adsorbate was identified as the main stable intermediate of ammonia oxidation on Pt(111), based on the observation of the 44 mV/decade Tafel slope of the feature corresponding to the formation of the adsorbate (peak at 0.55 V in the dashed line in the inset of Figure 6), which can only be explained if at least two electrons are transferred. The surface remained blocked at potentials corresponding to OH adsorption (ca. 0.6 V vs RHE in 0.1 M NaOH), although a further dehydrogenation of NH to N seems possible. According to recent DFT calculations, the NH and N intermediates adsorb strongly on Pt(111) with preference for multifold-coordination sites.[46−48] No gaseous products (e.g., N_2O, NO, NO_2) have been detected in the potential region in which the Pt(111) surface maintains its structural order (up to ca. 0.9 V vs RHE),[43,46] except for a very small

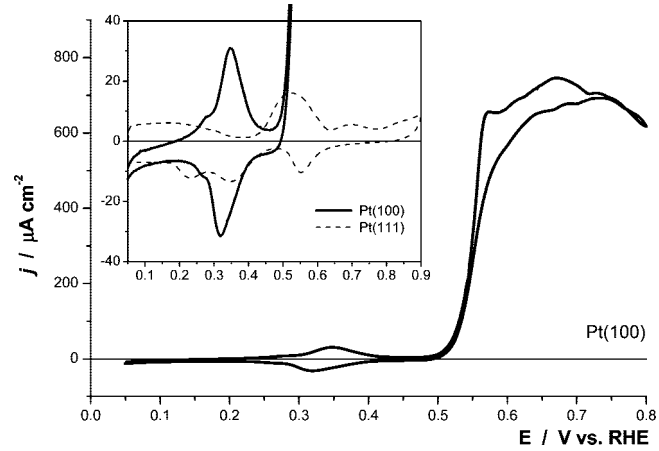

Figure 6. Ammonia oxidation on Pt(100) in 0.1 M NaOH. The inset compares the oxidation of ammonia on Pt(100) (solid line) and Pt(111) (dashed line) surfaces. Experimental conditions: starting potential 0.05 V; scan rate 10 mV s^{-1}; 5×10^{-3} M NH_3. Reproduced with permission from ref 46 Copyright 2006 PCCP Owner Societies.

amount of N_2.[43] These observations indicate that ammonia oxidation to nitrogen−oxygen compounds and hence the formation of N−O bond is very sluggish on Pt(111).

The electrochemical oxidation of ammonia on Pt(100) starts at potentials corresponding to the H_{upd} region, resulting in the formation of a monolayer of NH_x adsorbate at moderate oxidative potentials. The $NH_{x(ads)}/NH_{3(ads)}$ surface redox couple is characterized by oxidation and reduction peaks at 0.32−0.33 V (see Figure 6; we exclude N−N bond formation at these potentials because no N_2 has been detected in the DEMS experiments[43] and hydrazine should oxidize irreversibly at these potentials, see section 3.1). The Tafel slopes for the oxidation and reduction features are ca. 100 and 120 mV/decade, respectively, which together with the charge associated with these peaks strongly suggest that $x = 2$, implying that the stable adsorbate on Pt(100) is $NH_{2(ads)}$. There is no indication that the first dehydrogenation step would require participation of co-adsorbed OH. In the potential region between ca. 0.5 and 0.7 V vs RHE, ammonia is oxidized quantitatively to N_2 in a fast continuous process (Figure 6). Based on a Tafel slope of 30 mV/decade for the main oxidation peak to N_2, the following mechanism was proposed for ammonia oxidation to N_2 at Pt(100):[46]

$$NH_3 + * \leftrightarrows NH_{3,ads} \quad (6)$$

$$NH_{3,ads} + OH^- \leftrightarrows NH_{2,ads} + e^- + H_2O \quad (7)$$

$$2NH_{2,ads} \rightarrow N_2H_{4,ads} \quad \text{rds} \quad (8)$$

$$N_2H_{4,ads} \rightarrow \ldots \rightarrow N_2 + 2* \quad \text{fast} \quad (9)$$

(where "*" denotes a free site on the Pt surface). This mechanism identifies the surface-confined hydrazine as the key precursor in dinitrogen formation. The involvement of hydrazine agrees very well with the SERS measurements by Vidal-Iglesias et al.[38] mentioned earlier, who found evidence for the formation of azide from the reaction between ammonia and hydrazine. The high oxidation activity of hydrazine on Pt at these potentials, as implied by the above mechanism, will be discussed in section 3.1. At oxidative potentials higher than 0.7 V vs RHE, the selectivity gradually shifts toward the formation of oxygen-containing compounds.[43]

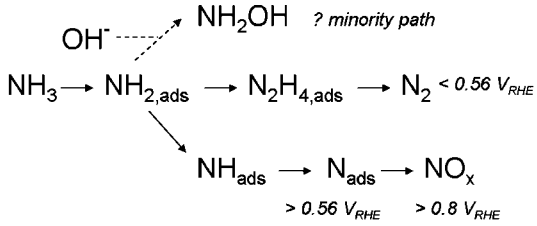

Figure 7. General scheme for ammonia oxidation on Pt in alkaline solution.

A comparison of ammonia oxidation on Pt(111) and Pt(100) allows us to identify the factors that control the activity and selectivity. The above findings point to the importance of an "early" stabilization of the intermediates of ammonia dehydrogenation. The deeper the ammonia dehydrogenation, the higher the coordination and the higher the adsorption energy of the resulting adsorbed species.[46−48] Accordingly, on Pt(111) the hydrogenation of ammonia results in the formation of strongly bound NH and N fragments, which are not able to participate in the dinitrogen formation. By contrast, the Pt(100) surface can stabilize the NH_2 adsorbate, which is significantly less strongly bound and, importantly, provides an active precursor for the formation of the N−N bond in the form of hydrazine. Interestingly, this preference of Pt(111) and Pt(100) for NH and NH_2 fragments, respectively, has also been predicted in a recent computational DFT study[48] and is also in agreement with a recent UHV study of ammonia oxidation on stepped Pt surfaces.[49]

Figure 7 summarizes the overall mechanistic picture of ammonia oxidation on Pt that may be derived from the above discussion. The formation of hydroxylamine is hypothesized tentatively on the basis of the RDDE experiments of Endo et al.,[39] although the escape of hydrazine from the Pt surface would also explain their results.

2.2. Ammonia Oxidation on Other Metal and Alloy Electrodes

De Vooys et al.[30] studied ammonia oxidation on a series of transition and coinage metals. The coinage metals copper, silver, and gold showed no activity for ammonia oxidation, due to their low dehydrogenation capacity. The transition metals rhodium, ruthenium, and palladium were found to poison very rapidly during ammonia oxidation without showing any steady-state activity, and SERS measurements indeed indicate the formation of adsorbed atomic nitrogen on palladium.[37] Only platinum and iridium show steady-state activity for ammonia oxidation, presumably because they are able to stabilize the key NH_x intermediate (with probably $x = 2$, see section 2.1).

Several authors have looked for better ammonia oxidation catalysts by studying platinum-based alloys, such as Pt−Ir,[50−54] Pt−Ru,[52,53] Pt−Ni,[52,55] Pt−Cu,[51] Pt−Pd,[53] and Pt−Rh.[53] Of these bimetallic catalysts, Pt−Ir and Pt−Ru have shown small enhancements in catalytic activity compared with polycrystalline Pt. However, Pt(100) and Pt nanoparticle catalysts with Pt(100) domains remain the most active catalysts for ammonia oxidation.[53]

2.3. Comparison to Enzymatic Ammonia Oxidation

Ammonia oxidizing bacteria extract energy for growth from the oxidation of ammonia to nitrite. Together with nitrite oxidation to nitrate by nitrite-oxidizing bacteria, this overall process is called nitrification (see Figure 1). For many years, bacterial ammonia oxidation was considered to be a strictly aerobic process, with oxygen as the electron acceptor (and oxygen donor). More recent discoveries have shown that the anaerobic oxidation of ammonia is possible, utilizing other species from the nitrogen cycle as electron acceptors.

In aerobic ammonia-oxidizing bacteria, the catabolism of ammonia takes place in two stages.[3] Ammonia is first oxidized to hydroxylamine by an enzyme called ammonia monooxygenase (AMO). Hydroxylamine is then oxidized to nitrite by hydroxylamine oxidoreductase (HAO), an enzyme that we will discuss briefly in section 4.4. The molecular structure of AMO has not been fully clarified yet, but it is considered that the enzyme consists of three subunits and metal centers of copper and iron. In the mechanisms described in the literature, molecular oxygen serves as both the oxygen donor and (partial) electron acceptor; that is, one oxygen atom is inserted into ammonia to form hydroxylamine, whereas the other oxygen picks up two electrons and two protons to form water. The two electrons needed for the overall reaction are likely donated by the quinone reductant pool. Note that this mechanism is very different from the electrochemical mechanism outlined in Figure 7. Although there is some evidence that hydroxylamine may be formed as a byproduct of ammonia oxidation on platinum, there is no evidence that the further oxidation of hydroxylamine would play any role. Rather, nitric oxides such as NO, nitrite, and nitrate are formed from the oxidation of surface-adsorbed atomic nitrogen or NH.

Interestingly, the processes featuring in the anaerobic ammonia oxidation ("anammox")[56] bear much closer resemblance to the mechanism of the platinum-catalyzed ammonia oxidation. Anammox uses nitrite as the electron acceptor to oxidize ammonia to dinitrogen:

$$NH_3 + NO_2^- \rightarrow N_2 + H_2O + OH^- \qquad (10)$$

Hydrazine appears to be the key intermediate, although the mechanism by which ammonia combines with nitrite to form hydrazine is currently unknown. Hydrazine is then converted to N_2 by an enzyme called hydrazine dehydrogenase (see also section 3.3). The resemblance to platinum is striking, with the difference that platinum carries out both the conversion of ammonia to hydrazine and of hydrazine to dinitrogen. Anammox uses two separate enzymes for the two conversions, and also uses another nitrogen donor (nitrite) to accomplish the N−N bond formation.

3. Hydrazine Oxidation

3.1. Hydrazine Oxidation on Pt Electrodes in Acidic and Alkaline Media

Hydrazine oxidation in an electrochemical environment has been of interest for various applications, including fuel cells, electrochemical detection, and its use as a reducing or anticorrosion agent. When compared with ammonia oxidation, electrochemical hydrazine oxidation is a seemingly facile process, quickly reaching mass-transport limitations. However, the reaction still occurs with significant oxidation overpotential both in acidic and in alkaline media. The theoretically calculated standard equilibrium potential in acidic media,[16]

$$N_2H_5^+ \leftrightarrows N_2(g) + 5H^+ + 4e^- \qquad E^0 = -0.23 \text{ V (vs NHE)} \quad (11)$$

and in alkaline media,[16]

$$N_2H_4 + 4OH^- \leftrightarrows N_2(g) + 4H_2O + 4e^- \qquad E^0 = -0.33 \text{ V (vs RHE)} \quad (12)$$

are some 0.3 V more negative than the potentials at which hydrazine starts to oxidize at platinum surfaces in dilute acidic or alkaline solutions.[17] Therefore, dehydrogenation of hydrazine to molecular nitrogen, a presumably facile transformation, is associated with significant kinetic limitations even at a catalytically active metal such as platinum.

The electrooxidation of hydrazine on polycrystalline platinum has been the subject of extensive studies, often in relation with the possible application of hydrazine in fuel cells.[57−60] In acidic media, hydrazine oxidation typically starts just positive of the hydrogen UPD region, implying an anodic overpotential of ca. 0.5 V (see eq 11), quickly reaching diffusion limitations at higher potential. From the early studies, it was concluded that hydrazine oxidation takes place as a stepwise electrochemical dehydrogenation process with molecular nitrogen as the product.[57] Online electrochemical mass spectrometry (MS) measurements confirmed that at polycrystalline platinum, molecular nitrogen is the main product without any evidence for N−N bond breaking.[60] Harrison and Khan[59] found that the first electron transfer step is rate-determining and inverse first order in H^+ concentration, leading them to suggest the following reaction scheme:

$$N_2H_5^+ \leftrightarrows N_2H_4(ads) + H^+ \quad (13)$$

$$N_2H_4(ads) \rightarrow N_2H_4^+ + e^- \quad \text{rds} \quad (14)$$

$$N_2H_4^+ \rightarrow N_2 + 4H^+ + 3e^- \quad \text{fast} \quad (15)$$

though in our opinion the following scheme would also be in agreement with their experimental results:

$$N_2H_4(ads) \rightarrow N_2H_3(ads) + H^+ + e^- \quad \text{rds} \quad (16)$$

$$N_2H_3(ads) \rightarrow N_2 + 3H^+ + 3e^- \quad \text{fast} \quad (17)$$

The structure sensitivity of hydrazine oxidation on Pt in acidic media was explored by García Azorero et al.,[61,62] who found that (100)-type facets on electrofaceted electrodes were able to shift the oxidation potential negatively. More recent studies of hydrazine oxidation on single-crystal metal surfaces in acidic media confirmed the structure sensitivity of hydrazine oxidation, and brought new insight into the mechanism of the reaction. Nishihara et al.[63] and Gomez et al.[64] reported voltammetric studies of hydrazine adsorption and oxidation on platinum single-crystal surfaces in 0.5 M sulfuric acid. As illustrated in Figure 8 for Pt(100), the voltammetry of hydrazine at single-crystal platinum surfaces in acidic media shows a modified hydrogen UPD region (0.05−0.25 V in Figure 8), presumably influenced by hydrazine adsorption, followed by a diffusion-controlled oxidation wave (>0.3 V in Figure 8). Nishihara et al.[63] studied hydrazine adsorption and oxidation on Pt(111) and Pt(322) surfaces and found that hydrazine adsorbs more easily on steps of (100) orientation than on terraces of (111) orientation, whereas hydrazine oxidation occurs at lower overpotentials on terraces. Hydrazine adsorbates were also found

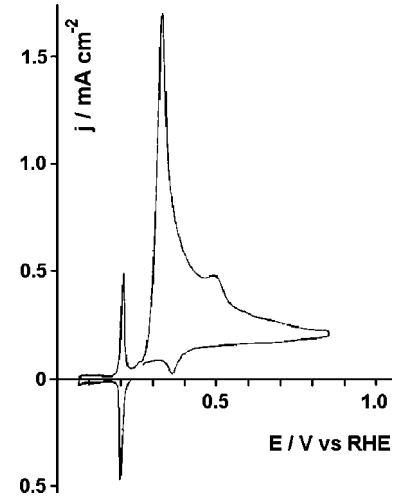

Figure 8. Voltammograms for a Pt(100) electrode in 10^{-3} M hydrazinium sulfate solution in 0.5 M H_2SO_4, showing hydrazine oxidation in the first potential excursion up to 0.89 V after recording the stationary voltammogram in the low potential range. Scan rate is 50 mV/s. Reproduced with permission from ref 64. Copyright 1993 Elsevier.

to be relatively weakly adsorbed, since the hydrazine-related voltammetric features in the H-upd region did not survive when the electrode was transferred to a clean solution. Of the three basal planes of platinum, Gomez et al.[64] found that Pt(100) has the lowest overpotential for hydrazine oxidation, in agreement with the earlier findings of García Azorero et al.[61,62] Their experiments also suggested that on Pt(111) and Pt(100), hydrazine adsorbs relatively weakly, as evidenced by the reversible nature of the modified hydrogen UPD region (Figure 8, peak at 0.2 V), whereas on Pt(110) hydrazine adsorption is stronger and irreversible.

More recently, Alvarez-Ruiz et al.[65] investigated in greater detail hydrazine adsorption and oxidation on platinum surfaces in perchloric acid solution by combining cyclic voltammetry, Tafel slope analysis, and CO displacement experiments. The adsorption prewave on Pt(111) and Pt(100) is considerably less sharp than that in sulfuric acid, implying the involvement of anions in the latter solution. The authors suggested that in the prewave, hydrazine is reversibly dehydrogenated to surface-bonded N_2H_3,

$$N_2H_5^+ \leftrightarrows N_2H_3(ads) + 2H^+ + e^- \quad (18)$$

which is then oxidized to N_2 in the main peak,

$$N_2H_3(ads) \rightarrow N_2 + 3H^+ + 3e^- \quad (19)$$

The authors ascribed the high activity of Pt(100) to its low barrier to form the N_2H_2(ads) as the first step in the overall reaction 19.

In alkaline media, hydrazine oxidation typically starts at potentials *within* the hydrogen UPD region, at potentials as low as 0.1 V vs RHE.[66] This is at a lower potential than in acidic media (on the RHE scale) and also at a slightly lower overpotential (compare the equilibrium potentials of reactions 12 and 13). The older work on hydrazine oxidation on Pt in alkaline media[67−70] tends to be "rather confusing" (quotation from ref 70) and does not point to a single key intermediate as has been concluded from the work in acidic media. Rosca and Koper[66] have examined the mechanism and structure sensitivity of the electrocatalytic oxidation of hydrazine on platinum single-crystal electrodes in alkaline solutions using

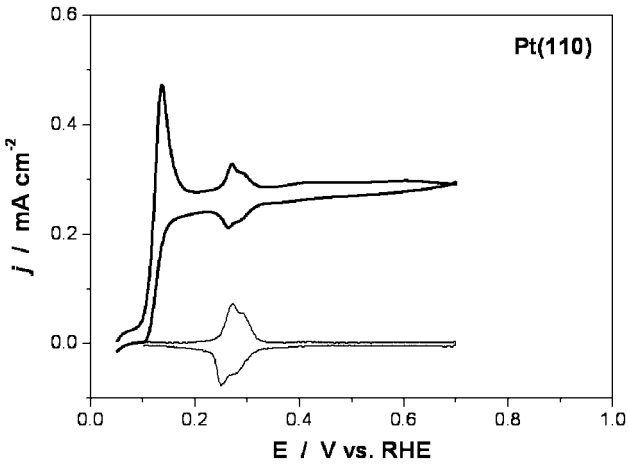

Figure 9. Voltammetry of hydrazine oxidation on a Pt(110) electrode in 0.1 M NaOH, 0.8 mM N_2H_4. Thin solid line is the Pt(110) blank voltammetry. Scan rate = 20 mV s^{-1}. Reproduced with permission from ref 66. Copyright 2008 Elsevier.

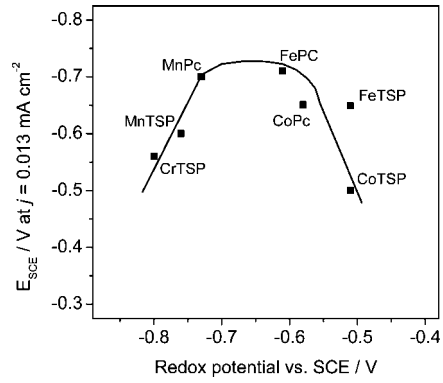

Figure 10. Potential leading to a hydrazine oxidation current of 0.013 mA cm^{-2} on a graphite electrode modified with different metal phtalocyanines plotted versus the redox potential of the corresponding phtalocyanine-modified electrode in the blank solution. Redox potential vs SCE. Redrawn from ref 82. Copyright 1986 Elsevier.

cyclic voltammetry, steady-state current measurements, and online electrochemical MS. As in acidic media, hydrazine oxidation on platinum in alkaline solutions is a diffusion-controlled process over a wide potential window. Pt(111), Pt(100), and Pt(110) show comparable activity, although in contrast to acidic media, Pt(110) is now the most active surface (see Figure 9). Note that the blank voltammetry of Pt(110) is "superimposed" on the hydrazine oxidation current, suggesting that hydrazine oxidation involves only weakly adsorbed intermediates. Molecular nitrogen was the only product of oxidation on all three surfaces, leaving the selectivity insensitive to the electrocatalyst structure. In alkaline media, no prepeaks are observed as on Pt(100) and Pt(111) in acidic media (compare Figure 9 to Figure 8), which is presumably related to the lower potentials at which hydrazine oxidizes to N_2, thereby not allowing for the stabilization of surface-bonded intermediates. Only on Pt(111) in alkaline media is there a visible prewave. When comparing the Tafel slopes between acidic and alkaline media, only that obtained for Pt(100) appears similar, 30 mV/decade in perchloric acid and 33 mV/decade in sodium hydroxide. Such a low Tafel slope would indicate the relative stability of a species such as N_2H_2(ads). Such a species has also been postulated as a reaction intermediate in the dehydrogenation of hydrazine on Pt(111) in UHV.[71]

White et al. have noted that, although in the gas phase the energy of the N−H bond (93.4 kcal mol^{-1}) is significantly higher than that of the N−N bond (38.4 kcal mol^{-1}), a significant cleavage of the N−N bond does not occur on Pt in UHV.[71] Based on the above discussion, we can draw a similar conclusion for the electrochemical environment. For the reaction under UHV conditions, this result may be explained by a Pt−NH_x bond being relatively weak compared with the Pt−H bond,[48,71] in addition to the stabilization of the N_2H_x species by having both nitrogens coordinated to a Pt surface atom.[71] Furthermore, as the extent of hydrazine dehydrogenation increases, the N−N bond becomes stronger. These factors likely play a role in keeping the N−N bond intact in electrochemical environments as well, and a N_2H_2 species with both nitrogens binding to Pt surface atoms has been postulated by Alvarez Ruiz et al.[65] The low-temperature conditions and the possibility of breaking of the N−H bond by electrochemical deprotonation (combined electron and proton transfer) would make cleavage of the N−N bond under electrochemical conditions an even less likely event.

3.2. Hydrazine Oxidation on Other Metal Electrodes

Very few systematic and comparative reports have appeared on the metal dependence of the hydrazine oxidation rate, although studies have been performed with Hg, Au, Ni, Pd, and Ag.[67,69,72−75] In acidic media, Alvarez-Ruiz et al.[65] have reported that gold may oxidize hydrazine, but at a much higher overpotential than platinum. Rhodium, on the other hand, is more active than platinum, with oxidation currents in perchloric acid starting below 0.2 V (vs RHE) on the most active Rh surface, Rh(100), which is about 0.1 V lower than those on Pt(100).[65] Kokkinidis and Jannakoudakis[76] have reported that the underpotential deposition of heavy metal ions such as Cd^{2+}, Tl^{+}, Cu^{2+}, Pb^{2+}, Bi^{3+}, and Ag^{+}, all have a pronounced inhibitive effect on the electrocatalytic activity of Pt for hydrazine oxidation.

3.3. Hydrazine Oxidation on Functionalized Electrodes

There is a vast body of electrochemical studies on the oxidation of hydrazine at modified electrodes, primarily devoted to its electroanalytical detection. Among the classes of electrode modifiers that have been studied in relation to hydrazine oxidation, are metal hexacyanoferrates (MHCF),[77−81] metal phtalocyanines (MPC),[82−84] and metal porphyrins (MP),[85,86] as well as organic and inorganic catalysts such as vitamin B12.[87] In many cases, the formation of N_2H_3 has been postulated to be rate-determining, based on Tafel slope measurements.

We would like to highlight one particularly systematic study on hydrazine oxidation here. Zagal and co-workers have published a number of papers on a series of metal phtalocyanine-modified graphite electrodes, in which various properties of the MPCs were varied.[82,88] The redox potential of the MPC is then correlated with the activity for hydrazine oxidation. Typically, it is found that such correlations show a volcano-type relationship (see Figure 10) with the most active phtalocyanines being the manganese, cobalt, and iron ones.[82] Volcano-type behavior here refers to a maximum observed in the catalytic activity as a function of a catalyst

property or reactivity parameter, in this case the catalyst redox potential, and typically results from applying Sabatier's principle to a two-step catalytic mechanism.[89] Similar correlations have been published in recent work by Zagal et al.,[83,88] though the plots appear more asymmetrical and scattered. The potentials in Figure 10 are on the saturated calomel electrode (SCE) scale and would for the most active catalysts correspond to an overpotential for hydrazine oxidation comparable to or somewhat higher than the most active platinum surface, i.e. ca. 0.4−0.5 V (in alkaline solution, to which Figure 10 applies). Moreover, it is found that active catalysts have a low Tafel slope of typically 40−60 mV/decade, whereas the least active catalysts have a high Tafel slope of ca. 120 mV/decade, which would suggest that good catalysts are able to stabilize the N_2H_3 or N_2H_2 adducts and poor catalysts are not. Zagal explains the observed volcano-type behavior in terms of a variation in the ability of the metal phtalocyanine to bind an extraplanar ligand such as the hydrazine molecule. Apparently, there is an optimum interaction of the frontier orbitals of the metal phtalocyanine with the frontier orbitals of the hydrazine when the adduct is formed. To study this interaction in more detail, Zagal and co-workers have performed DFT calculations of the interaction of hydrazine with Co(II) and Fe(II) phtalocyanines in the gas phase.[90,91] In contrast to what has been suggested for platinum, hydrazine, or rather N_2H_3, interacts with the metal center through only one nitrogen, that is, the one having only a single hydrogen. The DFT calculations showed that, with the successive dehydrogenation of the N_2H_3 adduct to N_2, the Fe metal center participates more strongly in the electron transfer than the Co metal center, as also reflected in the more favorable interaction energies (or reaction energies) for the various steps in the hydrazine oxidation at the Fe center as compared with the Co center. According to the authors, this could rationalize the high activity of Fe phtalocyanines for hydrazine oxidation as observed experimentally.

3.4. Hydrazine Oxidation by Enzymes

In microbial nitrogen conversions, hydrazine is rarely observed as an intermediate. However, in anammox bacteria,[56,92,93] already briefly mentioned in section 2.3, hydrazine is a key intermediate and hydrazine dehydrogenase is the enzyme that catalyzes reaction 12. Very little is known about the mechanism by which this enzyme catalyzes hydrazine oxidation. The electrons that become available in the process are supposed to be used for the oxidation of nitrite to hydroxylamine. Interestingly, the enzyme that normally oxidizes hydroxylamine, hydroxylamine oxidoreductase, is also capable of oxidizing hydrazine (see also section 4.4).

4. Hydroxylamine Oxidation and Reduction

4.1. Reactions of Hydroxylamine: Equilibrium Considerations

Hydroxylamine (HAM) is a key intermediate in the production of ε-caprolactam and a compound with various applications in industry, such as semiconductor etching. It may be obtained by the liquid-phase catalytic hydrogenation of nitric oxide or nitrate at carbon-supported platinum or palladium catalysts.[94,95] Although the relevance of electrochemistry for understanding the processes practiced in industry seems accepted, the application of electrochemical techniques is still not a very widespread approach.[9,94]

An important aim of the electrochemical research on HAM reactivity is the identification of the factors controlling the selectivity of nitric oxide or nitrate reduction to hydroxylamine. For this reason, HAM reduction and oxidation on platinum electrodes in acidic media, which are the conditions of interest from a practical point of view, are very relevant. Most of this section will be devoted to HAM reactivity on platinum, on which the majority of papers about hydroxylamine electrochemistry have appeared, but we will devote a few words to HAM reactivity on other metals and modified electrodes in section 4.3. Section 4.4 will briefly compare the properties of nature's catalysts for HAM conversion to the catalytic properties of platinum.

Thermodynamically speaking, hydroxylamine is one of the least stable compounds in the nitrogen cycle. It may exist in cationic and neutral form, depending on the solution pH:

$$NH_3OH^+ \leftrightarrows NH_2OH + H^+ \qquad pK_a = 5.8 \tag{20}$$

Because of the relatively low stability of hydroxylamine, a high reactivity is implied. Reduction to ammonia should be facile:

$$NH_3OH^+ + 2H^+ + 2e^- \leftrightarrows NH_4^+ + H_2O \qquad E^0 = 1.35\ \text{V (vs NHE)} \tag{21}$$

Possible oxidation products of hydroxylamine are

$$2NH_3OH^+ \leftrightarrows N_2O(g) + H_2O + 6H^+ + 4e^- \qquad E^0 = -0.05\ \text{V (vs NHE)} \tag{22}$$

$$NH_3OH^+ \leftrightarrows NO(g) + 4H^+ + 3e^- \qquad E^0 = 0.50\ \text{V (vs NHE)} \tag{23}$$

$$NH_3OH^+ + H_2O \leftrightarrows HNO_2 + 5H^+ + 4e^- \qquad E^0 = 0.64\ \text{V (vs NHE)} \tag{24}$$

$$2NH_3OH^+ \leftrightarrows N_2 + 2H_2O + 4H^+ + 2e^- \qquad E^0 = -1.87\ \text{V (vs NHE)} \tag{25}$$

From this list, we expect dinitrogen to be the thermodynamically preferred product of hydroxylamine oxidation, but as we will see below, it is typically not formed (at least not on platinum electrodes). This has, presumably, to do with the difficulty of breaking the N−O bond and making the N−N bond. The other products are all formed, as will be discussed below. Because of its low thermodynamic stability, hydroxylamine is also involved in a few pH-dependent homogeneous reactions. These reactions may play an important role in the kinetics and selectivity of the process. One prominent reaction of hydroxylamine is its disproportionation in acidic medium:

$$4NH_3OH^+ \rightarrow 2NH_4^+ + N_2O + 2H^+ + 3H_2O \tag{26}$$

It is not difficult to see from combining reactions 21 and 22 that reaction 26 should be a thermodynamically favorable process (again, N_2 formation should be even more favorable, but it seems that it is only formed to some extent in alkaline media[9]). Van de Moesdijk[9] has presented an extensive discussion of reaction 26 and has found that it may be catalyzed by platinum, though his experiments were carried out above room temperature (60 °C).

Another important reaction is that of hydroxylamine with nitrite or nitrous acid to yield nitrous oxide,[96] which is one of the common ways to produce N_2O (laughing gas):

$$NH_3OH^+ + NO_2^- \rightarrow N_2O + 2H_2O \quad (27)$$

$$HNO_2 \leftrightarrows H^+ + NO_2^- \qquad pK_a = 3.35 \quad (28)$$

Again, this is a thermodynamically favorable reaction, and it is a solution-phase reaction that does not require a catalyst to occur at appreciable rates.[96]

4.2. Hydroxylamine Oxidation and Reduction on Platinum

For the reasons outlined above, platinum has been the most studied electrode material for hydroxylamine oxidation, primarily in acidic media. Möller and Heckner[97−102] have carried out extensive measurements of hydroxylamine oxidation on platinum in both acidic and alkaline solution. In their mechanism, NOH (presumably in chemisorbed rather than dissolved form, although Möller and Heckner do not specify that) plays a central role. Hydroxylamine is first dehydrogenated to NOH, which dimerizes on the surface to $H_2N_2O_2$ (or $HN_2O_2^-$ in alkaline solution), which in turn serves as a precursor to N_2O, NO_2^-, or NO_3^- formation. In the past few years, the combination of electrochemistry with spectroscopic techniques such as DEMS and FTIR has thrown new light on the mechanism of hydroxylamine oxidation, and we will focus on these studies in the remainder of this section.

Karabinas et al.[103] presented a detailed study of hydroxylamine electrooxidation on polycrystalline Pt in neutral (buffered) and acidic solutions by combining voltammetry and online DEMS. In their mechanistic picture, the authors accepted the previously proposed dehydrogenation scenario that involves the formation of NOH species. The dimerization of NOH to hyponitrous acid ($H_2N_2O_2$) and its subsequent decomposition to N_2O and water were also supported. At potentials up to 0.7 V vs RHE (pH 6.5, phosphate buffer) NOH is partially oxidized to NO. Nevertheless, the NOH species was considered as the precursor in nitrite formation: the authors argued that as soon as Pt-OH species become available at the surface, NOH is oxidized directly to HNO_2. The reaction of HNO_2 with HAM (reaction 27) was held responsible for the formation of N_2O at potentials around 1 V. At higher potentials (ca. 1.1 V), nitrite is oxidized to nitrate. The oxidation involving Pt-OH species was perceived as the main reaction pathway in neutral solutions.

Piela and Wrona studied HAM oxidation at rotating platinum, gold, and glassy carbon disk electrodes in acidic media.[104] Only Pt showed a noticeable activity for HAM oxidation, which was explained by HAM adsorption on platinum and weak interaction of HAM with the other two electrode materials. The reaction was assumed to proceed via NHOH, NOH, and nitrite as intermediates, nitrate being the final oxidation product. The electrochemical transformations of HAM were shown to be accompanied by various homogeneous chemical reactions. For instance, the reaction of nitrite, a product of HAM oxidation, and HAM itself was shown to be an important source of N_2O accumulation in solution.

Our own laboratory studied the electrochemistry of HAM at polycrystalline platinum in acidic media using voltammetry, online DEMS, and in situ Fourier transform reflection−absorption infrared spectroscopy (FTIRRAS).[105] It was shown that the adsorption and reactions of HAM are essentially controlled by other species that interact strongly with the electrode surface (e.g., hydrogen, anions, strongly adsorbed intermediates). This explains the quite moderate current densities, for both HAM oxidation and reduction, observed between ca. 0 and 1 V vs RHE. Hydroxylamine is slowly reduced to ammonia in the H_{upd} region, though it becomes inhibited at high hydrogen coverages. The HAM electrooxidation is strongly influenced by the adsorption of its products, as well as by their transformations in solution. In disagreement with previous studies, adsorbed nitric oxide was considered to be the key intermediate in HAM oxidation, as deduced from both voltammetry and in situ infrared measurements. On the basis of a Tafel slope analysis, the following mechanism was proposed for HAM oxidation to NO(ads):

$$H_3NOH^+ \leftrightarrows H_3NOH^+(ads) \quad (29)$$

$$H_3NOH^+(ads) \leftrightarrows H_2NO(ads) + 2H^+ + e^- \quad (30)$$

$$H_2NO(ads) \rightarrow HNO(ads) + H^+ + e^- \qquad (rds) \quad (31)$$

$$HNO(ads) \rightarrow NO(ads) + H^+ + e^- \quad (32)$$

Nitric oxide forms an adlayer that is (electro)chemically stable in a wide potential window (ca. 0.4−0.8 V vs RHE, see also section 7.2.1 on NO reactivity), thus acting as a poison in HAM oxidation. At potentials corresponding to the oxidation of the platinum surface (above ca. 0.75 V), NO(ads) is oxidized to (adsorbed) nitrite. Finally, N_2O formation between ca. 0.4 and 1 V was shown to have multiple sources. Below 0.8 V, the most likely source of N_2O is the reaction between nitrite and HAM.

The electrochemistry of hydroxylamine at low-index single-crystal platinum surfaces (Pt(111), Pt(100), Pt(110)) in acidic media was studied using voltammetry, online electrochemical mass spectrometry, and in situ infrared spectroscopy.[106−108] Figure 11 shows the cyclic voltammetry of HAM at Pt(111) in perchloric acid. Starting at low potential, initially no reduction is observed due to a blocking by adsorbed hydrogen. Above 0.2 V, when the hydrogen coverage has become low enough, a strong reduction peak, E_{R4}, is observed owing to hydroxylamine reduction to ammonia. With more positive potential, the reduction current quickly changes into an oxidation current, leading to a peak E_{O1} at 0.45 V. From FTIR spectroscopy and reductive stripping voltammetry, it was concluded that this peak is related to the formation of an NO adlayer on the electrode. This layer blocks the electrode until a potential of ca. 0.9 V, when the adsorbed NO reacts with OH formed on the electrode to form HNO_2 (peak E_{O2}). Online electrochemical mass spectrometry shows the formation of N_2O and also significant amounts of NO at these positive potentials (see Figure 11). The formation of adsorbed NO is also evidenced in the cathodic return scan, in which the reduction peaks E_{R1}, E_{R2}, and E_{R3} are characteristic for the reductive stripping of an NO adlayer from Pt(111) (see section 7.2.1).

The reduction of hydroxylamine was found to be a structure-sensitive process, at least through a structure sensitivity of hydrogen adsorption. On Pt(111) and Pt(100), HAM reduction is completely blocked at potentials corresponding to a high H(ads) coverage (see Figure 11). On the other hand, a Pt(110) surface fully covered with H(ads) still

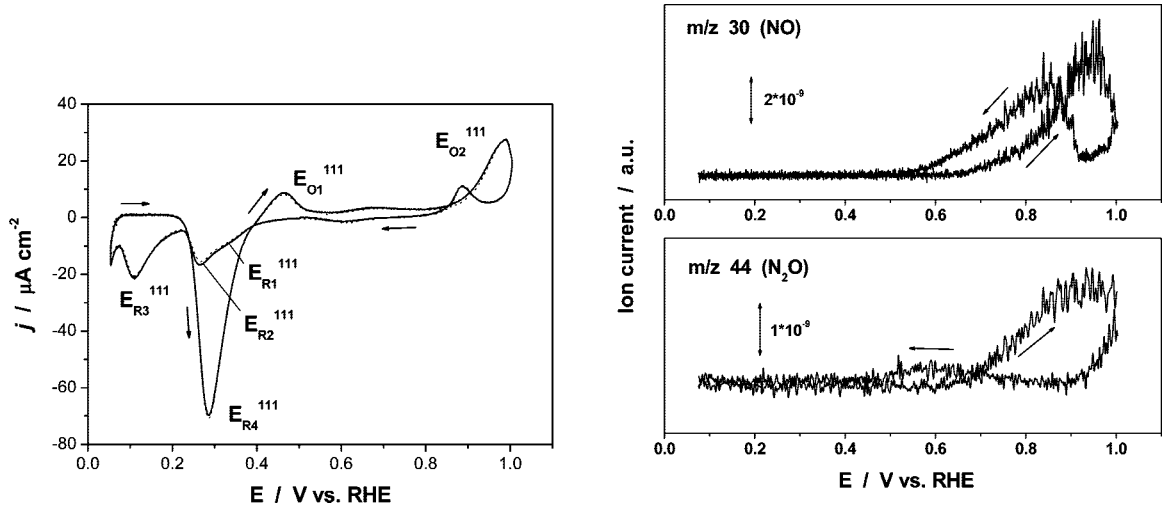

Figure 11. Voltammetry of hydroxylamine on Pt(111) (left panel) and the associated formation of NO and N_2O as detected by online electrochemical mass spectrometry (right panels). Twenty millimolar NH_3OH^+ in 0.5 M $HClO_4$, scan rate 5 mV s^{-1}, starting potential 0.06 V. Reproduced with permission from ref 108. Copyright 2006 Springer.

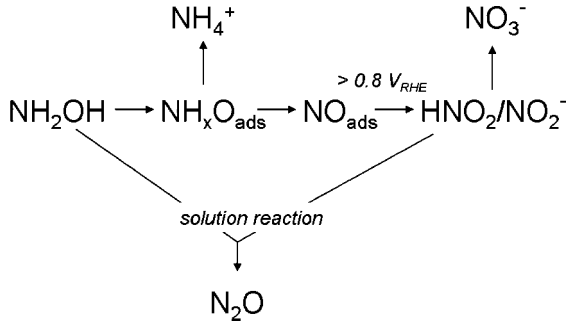

Figure 12. Schematic representation of the suggested mechanistic pathways during hydroxylamine oxidation and reduction on platinum.

shows considerable activity. No gaseous products were observed at potentials corresponding to the hydrogen UPD region. The observation that there seems to be an overlapping potential region for HAM reduction to ammonia and HAM oxidation to adsorbed NO is in agreement with thermodynamically favorable disproportionation of HAM (reaction 26). Experiments on Pt(100) show a reduction feature, which must be ascribed to an adsorbate with a higher oxidation state than HAM and which is also very similar to a reduction feature observed in the reductive stripping of NO from Pt(100).[107] This would suggest that reduction of hydroxylamine to ammonia may involve partial dehydrogenation of HAM, that is, an H_2NO or HNO intermediate would be formed first, which then acts as a precursor for the formation of both ammonia and adsorbed NO.

A schematic representation of the mechanism of HAM reduction and oxidation suggested by the experiments on Pt is given in Figure 12.

4.3. Hydroxylamine Reduction and Oxidation at Other Electrodes

There has been little work on the electrocatalysis of hydroxylamine reactivity on other metal electrodes than platinum. We briefly mentioned gold[104] (not active) in the previous section. The voltammetry of HAM on palladium is quite similar to that on platinum, except for a lower reduction activity of HAM on palladium.[109] Similar to hydrazine, however, there has been some work (though much less extensive than in the case of hydrazine) on hydroxylamine oxidation on modified electrodes, mainly in relation to its electroanalytical detection. Interestingly, the kind of modified electrodes used for the detection of hydroxylamine are very similar to those used for the detection of hydrazine, typically based on metal phtalocyanine (MPC) of metal hexacyanoferrate (MHCF) films on graphite electrodes.[110−115] Most papers conclude that the final product of the hydroxylamine oxidation on these electrodes is N_2O, and the mechanism typically suggested is similar to the mechanisms of Möller and Heckner[97−102] and of Karabinas[103] discussed above, namely, formation of NOH or HNO as intermediate, followed by dimerization to hyponitrous acid, which then quickly forms N_2O. Ebadi[111] realized that in order for this to happen, HNO would need to leave the metal compound and dimerize in solution, which we consider somewhat unlikely. Tafel slopes are normally close to 120 mV/decade, quite different from that observed for platinum (ca. 40 mV/decade). The possibility of the formation of N_2O from a reaction between NO_2^- and HAM (reaction 27) does not seem to have been suggested.

4.4. Comparison to Hydroxylamine Oxidoreductase

The structure and mechanism of the hydroxylamine oxidoreductase (HAO) enzyme from the autotrophic bacterium *Nitrosomonas europaea* has been studied extensively.[116,117] HAO is a large multiheme enzyme that catalyzes the oxidation of HAM to nitrite, NO_2^-. One of these hemes, the so-called P460, is considered to be the active site for the catalytic oxidation of HAM.[118] HAO is also capable of oxidizing hydrazine,[118] an interesting similarity with the modified electrodes used for hydrazine and HAM oxidation. Although the NO adduct has been detected spectroscopically after the addition of HAM to HAO, NO is not suggested to be part of the catalytic cycle.[119] Rather, the heme-bound HNO has been suggested to be the short-lived precursor to nitrite formation.[117] On the other hand, Fernández et al.[120] have recently studied a mechanism for HAM oxidation by HAO using DFT calculations in which the NO−heme adduct is a key intermediate for forming NO_2^-.

5. Nitrogen Reduction

The reduction of nitrogen to ammonia is one of the most remarkable reactions catalyzed by living organisms (a process known as nitrogen fixation) and a key reaction in the nitrogen cycle. From an industrial point-of-view, it is one of the most influential and successful high-temperature catalytic processes ever developed (the Haber−Bosch process). It is undoable to even briefly review here the process of biological nitrogen fixation; we refer the interested reader to textbooks.[121,122] As an important contrast to the mechanism typically considered for the Haber−Bosch process, involving N_2 dissociation leading to atomic nitrogen on the surface,[89] low-temperature nitrogen fixation is normally suggested to be initiated by proton−electron transfer steps forming hydrogenated dinitrogen species.[123,124]

Through the years, there have been several attempts at developing a low-temperature electrochemical process to reduce dinitrogen to ammonia.[125,126] None of these have been very successful in the sense that they would be viable replacements for the Haber−Bosch process or reach efficiencies close to that of nitrogen-fixating bacteria. Nevertheless, interesting results have been obtained, and it is worthwhile to selectively mention some of them. A paper by Marnellos and Stoukides[127] showed the possibility of the electrochemical synthesis of ammonia from dinitrogen at a palladium electrode in a solid-state electrochemical reactor at 570 °C with good yield. Kyriacou et al.[128] were able to carry out similar experiments at low temperature (100 °C) using a ruthenium cathode in 2 M KOH but with lower yield. Polyaniline-coated platinum is also able to reduce dinitrogen to ammonia, albeit at elevated N_2 pressures.[129] Very recently, Pospíšil et al.[130,131] reported the electrochemical conversion of N_2 to NH_3 at ambient pressure and 60 °C, mediated by a complex of C_{60} inside the molecular cavity of γ-cyclodextrin at a mercury electrode. The authors find that the activation of nitrogen takes place during the first two electron−proton transfer steps, with only a moderate overpotential. Although hydrazine was not detected during the experiments, it is assumed to be an intermediate in the reaction scheme.[131]

6. Nitrous Oxide Reduction

6.1. Nitrous Oxide Reduction on Transition-Metal Electrodes

The only known redox reaction involving the reaction of nitrous oxide, N_2O, is its reduction to N_2:

$$N_2O + 2H^+ + 2e^- \leftrightarrow N_2 + H_2O \qquad E^2 = 1.77\ \text{V (vs NHE)} \quad (33)$$

Ebert et al.[132] studied the electrocatalytic reduction of N_2O on polycrystalline and single-crystal platinum in sulfuric and perchloric acid solution. At all surfaces, N_2O starts to be reduced at ca. 0.5−0.6 V and goes through a maximum near 0.2−0.3 V after which the current drops to low values due to strong hydrogen adsorption. A typical example of Pt(111) in sulfuric acid solution is shown in Figure 13. Similar voltammetry was observed earlier by Johnson and Sawyer[133] during N_2O reduction on polycrystalline platinum in alkaline solution. Nitrous oxide is known to interact very weakly with Pt surfaces, explaining why adsorbed hydrogen is able to "poison" the N_2O reduction. However, Ebert et al. also suggested a catalytic role for adsorbed hydrogen. Since N_2O reduction was not observed on gold or iodine-protected platinum electrodes, they postulated the following mechanism:

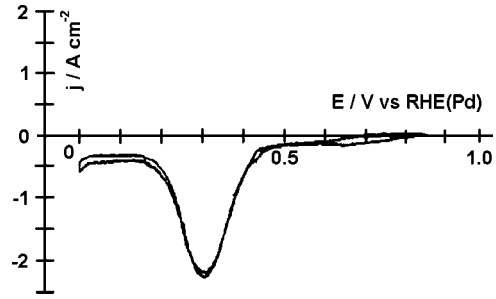

Figure 13. Voltammogram of Pt(111) in aqueous 0.1 M H_2SO_4, saturated with N_2O. Scan rate = 50 mV s^{-1}. Reproduced with permission from ref 132. Copyright 1989 Elsevier.

$$Pt{-}N_2O + Pt{-}H \rightarrow Pt{-}OH + N_2(g) \quad (34)$$

Since OH is unstable at the potentials considered, it quickly reacts with water and adsorbed hydrogen may be formed on the free Pt site. The rate of the reaction would be proportional to $\theta_H(1 - \theta_H)$, which would explain qualitatively the bell-shaped voltammetry. Attard et al.[134] took the work by Ebert et al.[132] a step further and studied N_2O on the other transition metal surfaces, iridium, rhodium, and palladium, in acidic media. All these metals show catalytic activity toward N_2O reduction, especially in the absence of specifically adsorbed anions. Palladium was found to be the most active metal in nitrous oxide reduction, even in the presence of sulfate anions. The authors were not able to reconcile their experiments with the model suggested by Ebert et al. but instead suggested the following mechanism:

$$N_2O + * \leftrightarrow N_2O(\text{ads}) \quad (35)$$

$$N_2O(\text{ads}) \rightarrow O(\text{ads}) + N_2(g) \qquad \text{slow irreversible reaction} \quad (36)$$

$$O_{ads} + 2H^+ + 2e^- \rightarrow H_2O + * \qquad \text{fast reaction} \quad (37)$$

The number of free sites is determined by the co-adsorption of species such as hydrogen, anions, and even OH and oxides, and this essentially determines the reaction rate. A reaction mechanism similar to reactions 35 and 36 has also been established for N_2O decomposition on metal surfaces in UHV, for instance, Pd(110).[135] According to DFT calculations, molecular N_2O binds weakly to Pd(110) (ca. 0.4 eV) by coordinating either with a single N to a Pd surface atom in a tilted fashion or in a bent horizontal fashion with N and O both binding to a Pd surface atom.[136] The latter configuration seems a more likely candidate as a precursor for reaction 36.

De Vooys et al.[137] studied the N_2O electroreduction on a series of metal surfaces in alkaline solution. Palladium was also found to be the most active metal in alkaline media, followed by platinum, rhodium, iridium, and ruthenium. Gold showed a very small activity for N_2O reduction.

6.2. Comparison to Nitrous Oxide Reduction by Enzymes

The reduction of nitrous oxide to dinitrogen is an essential step in the denitrification process because it is the final hurdle to be taken in the full reduction of nitrate to harmless

dinitrogen. Nitrous oxide reductase (N2OR) typically consists of two copper clusters, one used for electron transfer and the other one, the so-called Cu_Z center containing four copper atoms, acting as the catalytic center.[138] Solomon et al.[139] have suggested that N_2O binds to the Cu_Z center by coordinating the nitrogen and the oxygen to two copper atoms in the Cu_Z center in a kind of bridging mode, similar to one of the stable binding modes calculated for N_2O on Pd(110).[136]

7. Nitric Oxide Reduction and Oxidation

7.1. Reactions of Nitric Oxide: Equilibrium Considerations

Nitric oxide is an essential molecule in the nitrogen cycle. It was Science's "Molecule of the Year" in 1992 ("NO news is good news"),[140] and one of the very few molecules that has featured as the title and main topic of a novel.[141] NO serves as a messenger molecule in cells, and therefore there is great interest in developing electrochemical sensors for NO. The adsorption and reactivity of NO on transition metal surfaces in an electrochemical environment are also of considerable technological and scientific interest. Nitric oxide is an important intermediate or reagent in a series of environmentally and industrially important processes, such as nitrate and nitrite reduction (see sections 8 and 9) or the liquid-phase catalytic hydrogenation of nitric oxide or nitrate to hydroxylamine.[9,10,94] Electrochemical detection of nitric oxide[142] requires a thorough understanding of the electrochemistry of NO. Furthermore, adsorption, reduction, and oxidation of NO are relatively simple processes, which are in many respects attractive for fundamental investigations in electrochemical surface science and electrocatalysis and for comparison with similar processes at solid−gas and solid−liquid interfaces.

As with the other nitrogen compounds, the thermodynamically preferred reaction of NO is its conversion to N_2:

$$2NO(g) + 4H^+ + 4e^- \leftrightarrows N_2(g) + 2H_2O \qquad E^0 = 1.678\ \text{V (vs NHE)} \quad (38)$$

However, in practice, other products such as N_2O, hydroxylamine, and ammonia are also formed:

$$2NO(g) + 2H^+ + 2e^- \leftrightarrows N_2O(g) + H_2O \qquad E^0 = 1.59\ \text{V (vs NHE)} \quad (39)$$

$$NO(g) + 4H^+ + 3e^- \leftrightarrows NH_3OH^+ \qquad E^0 = 0.49\ \text{V (vs NHE)} \quad (40)$$

$$NO(g) + 6H^+ + 5e^- \leftrightarrows NH_4^+ + H_2O \qquad E^0 = 0.836\ \text{V (vs NHE)} \quad (41)$$

Oxidation products of NO are nitrous acid, nitrite, and nitrate:

$$NO(g) + H_2O \leftrightarrows HNO_2 + H^+ + e^- \qquad E^0 = 0.99\ \text{V (vs NHE)} \quad (42)$$

$$NO(g) + H_2O \leftrightarrows NO_2^- + 2H^+ + e^- \qquad E^0 = 1.202\ \text{V (vs NHE)} \quad (43)$$

$$NO(g) + 2H_2O \leftrightarrows NO_3^- + 4H^+ + 3e^- \qquad E^0 = 0.96\ \text{V (vs NHE)} \quad (44)$$

Nitrous acid is involved in two relevant acid−base equilibria:

$$NO_2^- + H^+ \leftrightarrows HNO_2 \qquad pK_a = 3.35 \quad (45)$$

$$HNO_2 + H^+ \leftrightarrows NO^+ + H_2O \qquad K_a = 2 \times 10^{-7} \quad (46)$$

The equilibrium potential for the redox reaction of the nitrosonium NO^+ ion and NO was reported by Plieth:[17]

$$NO^+ + e^- \leftrightarrow NO(g) \qquad E^0 = 1.45\ \text{V (vs NHE)} \quad (47)$$

7.2. Nitric Oxide Reduction on Platinum

The reduction of nitric oxide on platinum has been studied in two different ways: reductive stripping of strongly surface-bonded NO in the absence of NO in solution and continuous NO reduction, that is, in the presence of NO in solution. We will discuss the results of these two different methods in two separate sections.

7.2.1. Nitric Oxide Reductive Stripping

The reductive stripping of NO pre-adsorbed on a polycrystalline platinum electrode in acidic solution was studied by Gootzen et al.[143] and De Vooys et al.[144] using a combination of electrochemical techniques, DEMS, and FTIR. Reductive stripping of NO typically starts below 0.3 V, and DEMS measurements show no formation of N_2O or N_2. Gootzen et al.[143] excluded the formation of NH_3OH^+ because RRDE measurements did not detect any electroactive species on the ring. Ammonium is therefore the only product of NO adsorbate stripping in acidic solution. The Tafel slope of 50 mV/decade measured by de Vooys et al.[144] prompted them to suggest an EC mechanism, but more accurate values of the Tafel slope were obtained on single-crystal Pt (vide infra). De Vooys et al. suggested a similar mechanism for NO adsorbate stripping in alkaline solution.

More detailed insight into the mechanism of NO adsorbate reduction has been obtained with platinum single-crystal electrodes. From ultrahigh vacuum (UHV) studies, it is well-known that the site occupation, coverage, and structure of NO adlayers depend sensitively on the platinum surface structure. Generally, multifold coordination is preferred at low to moderate coverage. NO adsorbs molecularly on Pt(111) and Pt(110) surfaces under UHV conditions at low to near-room temperatures.[145−149] Adsorption of NO on Pt(100) seems to be (at least partially) dissociative even close to room temperature.[150] Breaking of the N−O bond strongly depends on the surface structure and is often the rate-determining step in NO reduction on platinum in UHV and is believed to occur prior to hydrogenation and to require free neighboring site(s).[145] Nevertheless, several UHV studies of NO reduction on Pt(111) at near-room temperature suggested the formation of an HNO intermediate.[151,152] At high NO coverage, linearly bonded NO may coexist with multifold-coordinated NO, as is the case for NO adsorption on Pt(111),[153−155] or a site switch to a lower coordination site may occur, as for NO adsorption on Pt(110).[148] On Pt(100), NO occupies a site between the atop and bridge site,[156] the "side-on" configuration being a possible stable configuration at low coverage values according to recent DFT calculations.[157]

Adsorption of NO on platinum single-crystal surfaces under electrochemical conditions, as well as on other platinum-group metals (e.g., Pd, Rh, Ir), turns out to be very

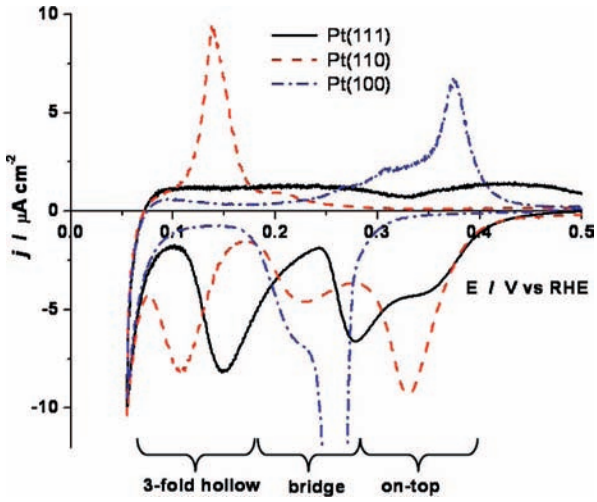

Figure 14. Stripping voltammograms for the reduction of saturated NO adlayers at low-index single-crystal platinum surfaces. Ammonia is the main product under the given experimental conditions. The terms "on-top", "bridge", and "3-fold hollow" refer to the adsorption site of NO species, which are stripped off in the indicated potential ranges. Experimental conditions: 0.5 M H_2SO_4; starting potential 0.5 V; 2 mV s^{-1}. Oxidative scans (positive currents) show that after NO stripping, all three surfaces are "clean".

similar to NO adsorption on platinum in UHV, as deduced from the in situ FTIRRAS studies.[158−161] Strong similarities in the vibrational spectral fingerprints imply identical site occupation and adlayer structure in UHV and in an electrochemical environment. Furthermore, the saturation coverage of the NO adlayer on single-crystal Pt electrodes estimated from a charge analysis of their reductive stripping agrees well with the NO coverages observed under UHV conditions. For example, the saturation NO coverages on Pt(111), Pt(100), and Pt(110) electrodes are 0.4−0.5 monolayer (ML),[158,162] 0.5 ML,[158,163] and 0.7−1 ML,[162] respectively. The measured value of the coverage can be affected by the nature of electrolyte. The variation on Pt(110), for instance, is explained by a saturation NO coverage of ca. 1 ML in perchloric acid (identical to the coverage under UHV conditions) and of ca. 0.7 ML in sulfuric acid.[162]

Reductive stripping of NO adlayers from single-crystal platinum electrodes has been the subject of a number of recent studies. NO adlayers can be formed by exposing the electrode surface to a dilute acidic solution of nitrite;[158] these layers are (electro)chemically stable in a wide potential window. Figure 14 compares the stripping voltammetry of a saturated NO adlayer from the three low-index planes, Pt(111), Pt(110), and Pt(100).[107,164] The various papers agree that ammonium is the final product of NO stripping, with no detectable formation of gases and hydroxylamine. Note from Figure 14 that the stripping takes place in the potential region between 0.1 and 0.4 V and that there is not a surface that is clearly more active in reducing the NO adlayer than the other surfaces. Although the reduction has a lower overpotential (at ca. 0.4 V vs RHE) on Pt(110) and Pt(111) compared with Pt(100), full reduction of the adlayer is favored on Pt(100) and Pt(110) (at ca. 0.18 V). Beltramo and Koper have studied the effect of steps on a series of stepped platinum single-crystal electrodes, Pt[n(111)×(110)], and also could not demonstrate a clear effect of the step density on the catalytic activity.[162] Therefore, they concluded that NO reductive stripping is not a strongly structure-sensitive reaction. This situation is in sharp contrast with the oxidative stripping of adsorbed CO, another important model reaction in electrocatalysis, for which steps act as the active sites as evidenced from their strong effect on both the voltammetry and chronoamperometry curves.[165,166]

On the basis of the Tafel slope of ca. 40 mV/decade observed on Pt(111), Pt(554), and Pt(110), Beltramo and Koper[162] proposed the following mechanism for NO(ads) reduction to ammonia:

$$NO(ads) + H^+ + e^- \leftrightarrows HNO(ads) \quad \text{equilibrium} \quad (48)$$

$$HNO(ads) + H^+ + e^- \rightarrow H_2NO(ads) \quad \text{rds} \quad (49)$$

$$H_2NO(ads) + 4H^+ + 3e^- \rightarrow NH_4^+ + H_2O \quad \text{fast} \quad (50)$$

The first two steps of the reaction are assumed to be combined proton−electron transfers, involving hydronium ions from solution. In agreement with the latter assumption, NO(ads) reduction on Pt(110) (and partly on Pt(111)) occurs at potentials at which the hydrogen coverage on clean Pt(110) is negligible.[162] Additionally, the reductive stripping of NO adlayers on polycrystalline platinum shows a 59 mV/pH dependence, in agreement with the electrochemical mechanism of NO(ads) hydrogenation.[144] The HNO and H_2NO intermediates are suggested on the basis of their lower energy (in vacuum) compared with NOH and HNOH species.[144,162] Note that in mechanism 48−50, the breaking of the N−O bond occurs after the rate-determining step. This mechanism gives a natural explanation for the lack of structure sensitivity of the NO reduction, because the rate-determining step involves only proton and electron transfer, whereas the real surface-sensitive step, that is, N−O bond breaking, occurs at a later stage. This electrochemical mechanism of NO reduction and bond breaking is in strong contrast with the situation in UHV, as discussed above, where N−O bond breaking is generally considered rate determining and hydrogenation happens on the dissociated fragments.

In a recent combined voltammetric and FTIR study, Rosca et al.[107,164] studied the relationship between the NO adsorption modes (atop, bridge, 3-fold hollow) and the reactivity of the NO species. Specifically, the voltammetric features observed for NO(ads) reduction on Pt(100), Pt(111), and Pt(110) were found to be determined by the reduction of NO molecules occupying different adsorption sites and not by consecutive reaction steps. As an example, we show in Figure 15 the FTIR spectra obtained during a slow voltammetric stripping of NO from Pt(110). At the most positive potentials, starting at 0.7 V, a broad band at 1710−1770 cm^{-1} corresponds to NO adsorbed in an atop fashion to the Pt(110) surface. The band red shifts with more negative potential in agreement with earlier work.[161] Between 0.5 and 0.4 V, where the NO adlayer starts to be reduced, the band loses intensity and a new band appears at ca. 1600 cm^{-1}. The latter band corresponds to NO bonded in bridged fashion to the Pt(110) surface (this band is not observed at high potentials and high coverage presumably due to a phenomenon called "intensity stealing", whereby a lower energy vibration loses intensity to a nearby higher energy vibration due to the strong interaction at high coverage). At 0.3 V, the broad feature corresponding to atop-bonded NO has disappeared, and only the feature due to bridge-bonded NO is observed. At this potential, there is a minimum in the stripping voltammogram (see Figure 14, dashed red line), which strongly suggests that the first stripping peak is related to the stripping of NO

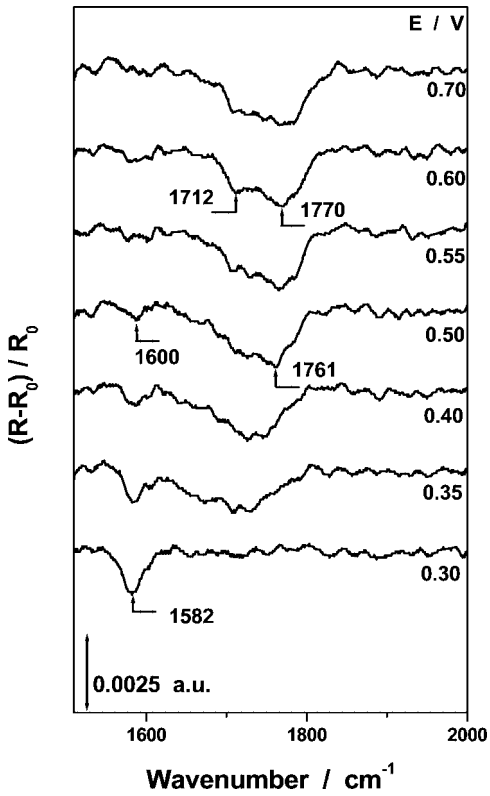

Figure 15. The potential difference infrared spectra acquired at a Pt(110) electrode covered with a pre-adsorbed NO adlayer. Numbers indicate the applied electrode potential on the RHE scale. Experimental conditions: 0.1 M $HClO_4$ (in D_2O), reference potential 0.1 V, p-polarized light. Reproduced with permission from ref 164. Copyright 2005 American Chemical Society.

adsorbed on atop sites. During the second smaller peak (0.2−0.3 V), the spectral band corresponding to the bridge-bonded NO disappears, suggesting that this peak is related to the stripping of bridge-bonded NO. Very similar observations were made for Pt(111) (see the solid curve in Figure 14), where the first peak (0.25−0.4 V) is the stripping of atop-bonded NO and the second peak (0.1−0.2 V) is the stripping of 3-fold-bonded NO. On Pt(100) there is only one stripping peak (see dash-dot blue line in Figure 14) and there is also only one type of NO observed in the FTIR, namely, bridge-bonded NO.[107] Comparing the voltammetric profiles for the reductive stripping of saturated NO adlayers at Pt(111), Pt(100), and Pt(110) surfaces, we conclude that the linearly bonded (on-top) NO molecules are the most reactive (react at more positive potentials), followed by bridged NO, and then 3-fold-coordinated NO species. The potential regions in which linearly bonded NO, on the one hand, and multifold-coordinated NO molecules, on the other hand, react on different surfaces are very much the same. Significantly, this trend has not been observed for NO reactions in UHV and is, therefore, unique to NO reduction under electrochemical conditions. In a recent surface-enhanced infrared reflection−absorption spectroscopy (SEIRAS) study on the reduction of adsorbed NO on polycrystalline Pt film electrode, Nakata et al.[167] found that atop NO has a higher rate constant for reduction than bridge-bonded NO, essentially confirming the above observations on single-crystalline electrodes.

The mechanism of NO reductive stripping on Pt(100) seems to be different from that on Pt(111) and Pt(110). First of all, the Tafel slope is higher than on the other two low-index planes, that is, 60 vs 40 mV/decade. Second, whereas on Pt(111) and Pt(110) it is possible to strip the NO adlayer partially by reversing the scan at any given potential during the scan, such an experiment leads to complete NO adlayer stripping on Pt(100), with the reduction continuing after scan reversal. This implies that the NO reduction becomes irreversible at a very early stage of the reaction. Together with the higher Tafel slope, we have ascribed this effect to an early N−O bond breaking, basically after the first proton transfer:

$$NO(ads) + H^+ + e^- \leftrightarrows HNO(ads) \qquad \text{equilibrium} \qquad (51)$$

$$HNO(ads) \rightarrow HN(ads) + O(ads) \qquad \text{rds} \qquad (52)$$

This high propensity of the Pt(100) surface to break the N−O bond is in agreement with the strong tendency for N−O bond breaking on Pt(100) under UHV conditions.

Cuesta and Escudero[168] have studied the stripping voltammetry of adsorbed NO on a Pt(111) electrode modified with prechemisorbed cyanide. Cyanide forms a $(2\sqrt{3} \times 2\sqrt{3})R30^0$ structure on Pt(111), consisting of hexagonally packed arrays each containing six CN molecules adsorbed atop on a hexagon of Pt atoms surrounding a free Pt atom, with a surface coverage of 0.5 ML. NO may be irreversibly adsorbed on such a surface, presumably on a free Pt atom. Compared with NO(ads) reduction on clean Pt(111), only one stripping peak is observed, namely, that corresponding to atop-bound NO, as also confirmed by FTIR spectroscopy. Interestingly, the Tafel slope corresponding to the stripping peak on Pt(111)/CN is ca. 60 mV/decade compared with ca. 40 mV/decade for unmodified Pt(111). Cuesta and Escudero suggested that this Tafel slope is due to the formation of H(ads) on the Pt(111)/CN surface, followed by a rate-determining chemical step between H(ads) and NO(ads). The minimal critical ensemble for the reduction of linear-bonded NO on Pt(111) was concluded to consist of two adjacent Pt atoms.

In addition to stripping voltammetry, Rosca and Koper have studied the mechanism of the reduction of adsorbed NO on Pt(111) and Pt(110) using the potential step method.[169] The current transients for NO reduction on Pt(111) show a hyperbolic (t^{-1}) rather than an exponential decay at moderate to high coverage. By comparison with kinetic modeling,[169,170] the hyperbolic decay was ascribed to (i) first-order kinetics in the NO coverage and (ii) strong lateral interactions between the NO adsorbates. The current transients for the reductive stripping of saturated NO adlayers on Pt(110) surface (with on-top NO as the reactive species) showed a potential-dependent maximum, which indicates a second-order kinetics in the NO coverage. This second-order kinetics was attributed to the necessity of having a neighboring free site next to the NO binding site required for breaking the N−O bond, suggesting that at high coverage N−O bond breaking may become rate determining, although this is difficult to establish experimentally. Such an ensemble for NO bond breaking is well-known from UHV surface science studies of NO reduction on single-crystal Pt. For the reduction of the saturated NO adlayers on the Pt(111) surface (with atop NO or 3-fold NO or both as the reactive species), the apparent first-order kinetics was explained by the availability of the required reaction site (sites) at all coverages, since the saturation coverage on Pt(111), ca. 0.5 ML, is much lower than that on Pt(110), ca. 1 ML. The second-order kinetics on Pt(110) is then related to the high initial

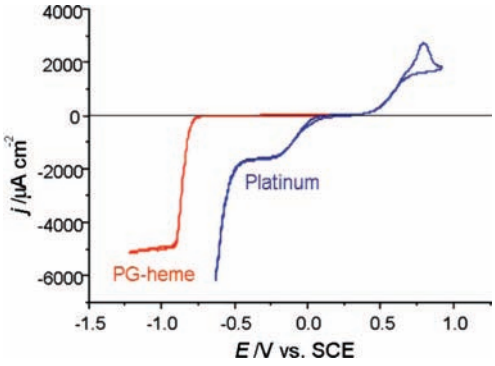

Figure 16. Polarization curves of adsorbed hemin on pyrolytic graphite (PG-heme, red curve) and platinum (blue curve) in saturated NO solution. Both PG and platinum rotating disk electrodes have the same geometry. Buffer 0.5 M phosphate, pH 7.0; scan rate 50 mV/s; disk rotation rate 2940 rpm.

coverage (1 ML); indeed, as the initial coverage on Pt(110) is lowered, the maximum disappears.[169]

7.2.2. Continuous Nitric Oxide Reduction on Platinum

The continuous reduction of nitric oxide (i.e., with NO in solution) on a polycrystalline platinum electrode in sulfuric acid has been studied by various authors.[143,144,171−176] Figure 16 illustrates that the polarization curve shows two reduction waves: a diffusion-limited wave at more positive potential (−0.5/−0.2 V vs SCE for pH = 7 in Figure 16, at ca. 1.0 V overpotential; the polarization curve in acidic solution looks the same), in which nitrous oxide is the only reduction product, and a wave at higher overpotential (below −0.5 V vs SCE), essentially the potential range in which the NO adsorbate reduction takes place, in which hydroxylamine, ammonium, and nitrous oxide are the main products. Depending on potential, the selectivity for hydroxylamine can reach up to 70%.[173]

Based on the Tafel slope of the wave in which N_2O is produced, which is close to 120 mV/decade, the first electron transfer step is considered to be rate determining. The pH dependence suggests that a proton is involved in the rate-determining step as well. Early studies on polycrystalline platinum[38,40,41,51] suggested that the formation of the N−N bond would result from dimerization of NOH (or HNO) adsorbed intermediates, followed by a decay of the resulting dimer to N_2O.[172−174] However, since the reduction of adsorbed nitric oxide does not yield any N_2O, de Vooys et al.[144] proposed an alternative mechanism for N_2O formation:

$$NO(ads) + NO(soln) + H^+ + e^- \rightarrow HN_2O_2(ads) \quad \text{rds} \tag{53}$$

$$HN_2O_2(ads) + H^+ + e^- \rightarrow N_2O + H_2O \quad \text{fast} \tag{54}$$

The formation of a (protonated) NO dimer as a precursor to N_2O formation is the key feature of this mechanism. This hyponitrous acid-like intermediate is formed only when NO is present in solution, in agreement with the observation that the formation of N_2O is first order in the concentration of NO in solution and also with the fact that in the absence of NO in solution, no N_2O is formed. In relation to the heterogeneous catalysis of NO reduction, the relevance of the formation of NO dimers on metal surfaces in UHV or in the gas phase has been the topic of a number of recent papers.[177−179]

In the low-potential reduction wave, both ammonia and hydroxylamine are observed as reduction products,[178] whereas in the same potential region the reduction of the NO adsorbate gives only ammonia.[143,144] Foral and Langer[180,181] studied the effect of pre-adsorbed sulfur on nitric oxide reduction on platinum and found that sulfur strongly inhibits ammonia formation and increases the selectivity for hydroxylamine. They explained this by an ensemble effect similar to that discussed in section 7.2.1 for NO reduction on Pt(110): NO needs neighboring free sites to dissociate and form ammonia. The density of these ensemble sites is lower in the presence of pre-adsorbed sulfur. A similar argument can be applied to rationalize the formation of hydroxylamine in the continuous reduction of NO: the high coverage of NO in the case of continuous NO reduction reduces the likelihood of N−O bond breaking.

7.3. Nitric Oxide Reduction on Other Metals

7.3.1. Nitric Oxide Reductive Stripping

The Alicante group has investigated the adsorption and reduction of NO on rhodium single-crystal electrodes in the absence and presence of HNO_2 in solution.[182,183] As with platinum, the NO adlayer was obtained by decomposition of nitrous acid in solution. On Rh(111), a saturation coverage close to 0.5 was found, similarly to the Rh(111)/NO system in UHV.[184] At low potential, in the hydrogen region just positive of the NO reduction stripping peak, the saturated NO layer shows a single IR band corresponding to bridge-bonded NO, also in agreement with the situation in UHV. At more positive potential, an additional peak is observed, attributed to atop-bonded NO. For NO adlayers with coverages lower than the saturation value (without HNO_2 in solution), the FTIR data suggest that co-adsorbed oxygen induces a change in the structure of the adlayer at positive potentials. Reductive stripping of NO on Rh(111), Rh(100), and Rh(110) occurs in a similar potential window as it does on platinum, typically displays multiple stripping peaks, and is mostly completed in a single potential scan, although some adsorbates seem to remain adsorbed on Rh(100) even after a low-sweep-rate potential excursion. From the stripping charges, assuming that ammonia is the only reduction product (formation of N_2O was not observed in the FTIR experiments), the saturation coverages on Rh(100) and Rh(110) were estimated to be close to 1 ML. In UHV, Villarubia and Ho[185] observed two types of NO on Rh(100), depending on NO coverage: a lying down or highly inclined species and a vertically adsorbed species. At low coverages, only the former is observed. The Rh(100)/N−O IR band reported by Rodes et al.[183] under electrochemical conditions at high NO coverage seems to correspond to the vertically adsorbed species. Interestingly, FTIR experiments failed to detect adsorbed nitric oxide on Rh(110), which could possibly be related to dissociation of the adsorbed NO molecule. There has as yet been no kinetic study of the NO stripping voltammetry on Rh nor any attempt to relate the observed multiple stripping peaks to different adsorption modes, as has been done for single-crystal Pt.[164] Nevertheless, it seems likely that an increased propensity for NO to dissociate on Rh, as compared with Pt, will play a role in the mechanism.

Nitric oxide adsorbed on Pd single crystals has been characterized spectroscopically by Weaver and co-workers.[161,186]

Alvarez et al.[187] have also studied the reduction of the NO adlayer, albeit on palladium-covered single-crystal platinum electrodes, which nevertheless give IR spectra for adsorbed NO similar to those observed for bulk Pd crystals. For these Pd_{ML}/Pt electrodes, they observed potential-dependent FTIR spectra that are qualitatively similar to those illustrated in Figure 15 for NO on Pt(110): as the NO adlayer is progressively reduced on a Pd/Pt(111) electrode, atop-bonded NO disappears and is replaced by multibonded NO. However, in the voltammetry, only a single stripping peak is observed. No gaseous products are formed during the stripping of NO from these electrodes.

Yan et al.[188] recently published a combined ATR−SEIRAS and voltammetry study of reductive NO stripping on a polycrystalline ruthenium electrode. In the absence of HNO_2 in solution, a single band located at 1840−1874 cm^{-1} was observed, the lower wavenumber corresponding to the lowest potential at which the band was still observed (0.1 V vs RHE), just before the NO reductive stripping from Ru was completed. By comparison with vibrational features of NO on clean Ru(0001) and NO co-adsorbed with atomic oxygen on Ru(0001) in UHV,[189] the authors concluded that the spectral band observed under electrochemical conditions is due to atop-bonded NO co-adsorbed with oxygen, termed an υ_2(O)-NO species. This co-adsorption of NO and oxygen on Ru is not surprising given the high oxophilicity of the Ru surface. As a result, the reductive stripping current observed on Ru is due to both oxide reduction and reduction of adsorbed NO. Importantly, NO chemisorbed on clean Ru sites without co-adsorbed oxygen, which according to the UHV results should have a distinct vibrational signature, was never observed in the ATR−SEIRAS experiments.[188]

7.3.2. Continuous Nitric Oxide Reduction on Transition Metal Electrodes

Colucci et al.[190] and De Vooys et al.[191] studied the continuous reduction of NO on a series of transition-metal electrodes. Many of the mechanistic features observed for NO reduction on Pt in acidic media, also apply to other metals such as ruthenium, iridium, rhodium, palladium, and gold. In particular, all transition metals show a high selectivity to N_2O at high potentials and a high selectivity to NH_4^+/NH_3 at low potentials, with N_2 formed at intermediate potentials (see Figure 17). However, a coinage metal such as gold forms mainly N_2O and very little NH_4^+/NH_3 and N_2, although we note that, in contrast with the results shown in Figure 17, DEMS experiments by Suzuki et al.[192] indicate that on single-crystal gold electrodes in alkaline solution, continuous reduction of NO leads mainly to hydroxylamine. As with platinum, in the absence of NO in solution, no N_2O is observed on Rh and Ru electrodes, which strongly suggests that the "dimerization mechanism" (reactions 53 and 54) also applies to other metals. Moreover, the experiments indicate that N_2O is the precursor for the formation of N_2, through reaction 33. This conclusion is also supported by the observation that the metal that is the most *active* in reducing N_2O to N_2, that is, palladium (see section 6.1), is also the most *selective* in reducing NO to N_2.[191,193]

Figure 18 gives the general scheme for the reduction of NO on platinum and other electrodes, emphasizing again the difference between NO(ads) and NO(soln) (NO in solution) reduction and the role of surface blocking (adsorbate coverage) in breaking the N−O bond. A main characteristic of the scheme is also that N_2 is formed through the reduction

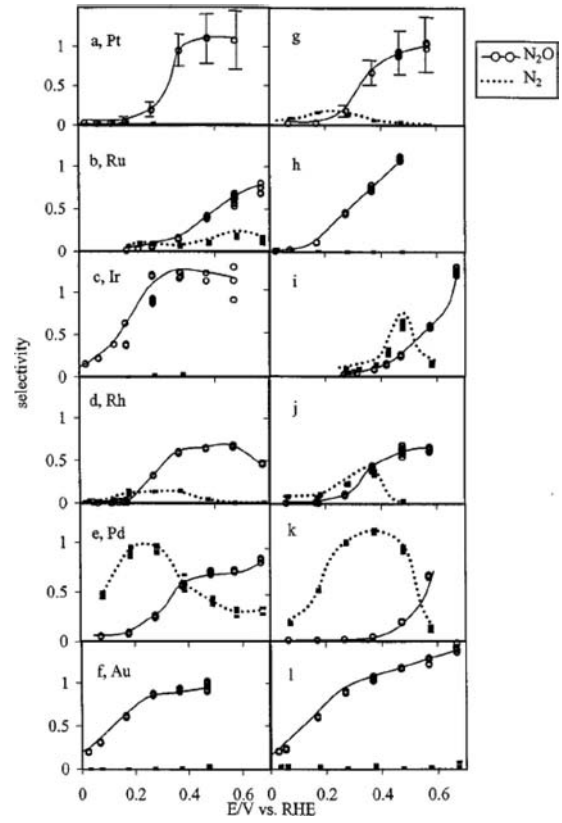

Figure 17. Selectivity of the continuous reduction of NO on various metal electrodes. Solution saturated with NO: (a−f) 0.1 M H_2SO_4; (g−l) 0.1 M KOH; (a, g) Pt; (b, h) Ru; (c, i) Ir; (d, j) Rh; (e, k) Pd; (f, l) Au. Solid lines and filled circles, selectivity for N_2O; dotted lines and rectangles, selectivity for N_2. A value of 1 on the selectivity axis corresponds to 100%. Reproduced with permission from ref 191. Copyright 2001 Elsevier.

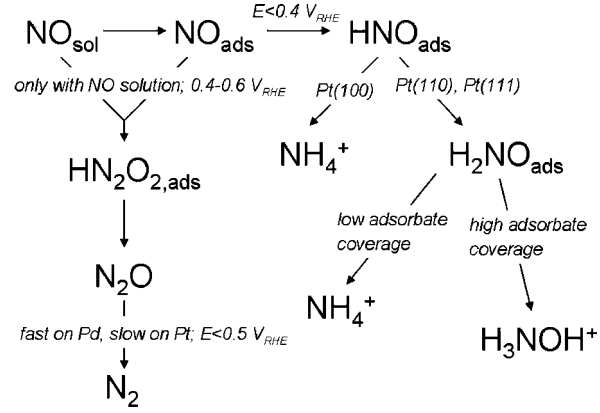

Figure 18. General scheme for the reduction of nitric oxide on metal electrodes.

of N_2O and not through the recombination of 2N(ads). In fact, the scheme in Figure 18 suggests that N(ads) plays no significant role in NO reduction under electrochemical conditions.

7.4. Nitric Oxide Reduction on Functionalized Electrodes

Functionalized electrode surfaces have been employed extensively for NO reduction. In many of these studies, the catalytically active compound is a macrocycle supposed to resemble the catalytic site of a NO reducing enzyme (nitric oxide reductase) or a protein containing a

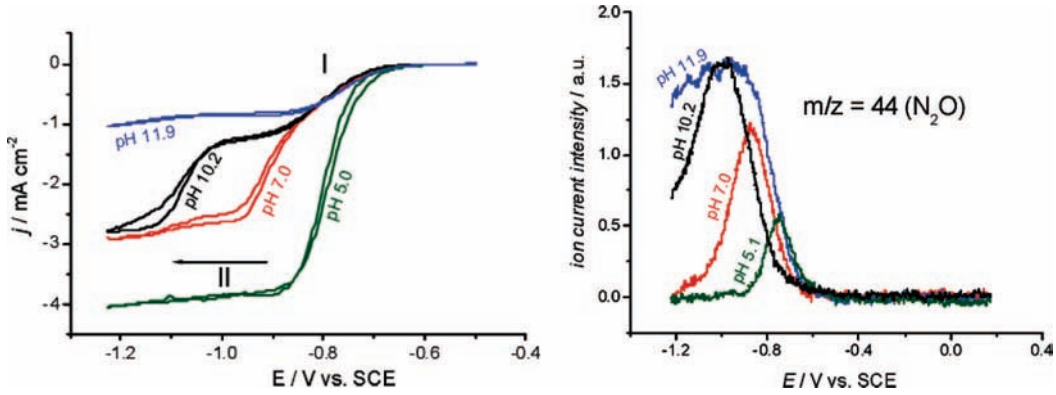

Figure 19. The pH dependence of the reduction of nitric oxide at pyrolytic graphite electrodes modified with heme−DDAB films. Left panel, voltammetry at a rotating disk electrode at various pHs; potential scan rate 50 mV/s; disk rotation rate 16 rps. Right panel, online electrochemical mass spectrometry measurements on a nonrotating electrode with continuous bubbling of NO. Reproduced with permission from ref 201. Copyright 2005 American Chemical Society.

site that is able to bind NO, such as myoglobin. In addition to the electrocatalytic properties of such modified electrodes, the main reason for the investigation of these functionalized electrodes is their potential use as sensitive biosensors for the detection of NO, which is an important messenger molecule in living organisms.[140]

One of the most widely investigated functionalized electrodes is iron protoporphyrin IX immobilized on graphite. The reason that iron protoporphyrin IX, better known as heme, is regarded as an interesting catalytic compound is because of its role as the active site in many enzymes, including the fungal and bacterial nitric oxide reductases.[5,194] Iron protoporphyrin IX can be easily immobilized on graphite electrodes either by direct adsorption[195−198] or by incorporation in different types of films.[199−201] Apart from graphite, iron protoporphyrin IX can be relatively easily immobilized on gold.[202,203] It has not only been investigated for the reduction of nitric oxide[198,201,204] but also for many other reactions, including nitrite reduction (see section 8) and oxygen reduction.[205,206]

Figure 16 compares the catalytic activity for the reduction of NO of a pyrolytic graphite electrode with directly adsorbed hemin to a platinum electrode, both in buffered solution of pH = 7.[198] The PG−heme is clearly less active. More interestingly, it also exhibits a remarkably different selectivity pattern compared with Pt as deduced from online electrochemical mass spectrometry (OLEMS, a technique very similar to DEMS but using a small inlet tip and only a single pump), from rotating ring-disk voltammetry, and from a comparison of the mass-transport limited currents on PG−heme and Pt. At pH = 7, the sole product observed in the reduction wave at −1.2/−0.8 V (vs SCE) is hydroxylamine, whereas no N_2O is observed, which is the product of the diffusion-limited reduction of NO on Pt. Also the reduction of NO pre-adsorbed on PG-heme, that is, without NO in solution, yields only hydroxylamine as the product.[198]

The selectivity of the continuous NO reduction on PG−heme changes with pH and with the way in which heme is immobilized. This is illustrated in Figure 19, which shows the NO reduction voltammograms for four different pH values for heme immobilized in a didodecyldimethylammonium bromide (DDAB) film. On such electrodes, not only hydroxylamine but also nitrous oxide is observed as a product. The main product observed at pH = 5.0 is hydroxylamine, but a small amount of N_2O is observed in the OLEMS at the foot of the reduction wave (note that the conditions of this experiment are different from those in Figure 16, because Figure 19 pertains to a heme−DDAB film). At pH = 7.0, the main product is still hydroxylamine, but the amount of N_2O is increasing. At pH = 10.2, the first reduction wave (−1.0/−0.7 V) corresponds to the formation of N_2O and the second reduction wave (<−1.0 V) to formation of hydroxylamine. At pH = 11.9, hydroxylamine production has been suppressed, and now N_2O is produced with 100% selectivity. Clearly the reaction products of NO reduction on these heme-modified graphite electrodes are formed by two different pathways: one to hydroxylamine and one to nitrous oxide. Which pathway occurs depends primarily on pH: hydroxylamine formation shows a pH dependence of 60 mV/pH, whereas N_2O production is pH independent, the latter observation being in interesting contrast to continuous NO reduction on Pt, which exhibits a "regular" 60mV/pH dependence (see section 7.2.2). Other conditions, such as NO concentration and immobilization method of the heme, also influence the preferred pathway at a given pH and potential.

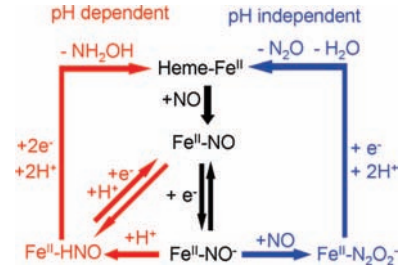

Figure 20. Mechanisms of the two pathways for NO reduction observed for immobilized heme on pyrolytic graphite.

The rate-determining steps in both mechanisms have been determined from Tafel slope measurements.[198,201,204] For the mechanism leading to hydroxylamine the Tafel slope of ca. 60 mV/decade suggests that an electrochemical equilibrium is followed by a rate-determining chemical step. Given the pH dependence, it was suggested that the rate-determining chemical step could be the proton transfer from $Fe^{II}-NO^-$ to $Fe^{II}-HNO$. For the mechanism leading to nitrous oxide, a Tafel slope of ca. 110 mV/decade suggests that the first electrochemical step is rate-determining, that is, the formation of $Fe^{II}-NO^-$. The overall mechanistic scheme for NO reduction on PG−heme is given in Figure 20.

Apart from iron protoporphyrin IX, nitric oxide reduction has also been investigated on other iron porphyrins[207,208] and iron phthalocyanines.[209] In the case of nitric oxide reduction on iron phthalocyanines immobilized on graphite, hydroxy-

lamine was found as the major product with almost no ammonia formation,[209] presumably by a mechanism similar to NO reduction on PG−heme. NO reduction by cobalt porphyrins and cobalt phthalocyanines has also been investigated,[210,211] but no in situ techniques have been employed to determine the reaction products. From long-term electrolysis experiments of NO reduction on a glassy carbon electrode modified with vitamin B_{12} (a cobalt phthalocyanine), Vilakazi and Nyokong observed the formation of both hydroxylamine and ammonia. Su et al.[212] also reported the formation of both ammonia and hydroxylamine during NO reduction on a Prussian blue film modified electrode in prolonged electrolysis experiments. The difficulty with such long-term electrolysis experiments is that they cannot be easily related to the short-term voltammetry experiments. It is conceivable that hydroxylamine is produced at the electrode and then slowly reduced further to ammonia. For instance, hydroxylamine was observed to have a low but nonzero reduction activity on PG−heme.[198] It is therefore likely that during prolonged electrolysis experiments, this surface would also produce measurable amounts of ammonia. Also the role of solution-phase reactions cannot be easily excluded, and they are likely to be important when hydroxylamine is involved (see section 4). Hence, due to a lack of detailed comparative in situ experiments, it is as yet unclear to what extent the nature of the adsorbed molecular catalyst affects the activity and selectivity of the reaction and on which time scale.

The reduction of NO has also been studied using electrodes with immobilized heme enzymes and heme proteins.[213−215] However, recent experiments indicate that the specific method that was employed to immobilize these heme proteins, namely, incorporation in a film of DDAB, may result in the release of the heme group from these proteins.[201,216,217] Denatured heme protein films can therefore be regarded as equivalent to films with immobilized heme, the NO reduction properties of which were discussed above (see Figure 19). Bearing this in mind, myoglobin− and hemoglobin−DDAB film-modified graphite electrodes have been studied for NO reduction,[213,215] with N_2O as the main reduction product (from prolonged electrolysis[213]). Cytochrome P450nor, a fungal enzyme, which catalyzes the reduction of NO to N_2O, was immobilized in the same way and studied for its nitric oxide reduction activity.[214] Also on this electrode, N_2O was the main product observed.

7.5. Nitric Oxide Oxidation

7.5.1. Nitric Oxide Oxidative Stripping on Platinum

The oxidation of adsorbed NO on platinum depends sensitively on the Pt surface structure. On all Pt surfaces, apart from Pt(111), NO adlayer oxidation is irreversible. On Pt(111), an interesting redox couple is found, first reported by Ye and Kita[218] and later studied by a number of other groups.[162,183,219,220] At a scan rate of 50 mV/s, NO(ads) on Pt(111) in perchloric acid exhibits an oxidation peak at 1.05 V (vs RHE) and a corresponding reduction peak at 0.65 V in the negative-going scan. Following the original suggestion of Ye and Kita, Beltramo and Koper have proposed that this redox couple involves a monoelectronic reaction between NO(ads) and HNO_2(ads) with some simultaneous adsorption of OH(ads):

$$\mathrm{NO(ads)} + (1 + x)\mathrm{H_2O} \leftrightarrows \mathrm{HNO_2(ads)} + x\mathrm{OH(ads)} + (1 + x)\mathrm{H^+} + (1 + x)\mathrm{e^-} \quad (55)$$

The fact that the charge corresponding to the redox feature depends on the electrolyte (i.e., perchloric vs sulfuric acid) may be explained by the formation of co-adsorbed OH, which will be blocked by the adsorbing sulfate anion. On more open surfaces, such as Pt(110), the redox couple cannot be resolved, presumably due to further oxidation of platinum and of the surface-bonded HNO_2 to nitrate. Nevertheless, full oxidation of NO(ads) appears very difficult: on polycrystalline Pt, NO(ads) reduction features were still observed even after 15 min of oxidation at 1.4 V (vs RHE).[221] We are not aware of any detailed studies of NO(ads) oxidation on other electrode materials than Pt.

7.5.2. Continuous Nitric Oxide Oxidation

De Vooys et al.[221] have studied the continuous electrooxidation of NO on platinum and a number of other metal electrodes. In general, NO oxidation experiments suffer from poor reproducibility because of the extensive oxidation of the electrode surface at the potentials at which NO is oxidized. With NO in solution, the oxidation of NO takes place in two oxidation waves, as was first shown by Dutta and Landolt.[222] From rotating disk electrode experiments, the first wave (0.9−1.1 V vs RHE) corresponds to the oxidation of NO to HNO_2, whereas the second wave (>1.1 V vs RHE) corresponds to the further oxidation to nitrate. The oxidation of NO to HNO_2 requires only a low overpotential and seems to occur with a very similar rate on most electrode materials, including gold.[221] The second oxidation wave, which represents the further oxidation of HNO_2 to NO_3^-, does also not appear to be very metal dependent, although it is inhibited by the formation of surface oxides (see section 8.3.1). In general, however, since NO oxidation occurs on platinum and gold with very similar rates, the conclusion seems justified that NO oxidation is a relatively fast reaction that does not require a strong interaction with the metal electrode.

7.5.3. Nitric Oxide Oxidation on Functionalized Electrodes

The oxidation of nitric oxide has been studied on electrodes modified with various different macrocycles, such as metalloporphyrins,[223,224] metallophtalocyanines,[225] and other compounds.[212,226] Although the list of cited references is far from complete, we have not been able to find many studies that give a clear insight into the mechanism of nitric oxide oxidation on these modified electrodes. Su et al.[212] suggested that on a Prussian blue (iron hexacyanoferrate) modified electrode, nitrate is the main oxidation product. Most likely, NO_2^- will feature as an intermediate.

7.6. Comparison to Nitric Oxide Reduction by Enzymes

The literature on the enzymology of nitric oxide is vast, especially in connection with NO reductases. A good relatively recent review is the paper by Wasser et al.[5] In this section, we will mainly focus on a comparison between heme-modified electrodes (because heme is the active center

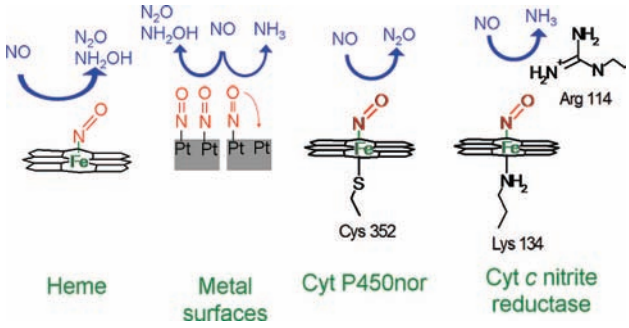

Figure 21. Schematic overview of the selectivity of NO reduction by immobilized heme, metal electrodes, cytochrome P450nor, and cytochrome *c* nitrite reductase

in many NO reductases), platinum, and two representative NO reductases, following two recent papers from our group.[201,204]

When comparing NO reduction on immobilized heme groups with NO reduction on metal catalysts such as platinum (see Figure 21), one may conclude that both catalysts resemble each other in the sense that they can reduce NO via two pathways, one leading to N_2O and another leading to NH_2OH/NH_3. The most striking difference is that, at low pH, immobilized heme selectively reduces NO to NH_2OH without producing NH_3, whereas platinum reduces NO to a combination of NH_2OH and NH_3. This is in line with the low reactivity of immobilized heme groups in NH_2OH reduction and the higher activity of platinum toward NH_2OH reduction. It has been suggested that NH_3 formation is only possible if the oxygen of ligated NO has space to tilt and can coordinate to a second metal site (Figure 21).[177] If this is not possible, as for immobilized heme, the bond between oxygen and nitrogen is insufficiently weakened and therefore no NH_3 can be formed.

When immobilized heme is compared to NO reducing heme enzymes, it can be concluded that similar to the fungal nitric oxide reductase cytochrome P450nor[227−230] and the bacterial nitric oxide reductases[231,232] immobilized heme can reduce NO to N_2O. The mechanism of NO reduction by immobilized heme resembles that of cytochrome P450nor. The enzyme also has an $Fe^{II}-NO^-$ or $Fe^{II}-HNO$ intermediate that reacts with a second NO molecule to form N_2O. The major difference is that in the case of cytochrome P450nor, the electron donor is NADH, which probably provides a direct hydride transfer to $Fe^{III}-NO$.[233] This hydride transfer is equivalent to the transfer of two electrons and one proton and hence avoids the formation of the stable $Fe^{II}-NO$ intermediate. This could be one of the reasons why this enzyme is able to reduce NO at much more positive potentials than immobilized heme. Mechanistic comparison to bacterial NO reductases is more difficult, since a nonheme iron plays an important role in the catalytic mechanism of these enzymes. It has been suggested that in nitric oxide reductases, the enzyme binds the two nitric oxide molcules to a heme and a nonheme iron in order to generate N_2O.[5]

The pathway leading to NH_2OH observed for immobilized heme resembles the NO reduction pathway observed for cytochrome *c* nitrite reductase,[234,235] an enzyme that can reduce both nitrite and nitric oxide to ammonia. However, a major difference is the fact that cytochrome *c* nitrite reductase reduces NO to NH_3 and not to NH_2OH as immobilized heme does. The reason for this difference in selectivity is probably related to the interaction of NO with other protein residues surrounding the heme group or the influence of the lysine residue that is in a trans configuration with respect to NO (see Figure 20). Apparently, these residues sufficiently weaken the NO bond to allow for bond breaking. This is also reflected in the fact that NO-bound heme proteins have lower stretching frequencies (around 1600 cm^{-1})[236,237] than iron porphyrins with bound NO (1670−1680 cm^{-1})[238] and the fact that cytochrome *c* nitrite reductase readily reduces hydroxylamine.[239]

We conclude that the mechanisms by which immobilized heme reduces NO resemble the mechanisms observed for NO reducing enzymes. In contrast to the enzymes, immobilized heme can reduce NO via two different pathways, whereas the enzymes only catalyze one specific pathway. This is related to the fact that the enzymes are optimized for their specific pathway, which is not the case for immobilized heme.

8. Nitrite and Nitrous Acid Reduction and Oxidation

8.1. Reactions of Nitrite and Nitrous Acid: Thermodynamic Considerations

Nitrite is one of the more reactive compounds in the nitrogen cycle. It has a significant toxicity for humans, being the main cause of blue baby syndrome. As was mentioned in section 7.1, in acidic solutions, nitrite is involved in two acid−base equilibria, reactions 45 and 46, leading to the formation of nitrous acid and NO^+. Under typical reaction conditions, say 10 mM in an acid of pH = 1, this implies 9.9 mM HNO_2, 0.1 mM NO_2^-, and 2×10^{-7} mM NO^+. However, in highly acidic solution, the concentration of NO^+ becomes significant, and it is likely the main electroactive form of nitrite.[247] This implies that nitrite may take on three different electroactive forms: NO_2^- in alkaline and neutral media, HNO_2 in moderately acidic media, and NO^+ in highly acidic media. We will discuss below that this has important consequences for the reactivity, both at an electrode and in solution.

As far as the electrode reactions are concerned, the thermodynamically preferred product of nitrite reduction is N_2:

$$2NO_2^- + 8H^+ + 6e^- \leftrightarrow N_2(g) + 4H_2O \qquad E^0 = 1.520 \text{ V (vs NHE)} \quad (56)$$

However, other products such as NO(g), N_2O(g), hydroxylamine, and ammonia are also formed:

$$NO_2^- + 2H^+ + e^- \leftrightarrow NO(g) + H_2O \qquad E^0 = 1.202 \text{ V (vs NHE)} \quad (57)$$

$$2NO_2^- + 6H^+ + 4e^- \leftrightarrow N_2O(g) + 3H_2O \qquad E^0 = 1.396 \text{ V (vs NHE)} \quad (58)$$

$$NO_2^- + 6H^+ + 4e^- \leftrightarrow NH_3OH^+ + H_2O \qquad E^0 = 0.673 \text{ V (vs NHE)} \quad (59)$$

$$NO_2^- + 8H^+ + 6e^- \leftrightarrow NH_4^+ + 2H_2O \qquad E^0 = 0.897 \text{ V (vs NHE)} \quad (60)$$

The oxidation product of nitrite is nitrate:

$$NO_2^- + H_2O \leftrightarrow NO_3^- + 2H^+ + 2e^- \qquad E^0 = -0.835 \text{ V (vs NHE)} \quad (61)$$

In all these reactions, NO_2^- may be replaced by HNO_2, with the appropriate correction for the standard equilibrium potentials.

Especially in acidic media, HNO_2 may also take part in various solution-phase reactions, and these reactions should be kept in mind when discussing HNO_2 electrochemistry in acidic media. One reaction already discussed is reaction 27, the reaction between nitrite and hydroxylamine leading to the formation of nitrous oxide:

$$NH_3OH^+ + NO_2^- \rightarrow N_2O + 2H_2O \quad (27)$$

Another well-known reaction is that between nitrite and ammonium, already alluded to in section 2.3 as reaction 10, giving rise to the formation of N_2:

$$NO_2^- + NH_4^+ \rightarrow N_2 + 2H_2O \quad (10)$$

This is a spontaneous solution reaction responsible for the decomposition of ammonium nitrite solutions. For detailed discussions and references on the pH dependence and the mechanism of this reaction, see the paper by Harrison et al.[240] and references therein.

Furthermore, solutions of HNO_2 decompose. Park and Lee[241] have published a detailed account of the aqueous-phase decomposition of nitrous acid according to

$$2HNO_2(aq) \leftrightarrows NO(aq) + NO_2(aq) + H_2O \quad (62)$$

Another disproportionation reaction often found in the HNO_2 reduction literature is

$$3HNO_2 \leftrightarrows HNO_3 + 2NO + H_2O \quad (63)$$

These disproportionation reactions are most prominent at high HNO_2 concentration and depend on solution agitation.

The simplest oxidized form of nitrite is nitrogen dioxide, NO_2, a redox couple that has a standard equilibrium potential of

$$NO_2^- \leftrightarrows NO_2 + e^- \qquad E^0 = 0.78 \text{ V (vs NHE)} \quad (64)$$

At low temperature, the reddish-brown gas NO_2 converts to the colorless gas dinitrogen tetroxide N_2O_4, which disproportionates in aqueous solution to nitrous acid and nitric acid:

$$2NO_2 \leftrightarrows N_2O_4 \quad (65)$$

$$N_2O_4 + H_2O \leftrightarrows HNO_2 + HNO_3 \quad (66)$$

The latter reaction has a very high equilibrium constant, 8.5×10^8, but in highly acidic solutions of nitric and nitrous acid, some N_2O_4 and NO_2 may be formed. Nitrogen dioxide may be further oxidized to the nitronium ion, NO_2^+:[242]

$$NO_2 \leftrightarrows NO_2^+ + e^- \qquad E^0 = 1.56 \text{ V (vs NHE)} \quad (67)$$

Again, it has been suggested that this ion forms in highly acidic solutions and may be reduced to NO^+.

Note that reaction 63 follows from the more elementary reaction 62 by combining it with reactions 65 and 66.

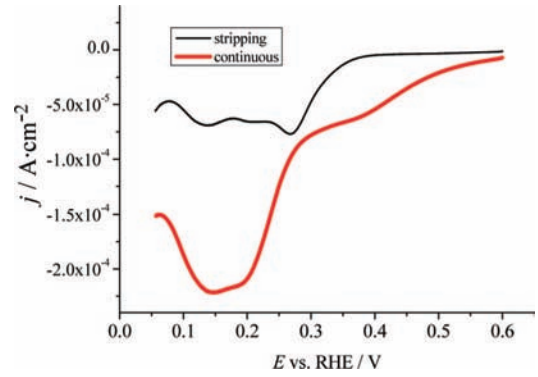

Figure 22. Continuous reduction of nitrous acid (ca. 0.8 mM $NaNO_2$ in 0.1 M $HClO_4$) on a polycrystalline platinum electrode in comparison with the stripping current of a NO-saturated platinum electrode. Scan rate = 20 mV/s. No stirring of the solution.

8.2. Nitrite and Nitrous Acid Reduction

8.2.1. Nitrite Reduction on Platinum Electrodes

Gadde and Bruckenstein[243] studied the reduction of HNO_2 on a rotating platinum disk electrode in 0.1 M perchloric acid solution. Figure 22 shows the voltammetry of a ca. 1 mM HNO_2 solution at a platinum electrode in perchloric acid. The thin line in Figure 22 is the stripping current due to the reduction of the NO adlayer that is formed because of the interaction of Pt with the HNO_2 solution, in the absence of HNO_2 in solution. Essentially two HNO_2 reduction features are observed: a prewave at lower overpotentials (ca. 0.6−0.3 V vs RHE) and a main wave at higher overpotential (<0.3 V vs RHE). As Figure 22 illustrates, this main wave corresponds to the potential region in which the NO adlayer is being reduced. According to Gadde and Bruckenstein,[243] the current in the main wave satisfies the Koutecky−Levich relationship, implying that it is diffusion limited. However, recent measurements in our own laboratory have shown deviations from ideal Koutecky−Levich behavior, which suggest the importance of taking into account HNO_2 decomposition.[262] Measurements with the rotating ring-disk electrode suggested that the only electroactive reaction product produced at low Pt disk potential (ca. 0.02 V vs RHE), that is, in the diffusion-limited main wave, was hydroxylamine. Using online electrochemical mass spectrometry, Gadde and Bruckenstein detected the formation of N_2O from ca. 0.6 V, with a maximum in the prewave region. Some NO was detected, but it was ascribed to the decomposition of HNO_2 (reaction 62). No N_2 was detected in the online mass spectrometry. From bulk electrolysis experiments, the product distribution at low potential (0.02 V vs RHE) was found to be 60% hydroxylamine, 20% nitrous oxide, and 20% ammonia. Some N_2 was found in the bulk electrolysis experiments, but again it was ascribed to a solution-phase reaction between nitrous acid and ammonia. One of the reactions held responsible for the formation of N_2O was the reaction between hydroxylamine and nitrite (reaction 27).

Nishimura et al.[244] studied the same reaction on a porous platinum electrode in sulfuric acid with DEMS. In contrast to the results reported by Gadde and Bruckenstein, they observed the formation of NO and N_2 in the DEMS during the voltammetry, simultaneously with the formation of N_2O. They concluded that N_2 was formed in an electrochemical reaction, not by solution-phase chemical reactions. Bae et al.[245] were able to resolve N_2O formation during nitrite

reduction on Pt using FTIR spectroscopy and found a good correlation with the experiments by Nishimura et al.[244] They suggested that the DEMS results of Nishimura et al. may be interpreted as N_2 being formed electrochemically from N_2O through reaction 33. Da Cunha and Nart[246] studied nitrite reduction on a platinum electrode with 10% rhodium with DEMS and FTIR and obtained similar results to Nishimura et al., that is, the evolution of NO and N_2O, but no N_2. They also observed a spectroscopic feature at ca. 1820 cm^{-1}, which they ascribe to a dinitrosyl species (i.e., dimeric NO), presumably as a precursor to N_2O formation.

Rodes et al.[159] have studied HNO_2 reduction on platinum single-crystal electrodes. No strong structure sensitivity was observed, which is in agreement with their observation that HNO_2 is strongly controlled by the reduction of adsorbed NO, which is also not a strongly structure-sensitive reaction (see section 7.2.1). There have been no detailed studies into the products formed during HNO_2 reduction on single-crystal platinum electrodes.

The electrocatalytic reduction of nitrite in highly concentrated acidic media has been reported in a number of papers.[247−250] Under these conditions, it is necessary to consider the additional acid−base equilibrium, reaction 46. Heckner and Schmid[248] investigated the reaction at a Pt electrode in concentrated perchloric acid (2−9 M), and established the key role of the nitrosonium ion (NO^+) as the actual electroactive species.

Van der Plas and Barendrecht[250] performed a detailed study of the electrochemical characteristics of nitrite reduction at a Pt RRDE in 7.5 M sulfuric acid. The RDE voltammetry shows three reduction waves, which are ascribed to three different reaction products. The reduction wave at most positive potential (starting at ca. 1.0 V vs RHE) corresponds to the reduction of the nitrosonium ion NO^+:

$$NO^+ + e^- \rightarrow NO(g) \quad (68)$$

In the second reduction wave, another one-electron reaction (per NO) takes place:

$$2NO(g) + 2H^+ + 2e^- \rightarrow N_2O(g) + H_2O \quad (69)$$

In the third reduction wave, hydroxylamine is the main product, yielding overall four electrons from NO^+:

$$NO^+ + 4H^+ + 4e^- \rightarrow NH_3OH^+ \quad (70)$$

Van der Plas and Barendrecht suggested that the last two reactions share a common adsorbed intermediate, namely, HNO (they do not specify whether it is adsorbed on Pt), which is at variance with the NO reduction mechanism suggested in section 7.2.2. It was established only after the work by Van der Plas and Barendrecht that adsorbed NO or adsorbed HNO alone cannot produce N_2O; the solution species is essential. We note that Snider and Johnson[247] have argued in favor of another mechanism in highly acidic solution, in which the second reduction wave is due to the reduction of N_2O_3, which is formed from NO and NO_2 in solution.

The reduction of nitrite in alkaline solutions is expected to be simpler compared with that in acidic media owing to the absence of the various above-mentioned solution-phase reactions. Furthermore, additional interest in the nitrite reduction in basic media is motivated by the occurrence of nitrite in alkaline low-level nuclear waste.[251] Horanyi and Rizmayer[252] studied the reduction of nitrite on polycrystalline Pt in 1 M NaOH. The reduction starts at ca. 0.4 V (vs RHE), shows a small plateau or minimum in current near 0.25 V, and seems to be partially inhibited by adsorbed hydrogen at potentials below 0.1 V. From an electrolysis experiment, the overall reaction was formulated as a six-electron reduction to ammonia. Wasmus et al.[28] observed NH_3, N_2, NO, and N_2O during the reduction of nitrite on a Pt-black electrode in 0.5 M NaOH using DEMS, but surprisingly the current in their voltammetry hardly differs from the blank electrolyte. Ye et al.[253] investigated the reduction of nitrite at low-index Pt single-crystal electrodes in alkaline solutions (pH = 13). A high structure sensitivity for the reduction of nitrite was reported, with a large reduction current for Pt(100) at ca. 0.3 V (vs RHE) and much smaller reduction currents for Pt(110) and Pt(111). From electrolysis experiments, it was concluded that the overall reduction of nitrite on Pt(100) followed a six-electron reaction to give ammonia as the main product.

From the above, it can be concluded that the nitrite reduction on platinum in alkaline solution, where ammonia has been suggested as the main or even only product, seems to be different from that in acidic solution, where N_2O and hydroxylamine are the dominant reaction products. Due to a lack of detailed studies, especially as a function of pH and in alkaline media in particular, the reasons for these discrepancies are as yet unclear. This issue is currently under investigation in our laboratory.[262]

8.2.2. Nitrite Reduction on Other Metal Electrodes

There have been a few studies on nitrite reduction on transition metals other than platinum. Rodes et al.[159] have studied the HNO_2 reduction on single-crystal rhodium electrodes and noted that the reduction typically starts at less positive potentials than on platinum. Brylev et al.[254] observed only ammonia as the product of nitrite reduction on electrodeposited Rh in neutral chloride-containing solution. Alvarez et al.[187] studied HNO_2 reduction on Pd-modified platinum electrodes and reported the detection of adsorbed NO and dissolved NO and N_2O during reduction using FTIR and DEMS. The catalytic activity of Pd seems somewhat lower than that of Pt. De Vooys et al. found that palladium is more active than copper for nitrite reduction in acidic media and mainly produced N_2.[255] Yan et al.[188] studied HNO_2 on Ru with ATR−SEIRAS and observed three different kinds of NO species on the surface during reduction, namely, (1) the υ_2(O)−NO species as already alluded to in section 7.3.1 since it was also observed during NO adlayer reduction, which corresponds to a NO linearly bonded to Ru with co-adsorbed oxygen; (2) an υ_1(O)−NO species corresponding to multicoordinated NO co-adsorbed with oxygen; (3) an atop-NO without co-adsorbed oxygen at very negative potentials. The reduction of the surface-bonded NO is observed before the complete reduction of the Ru surface oxides.

Nitrite reduction on Cu single-crystal electrodes was studied by Gewirth et al.,[256] but we will postpone discussion of those results to section 9.2.2 where nitrite reduction will be compared with nitrate reduction on the same Cu surfaces.

In alkaline media, silver and copper show some activity for nitrite reduction, but the activity is generally lower than that for nitrate or hydroxylamine reduction.[257] Ammonia was suggested to be the final product. On palladium, Pletcher et al.[258] speculated about the role of adsorbed H in reducing

nitrite. Finally, De et al.[259−261] have performed rather extensive studies on nitrite reduction on iridium-modified carbon fiber electrodes. Iridium is typically a less active catalyst for nitrite reduction than Pt,[262] an observation that we would tend to ascribe to the role of the oxide layer.

8.2.3. Nitrite Reduction on Functionalized Electrodes

The reduction of nitrite on a pyrolytic graphite electrode modified with a heme−DDAB film (see Figure 19 for results with NO) has been reported to be more sluggish than the reduction of nitric oxide on the same electrode by about 0.2 V.[201] The reduction product has not been determined, but preliminary results from our group suggest it to be mainly N_2O in neutral media and hydroxylamine in more acidic media. There have been quite a few other studies of nitrite reduction on electrodes modified with iron protoporphyrin films or films containing DDAB and heme proteins such as myoglobin, hemoglobin, and catalase.[199,263−265] Typically, a variety of reduction products (NH_3OH^+, NH_4^+, N_2O, NO, and N_2) has been found. Mimica et al.[264] have suggested that on electrodes modified with films of myoglobin or hemoglobin and DDAB, the first electron transfer of the iron−nitrosyl adduct is the rate-determining step. Younathan et al.[199] have used electropolymerized films of iron protoporphyrin IX dimethyl ester for nitrite reduction and also observed a variety of products in long-term electrolysis experiments. Especially the formation of some 40% N_2 is very interesting. Ammonia was found in increasing amounts with more negative potentials. The authors speculated on a mechanism including an iron−nitrido (Fe^V-N^{3-}) intermediate as a precursor to N−N bond formation. The Meyer group has studied various metal complexes in solution for the electrochemical reduction of nitrite, and they all seem to lead to the four mentioned final products, though in varying amounts, in long-term electrolysis experiments.[266−268] Other iron complexes that have a known catalytic activity for nitrite reduction are iron-substituted polyoxotungstates[269] and iron−alizarin complexone.[270] The latter complex has been studied on a graphite electrode using RRDE voltammetry, which identified hydroxylamine and ammonia as the main products.

Taniguchi et al.[271] reported that metal cyclams, especially Co(III)-cyclam (cyclam = 1,4,8,11-tetra-azacyclotetradecane), have an interesting catalytic effect on the reduction of nitrite (and nitrate), leading primarily to hydroxylamine. Li et al.[272] have incorporated these compounds into Nafion films on gold electrodes and showed catalytic activity to hydroxylamine in alkaline media. The applied potential for catalytic activity is rather negative, however, ca. −1.3 V vs SCE, which is much more negative than nitrite reduction on, for example, platinum.

Chebotareva and Nyokong[273] have studied nitrite reduction on glassy carbon electrodes modified with various metallophthalocyanine (MPC) complexes in alkaline solution. CuPC appeared to the most active complex, producing mainly ammonia.

8.3. Nitrite Oxidation

8.3.1. Nitrite Oxidation on Metal Electrodes

The interest in the electrochemical oxidation of nitrite or nitrous acid is primarily motivated by analytical purposes in relation to the quantitative determination of nitrate, nitrite, and NO_2. There have been quite a few early studies on the oxidation of nitrite on platinum electrodes,[274−276] the most thorough one appearing to be the one by Guidelli et al.[277] From a detailed modeling of the electrochemical transients at a platinum microelectrode, they concluded that the oxidation mechanism consists of an electron-transfer reaction followed by a solution-phase disproportionation reaction:

$$HNO_2 \leftrightarrows NO_2 + H^+ \quad (71)$$

$$NO_2^- \leftrightarrows NO_2 + e^- \quad (72)$$

$$2NO_2 + H_2O \rightarrow HNO_2 + H^+ + NO_3^- \quad (73)$$

The latter reaction (being the sum of reactions 65 and 66) is rate-determining, and therefore, electrochemical techniques may be employed to determine the rate constant for this reaction.[277,278]

More recently, Piela et al.[278,279] have restudied the oxidation of nitrite on "clean" and oxidized platinum electrodes and found that the reaction is more sluggish on a oxide-covered electrode, which they ascribed to the inhibiting effect of the oxide layer on the overall reaction rate. The experimental data were fitted to an inhibition model previously proposed in the literature, suggesting that the rate constant depends on the oxide coverage in a rather complicated way.[279] According to the authors, this rate constant applies to the forward (oxidation) reaction of reaction 72, which was, however, suggested to be in equilibrium on clean electrodes in the earlier literature.[277,278] This must imply (the assumption of) a change in rate-determining step on oxide-covered electrodes, although this is not explicitly stated by the authors.

The same mechanism given above was also supported for gold electrodes by Xing and Scherson[280] and for glassy carbon electrodes by Piela and Wrona.[278] For pH > 6, oxide formation on gold starts interfering with nitrite reduction and the reaction rate drops, as with platinum.[278,279]

8.3.2. Nitrite Oxidation on Functionalized Electrodes

Nitrite oxidation as an analytical approach to detecting nitrite is often preferred over nitrite reduction because interference with nitrate and oxygen may be avoided. However, as we have seen in the previous section, high oxidation potentials are needed at which the electrode may form oxide layers or be unstable, compromising the analytical response. Nyokong and co-workers[281,282] have studied electropolymerized layers of substituted metalphthalocyanines on glassy carbon as electrodes for nitrite oxidation. These electrodes appear to exhibit good stability. The suggested mechanism for nitrite oxidation was similar to that for discussed platinum in section 8.3.1.

8.4. Comparison to Nitrite Reduction by Enzymes

Nitrite reductases refer to a class of enzymes that catalyze the reduction of nitrite. Typically two sets of nitrite reductases are distinguished: iron-containing heme enzymes that reduce nitrite to a variety of products and copper-containing enzymes that are optimized for the one-electron reduction of nitrite to nitric oxide. There is a great amount of literature on these enzymes,[3−5,138,283] and we will limit our discussion here to those enzymes that have been studied using protein film voltammetry, a technique that involves immobilization of the enzyme or protein on a conducting substrate and subsequent study of its activity electrochemically.

Of the multiheme nitrite reductases, cytochrome cd_1 reduces nitrite to NO, and cytochrome *c* nitrite reductase (ccNIR) reduces nitrite to ammonium. Both enzymes have been studied by protein film voltammetry,[284−286] though the latter with greater detail. Nitrite binds to ccNIR to form NO bound heme iron, which is further reduced to hydroxylamine and ammonium. As was discussed in section 7.6, it is believed that nearby amino acids facilitate the cleavage of the N−O bond to yield both NO from nitrite and ammonia from hydroxylamine (Figure 20). As hydroxylamine is also reduced by these enzymes, albeit at a much lower rate,[285] it is often assumed that hydroxylamine is a key intermediate on the way from NO to ammonium.

Nitric oxide is the end product of nitrite reduction by heme cd_1 and copper-containing nitrite reductases. Detailed discussions of the binding of nitrite and nitric oxide to the various oxidation states of the catalytic centers have been given by Averill.[4] Wijma et al.[287] have recently presented a protein film voltammetric study of a copper-containing nitrite reductase on a pyrolytic graphite electrode and were able to distinguish between various modes of nitrite activation.

9. Nitrate Reduction

9.1. Reactions of Nitrate: Equilibrium and General Considerations

The reduction of nitrate is currently attracting much attention in liquid-phase heterogeneous catalysis and electrocatalysis, for reasons outlined already in the Introduction. The list of products to which nitrate can be reduced and the corresponding equilibrium potentials are given below.

$$NO_3^- + 2H^+ + 2e^- \leftrightarrow NO_2^- + H_2O \qquad E^0 = 0.835 \text{ V (vs NHE)} \quad (74)$$

$$NO_3^- + 4H^+ + 3e^- \leftrightarrow NO(g) + 2H_2O \qquad E^0 = 0.958 \text{ V (vs NHE)} \quad (75)$$

$$2NO_3^- + 10H^+ + 8e^- \leftrightarrow N_2O(g) + 5H_2O \qquad E^0 = 1.116 \text{ V (vs NHE)} \quad (76)$$

$$2NO_3^- + 12H^+ + 10e^- \leftrightarrow N_2(g) + 6H_2O \qquad E^0 = 1.246 \text{ V (vs NHE)} \quad (77)$$

$$NO_3^- + 8H^+ + 6e^- \leftrightarrow NH_3OH^+ + 2H_2O \qquad E^0 = 0.727 \text{ V (vs NHE)} \quad (78)$$

$$NO_3^- + 10H^+ + 8e^- \leftrightarrow NH_4^+ + 3H_2O \qquad E^0 = 0.875 \text{ V (vs NHE)} \quad (79)$$

Although it is not the most active catalyst, platinum is the most actively studied electrode material for nitrate reduction. A large part of this section will be devoted to a discussion of the mechanism of nitrate reduction on platinum and on platinum electrodes modified by a second metal or a promoter. Moreover, nitrate reduction can follow two different mechanisms: one is operative at moderate nitrate concentrations and acidity and applies to most practical conditions; the second mechanism is operative at high nitrate concentrations (>1 M) and high acidity (pH < 0).[288] As we have discussed in previous sections, at such low pH, solution-phase reactions come into play, which influence the overall nitrate reduction very significantly. Table 1 compares the mechanisms in terms of the media in which they take place, the relevant electroactive species, the potential range, and the products. These mechanisms will be discussed in detail in sections 9.2 and 9.3.

Table 1. Comparison between the Two Nitrate Reduction Pathways on Platinum

	direct pathway	indirect pathway
medium	all media	highly acidic media
electroactive species	NO_3^-	NO^+
potential range (vs RHE)	0.3−0.1 V	0.9−0.5 V
products	mainly NH_4^+	HNO_2, NO, NO_2, N_2O

9.2. Nitrate Reduction in Acidic Solution at Low Nitrate Concentration

9.2.1. Nitrate Reduction at Platinum Electrodes

The reduction of nitrate on polycrystalline platinum at low nitrate concentration has been the subject of many studies.[244,289−296] Figure 23 shows the typical voltammetry of nitrate reduction on a polycrystalline platinum electrode in sulfuric and perchloric acid.[295] Under these conditions, we are probing the direct reduction pathway, which has significant overpotential on platinum. Moreover, as is clearly illustrated in Figure 23, the electrocatalytic reduction of nitrate on platinum is strongly hindered by the presence of specifically adsorbing anions, such as sulfate, as well as other anions.[290,291]

As also shown in the inset to the left panel of Figure 23, which gives the steady-state nitrate reduction current in sulfuric acid, the nitrate reduction current on Pt starts at ca. 0.3 V (vs RHE), initially increases, but then drops again below ca. 0.1 V. Safonova and Petrii[292,293] have argued that this inhibition is due to the formation of adsorbed hydrogen (upd H) on the platinum surface, and results obtained on single-crystal platinum electrodes, to be discussed below, have unambiguously shown the inhibitive role that adsorbed H exerts on nitrate reduction on platinum. Kinetic measurements in the initial reduction region (0.3−0.2 V) show a reaction order in nitrate of ca. 0.5 and a Tafel slope of ca. 120 mV/decade.[295] The current measured in Figure 23 does not involve any diffusion-limited contribution. FTIR measurements[294] and transfer experiments followed by stripping in a nitrate-free solution[295] demonstrated that the main surface-bonded intermediate formed from nitrate is nitric oxide (NO). In sulfuric acid, adsorbed NO is formed at potentials as high as 0.45 V, reaches a maximum coverage of ca. 0.1 monolayer at 0.3 V, and then rapidly disappears at lower potentials due to its reduction. Rotating ring-disk and online electrochemical mass spectrometry measurements showed that during nitrate reduction on platinum, no hydroxylamine and no gaseous products are formed,[295,297,298] leaving ammonia as the only possible product. A recent ATR−SEIRAS study of nitrate reduction at polycrystalline platinum by Nakata et al.[299] has argued that the main species observed spectroscopically at 1547−1568 cm^{-1} is adsorbed nitrate, more specifically a chelating bidentate nitrate chemisorbed on the Pt surface.

A more detailed view on nitrate reduction on platinum is obtained when working with single-crystal platinum surfaces. Dima et al.[300] have argued that the observed structure sensitivity of the nitrate reduction on platinum is primarily due to the structure-sensitive adsorption of other species, such as hydrogen and anions. The inhibitive effect of adsorbed hydrogen is clearly indicated in the cyclic voltammetry of

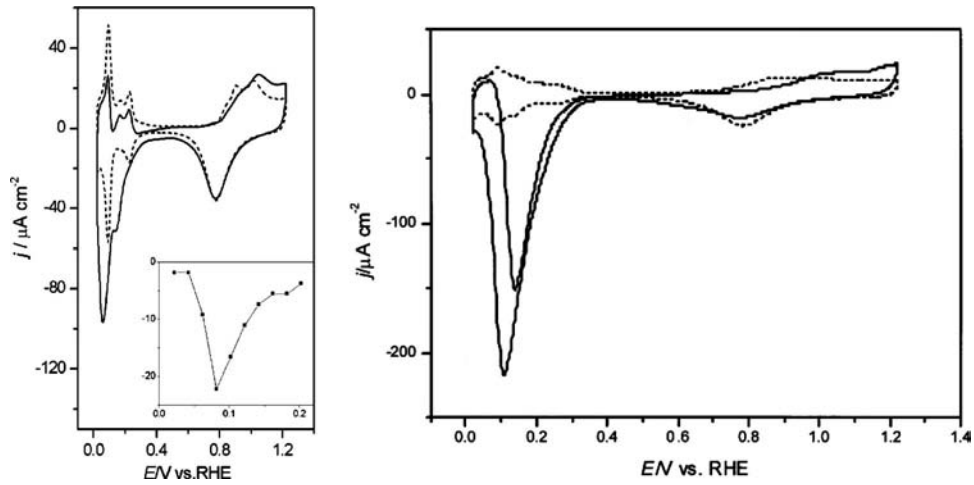

Figure 23. Voltammetry of the nitrate reduction on a platinum electrode in sulfuric acid (0.5 M H_2SO_4) electrolyte (left panel) and perchloric acid (0.5 M $HClO_4$) electrolyte (right panel). Dashed lines are base electrolyte; solid lines are base electrolyte plus 0.1 M $NaNO_3$. The inset in the left panel is the steady-state nitrate reduction current density as a function of potential. Reproduced with permission from ref 295. Copyright 2003 Elsevier.

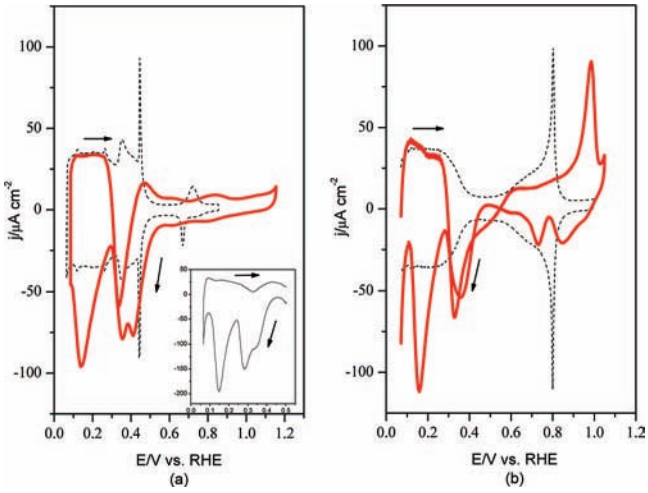

Figure 24. Cyclic voltammograms recorded at Pt(111) electrode in 0.5 M H_2SO_4 (a) and 0.5 M $HClO_4$ (b) in the absence (dashed line) and presence (bold solid red line) of nitrate. The blank voltammograms were recorded at 50 mV s^{-1}. The nitrate voltammograms were recorded at 5 and 2 mV s^{-1} in H_2SO_4 and $HClO_4$, respectively. Their currents have been multiplied by factors of 10 and 25, respectively, for comparison with the blanks. Experimental conditions: 1 mM $NaNO_3$, starting potential 0.06 V. Inset in panel a is the reduction of a saturated NO adlayer at a scan rate of 2 mV s^{-1} (current multiplied by a factor of 25). Reproduced with permission from ref 300. Copyright 2005 Elsevier.

Pt(111) in nitrate-containing solution (Figure 24). When the voltammogram is started at 0.05 V and scanned in the positive direction, the current initially traces the blank voltammogram, both in sulfuric and in perchloric acid, until ca. 0.25 V. Above 0.25 V, the hydrogen coverage drops below what is apparently a critical coverage (which we estimate is ca. 0.2 ML), and a negative current is observed that is due to nitrate reduction. The current observed is related to the formation of chemisorbed NO and its subsequent reduction to ammonia, the latter only at sufficiently low potentials. The formation of adsorbed NO is also evident from the voltammetry. In perchloric acid, the oxidation peak observed at 1.0 V and the subsequent reduction features between 0.7−0.9 V are due to the redox couple discussed in section 7.5.1, reaction 55, that is, the reversible conversion of adsorbed NO to nitrous acid. In the reduction scan at low potential, the features due to NO(ads) reduction are clearly observed, as compared with the stripping of a full monolayer of NO shown in the inset of Figure 24a. FTIR measurements also suggest the formation of adsorbed NO and indicate that at the low NO coverage one expects from nitrate dissociation, NO primarily occupies hollow sites on Pt(111) (although we should note again that Nakata et al.[299] have argued that the observed band is due to adsorbed nitrate rather than adsorbed NO, at least on polycrystalline Pt).

The most active platinum surface for nitrate reduction is Pt(110), but only in perchloric acid. In sulfuric acid, the Pt(110) surface is severely blocked, and the nitrate reduction activity is lower than that on Pt(111) in sulfuric acid. Of the two stepped surfaces considered for nitrate reduction by Dima et al.,[300] Pt(554) behaved more like Pt(111) and Pt(553) more like Pt(110). In addition, Dima et al. presented some evidence that NO tends to accumulate at step sites on stepped electrodes, and the presence of adsorbed NO on Pt(110) was confirmed by FTIR. A more detailed study of the influence of step density on nitrate reduction on single-crystal platinum was published recently by Taguchi and Feliu.[301] They found that the electrocatalytic activity for nitrate reduction depends on the step density in a nonlinear fashion, the activity strongly increasing when the terrace length is shorter than 5 atoms (i.e., Pt(553), we note that the nitrate concentration used was 10 mM compared with 1 mM used by Dima et al.). Furthermore, from their extensive voltammetry experiments, the authors concluded that in the hydrogen region, nitrate preferentially adsorbs and dissociates on step sites. In a subsequent study, Taguchi and Feliu[302] carried out a detailed voltammetric study on the kinetics of nitrate reduction on Pt(110). Interestingly, at the very low scan rate they employed (1 mV/s), the kinetics were quite different from those previously established on polycrystalline Pt. First of all, the reaction was zeroth order with respect to nitrate concentration, and first order with respect to proton concentration. The nitrate reaction order is in contrast with the positive reaction order observed by Dima et al. at low nitrate concentration. However, a negative order in nitrate concentration, suggesting strong inhibitive adsorption, was observed in acidic media at high nitrate concentration (>0.1 M).[288] Furthermore, the Tafel slope on Pt(110) measured by

Taguchi and Feliu[302] was close to 60 mV/decade, in contrast to the previously observed 120 mV/decade for polycrystalline Pt.

On the basis of the above discussion, one may suggest the following mechanism for nitrate reduction on platinum. The difficult step in nitrate reduction is its conversion to nitrite:

$$NO_3^- + 2H^+ + 2e^- \rightarrow NO_2^- + H_2O$$

On Pt(110), the most active surface, the Tafel slope and the reaction orders in nitrate and proton concentration suggest the following mechanism:

$$NO_3^-(sol) + * \leftrightarrows NO_3^-(ads) \quad (80)$$

$$H^+ + e^- \leftrightarrows H(ads) \quad (81)$$

$$NO_3^-(ads) + H(ads) \rightarrow ... \quad (82)$$

On the other surfaces, for which the Tafel slope is 120 mV/decade, the electron transfer may be involved in the rate-determining step. Because the adsorption of nitrate is relatively weak, it is strongly influenced by the adsorption of anions and hydrogen. Taguchi and Feliu[302] have suggested that two types of adsorbed upd hydrogen exist on Pt(110): H_s, adsorbed on (110) sites at low potential, and H_{nt}, adsorbed at higher potential presumably on narrow (111) terraces of the reconstructed Pt(110). The adsorbed hydrogen in reactions 81 and 82 is H_{nt}, and the adsorbed hydrogen that inhibits nitrate reduction is H_s.

Adsorbed NO is an important intermediate in nitrate reduction, as evidenced from FTIR and stripping measurements. Adsorbed NO is formed after the rate-determining step, most likely from nitrite, and is reduced to ammonia (see section 7.2.1). Because NO is adsorbed strongly on Pt, it does not desorb, and there is no NO in solution. As a result, the formation of N_2O and N_2 is prohibited, and ammonia is the only product of nitrate reduction on platinum.

9.2.2. Nitrate Reduction at Other Metal Electrodes

The first to compare the activity of various metals for the electrocatalytic reduction of nitric acid/nitrate was Vijh,[303] who based his volcano-type analysis on experimental results published by Khomutov and Stamkulov.[304] An interesting assertion made by Vijh was that metals that have a high overpotential for hydrogen evolution also have a high overpotential for the reduction of nitrate. More recently, Dima et al.[295] studied the reduction of nitrate on five transition-metal electrodes (Pt, Pd, Rh, Ru, Ir) and three coinage-metal electrodes (Cu, Ag, Au) in acidic media. Of the transition metals, rhodium is the most active catalyst for the reduction of nitrate, with the activity decreasing in the order Rh, Ru, Ir,[305] Pt, and Pd, when the comparison is made in sulfuric acid. The high catalytic activity of Rh for nitrate reduction was also observed by Wasberg and Horanyi,[306,307] who showed that nitrate reduction on rhodium may reach diffusion-limited values. Online electrochemical mass spectrometry revealed that no gaseous products are formed on Rh,[295] in agreement with the observation by Brylev et al.[254] that the main products on rhodium are ammonia and nitrite. Da Cunha et al.[308] observed the formation of NO and N_2O during nitrate reduction on rhodium, but they employed a high concentration (3 M) of nitrate, for which the mechanism is different (see section 9.3). The high activity of rhodium was ascribed to the high affinity of rhodium for anions. For instance, rhodium is also a good catalyst for the reduction of perchlorate,[309] whereas platinum does not reduce perchlorate. The Tafel slope for nitrate reduction on rhodium is close to 120 mV/decade,[295,306] suggesting that also on rhodium the slow step is the conversion of nitrate to nitrite. The addition of chloride to the solution inhibits the reaction rate, and may introduce galvanostatic potential oscillations.[306] Also the adsorption of methanol chemisorption products (carbon momoxide) has an inhibitive effect on nitrate reduction on rhodium.[307]

Of the coinage metals, copper is the most active surface for nitrate reduction, followed by silver and gold,[295] the latter metal showing very little activity. Copper has been widely investigated as a catalyst for nitrate reduction. Pletcher and Poorabedi[310] showed that in acidic media, the reduction of nitrate at copper electrodes is fast enough to lead to a diffusion-limited wave. They found that the main product on copper is ammonia. The reduction is inhibited by the addition of chloride and bromide to the solution. Dima et al.[295] found Tafel slopes of ca. 120 mV/decade for nitrate reduction on copper in sulfuric acid and ca. 200 mV/decade in perchloric acid. Interestingly, in contrast to Pt and Rh, gaseous products are detected during nitrate reduction on copper using online DEMS. The reduction current is accompanied by the formation of NO in solution, though N_2O was not observed. Dima et al. ascribed the formation of NO to the fact that the intermediate NO binds weakly enough to Cu to desorb. However, NO is not reduced further to N_2O, as would be expected according to the mechanism discussed in sections 7.2.2 and 7.3.2. We note that copper tends to be unstable in acidic media and to corrode,[311] which may influence the reduction of NO to N_2O. Reyter et al.[312,313] have looked at methods that activate copper for nitrate reduction, such as high-energy ball milling and alkaline pretreatment.

Detailed molecular-level studies of nitrate reduction on copper single-crystal electrodes were recently published by Gewirth et al.,[256,314] combining electrochemical techniques, STM, SERS, and DFT calculations. Comparison of the electrochemical data with STM and SERS suggests that at the most positive potential, nitrite is the main initial product of nitrate reduction on Cu(100). The reduction wave observed at lower potential would then be associated with the further reduction of nitrite, presumably also involving the formation of (adsorbed) NO. At these potentials, RDE measurements show that nitrate reduction is an eight-electron process on polycrystalline Cu, implying ammonia is the final reduction product, but a six-electron process on Cu(100). Gewirth et al. did not have a clear explanation for this difference but pointed out that the Cu(100) surface is the most stable Cu surface and does not seem to spontaneously dissolve in acidic media, whereas Cu(110), Cu(111), and Cu(poly) are unstable, leading to increased concentrations of Cu^{2+} and Cu^+ near the electrode. The cuprous Cu^+ ion is a known catalyst for nitrate reduction.[315] Cu(100) is indeed the least active surface for nitrate reduction. STM images suggest that step sites of (110) orientation on a Cu(100) surface are active sites for nitrate to nitrite conversion and may be a source of cuprous ion formation.[256] STM images of nitrate and nitrite on Cu(100) show (2×2) and $c(2 \times 2)$ structures, respectively, and their comparison, in combination with the SERS data on Cu(poly), suggests that at potentials just before the main reduction wave the nitrate adlayer is converted to a nitrite adlayer. The transition between the two adlayers proceeds through a nucleation and growth mechanism. DFT calcula-

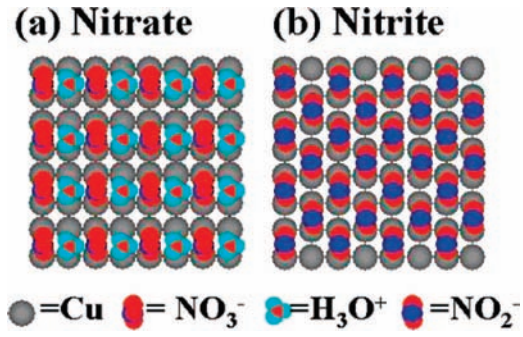

Figure 25. Schematic model of the nitrate (a) and nitrite (b) adlayer on the Cu(100) surface. Reproduced with permission from ref 256. Copyright 2007 American Chemical Society.

tions of nitrate and nitrite adsorption on Cu(100), without co-adsorbed water, show that both species prefer to interact with two oxygens coordinated to two neighboring Cu surface atoms in a bidentate bridge fashion.[256] On the basis of their STM and DFT results, they suggested that nitrate and nitrite interact with Cu(100) as illustrated in Figure 25. The differential reactivity of Cu(111) and Cu(100) was recently discussed by Bae and Gewirth.[314] Nitrate reduction on Cu(111) starts at 0.3 V lower overpotential than that on Cu(100). In the presence of nitrate, Cu(111) evinces oxide-like features at the potentials at which nitrate is reduced on this surface. These features are not found on Cu(100), except at the (111)-oriented step edges. During the cathodic sweep on Cu(111), the oxide monolayer is reduced finally forming flat surfaces exhibiting holes with monatomic depth. The oxide adlayer appears on Cu(111) in the potential range where nitrate is reduced but is absent without nitrate in solution. Therefore, Bae and Gewirth suggest that oxide formation is a key step in the nitrate reduction on Cu(111):

$$NO_3^- + Cu(111) \rightarrow NO_2^- + Cu(111) - O$$

This mechanism does not apply to Cu(100) because of the lower stability of the Cu(100)-O intermediate and therefore is restricted to step-like defect sites on the Cu(100) surface.

Gold is the least active nitrate reduction catalyst of the three coinage metals. Da Cunha et al.[316] observed vibrational bands of adsorbed nitrate on gold using FTIR, suggesting that nitrate does not lie flat on the gold electrode but with the molecular plane perpendicular to the surface, essentially in agreement with the adsorption structure suggested in Figure 25 for Cu(100). A weak feature corresponding to nitrite adsorption was also observed, which was suggested to correspond to nitrite binding in a bridge-type fashion to the gold surface.

Besides transition and coinage metals, there have been a few studies of nitrate reduction in acidic media on "poor metals" such as mercury,[317] indium,[318] cadmium,[319] and tin.[320,321] In agreement with Vijh's assertion[303] that there is a relation between the overpotential for hydrogen evolution and nitrate reduction, these metals have a high overpotential for the reduction of nitrate. Very recently, Kyriacou and co-workers[320−322] made the interesting observation that at very negative potentials (−2.8 V vs Ag/AgCl), tin is able to reduce nitrate to dinitrogen with very high selectivity (>90%). Nitrite and ammonia are the other products. At these very cathodic potentials, "cathodic corrosion" (destruction by hydride formation) of tin takes place, which may impair practical application of this process. There is as yet little insight into the mechanism of nitrate reduction on tin.

Scharifker et al.[323] have recently reported the catalytic action of thallium during nitrate reduction on vitreous carbon electrodes. The reduction of nitrate to ammonia was observed with the simultaneous reduction of the intermediate Tl^+ cation in the Tl^{3+} reduction. No catalysis was observed in the presence of Tl^+ without Tl^{3+}, suggesting a key role for the Tl^{2+} species, which arises from the disproportionation of Tl^+ and Tl^{3+}. This mechanism seems somewhat similar to the role of Cu^+ in the copper-catalyzed reduction of nitrate.

Since nitrite is a necessary intermediate in the reduction of nitrate, it is useful and insightful to briefly compare the activity for nitrite and nitrate reduction on various metals. On platinum, nitrite is more easily reduced than nitrate. Also, more products are formed from nitrite: N_2O, NH_2OH, NH_4^+. From nitrate, only ammonia is formed (at low nitrate concentrations). On rhodium, nitrite reduction is also more efficient than nitrate reduction.[254] However, only ammonia was found during prolonged electrolysis experiments of nitrite, whereas during nitrate reduction both nitrite and ammonia were observed. This could suggest a more sequential mechanism on rhodium, whereas side reactions are more important on platinum. On copper, nitrite and nitrate reduction display similar voltammetric characteristics, although nitrite reduction starts at a potential about 0.3 V more positive.[256] However, nitrite was observed as an intermediate in nitrate reduction on copper, and there was no evidence for additional side reactions as on platinum.

9.2.3. Nitrate Reduction at Bimetallic Electrodes

One of the goals of research into nitrate reduction is to achieve a high selectivity for the formation of hydroxylamine or dinitrogen. Because none of the common pure metals is able to reach such high selectivities, there have been many papers devoted to nitrate reduction on bimetallic alloys or monometals modified with foreign metal adatoms or adions.

Because copper is such an active albeit somewhat unstable catalyst for the reduction of nitrate and nitrite, there have been many investigations into the catalytic properties of platinum and palladium electrodes modified with copper, either as alloys or as pure Pt or Pd surfaces modified with small amounts of Cu. Palladium−copper catalysts have been suggested by Vorlop et al.[14] as selective catalysts for the reduction of nitrate to dinitrogen. The first thorough electrochemical study of palladium−copper electrodes for the reduction of nitrate was performed by De Vooys et al.[255] These authors prepared a series of Pd−Cu surfaces by underpotential deposition of Cu onto Pd, which allows tuning of the Cu surface coverage between 0 and 1. The presence of copper on the Pd surface significantly enhances nitrate reduction, because Pd is known to be a poor catalyst for nitrate reduction (see section 9.2.2). Figure 26 shows the activity and selectivity toward N_2 and N_2O as estimated from online DEMS experiments, measured at fixed potential as a function of the Cu coverage. The figure also clearly illustrates the inhibiting role of anions (sulfate in this case) in terms of both the activity and selectivity of the catalyst. From Figure 26, it is concluded that the highest selectivity toward N_2 (ca. 40%) is realized at low Cu coverage and that the higher reduction activity observed at higher Cu coverage is compromised by a lower selectivity toward N_2. De Vooys et al. have suggested the following explanation for these observations. Because palladium is not active for nitrate reduction, the copper sites on the surface are responsible for the reduction of nitrate to nitrite and NO. Both copper and

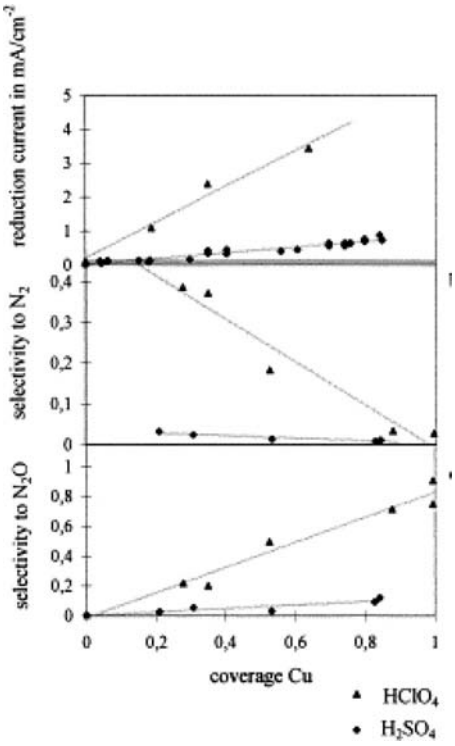

Figure 26. Activity and selectivity of the nitrate reduction on Pd−Cu electrodes vs Cu coverage in $HClO_4$ and H_2SO_4, electrode potential 0.02 V (vsRHE), pH = 0.3, $[NO_3^-]$ = 0.1 M. Reproduced with permission from ref 255. Copyright 2000 Elsevier.

palladium are active catalysts for the reduction of NO to N_2O, and palladium is the most active catalyst for the reduction of N_2O to N_2 (see section 6.1), whereas this reaction does not take place on Cu. As a result, Pd sites are needed on the surface for the production of N_2. We note that N_2O production was not observed during nitrate reduction on pure Cu (see section 9.2.2) but is a prominent reduction product on a Pd surface covered with a full monolayer of Cu (see Figure 26). Most likely, this has to do with the stability of Cu surface sites: upd Cu on Pd is stable, whereas pure Cu tends to corrode, and this may interfere with the N_2O production. Pronkin et al.[324] have recently described an in situ method for the preparation of PdCu bimetallic nanoparticulate catalysts. These catalysts produced a similar enhancement in nitrate reduction current as compared with the previously described flat "model" surface.

Platinum electrodes modified with upd Cu are different from Pd−Cu surfaces, because Pt is less active in the reduction of N_2O to N_2 and hence less selective in the reduction of NO to N_2. Therefore, it is understandable that PtCu catalysts produce more ammonia and less N_2, as has been observed by Kerkeni et al.[325] Addition of silver to Pt or Pd has a similar promotional effect as Cu, whereas the addition of Au has no effect.[326] A gold electrode modified with Cu upd is also active for nitrate reduction.[327] Nitrite was observed as one of the intermediates, but the other reduction products remained unidentified.

Another known promoter for the reduction of nitrate on platinum or palladium that also enhances the selectivity toward N_2 formation is tin.[15,328,329] Shimazu et al.[330] have carried out electrochemical investigations of the activity and selectivity for nitrate reduction on platinum modified with controlled amounts of tin. Figure 27 illustrates the enhancing effect of Sn for various coverages of Sn on Pt in perchloric

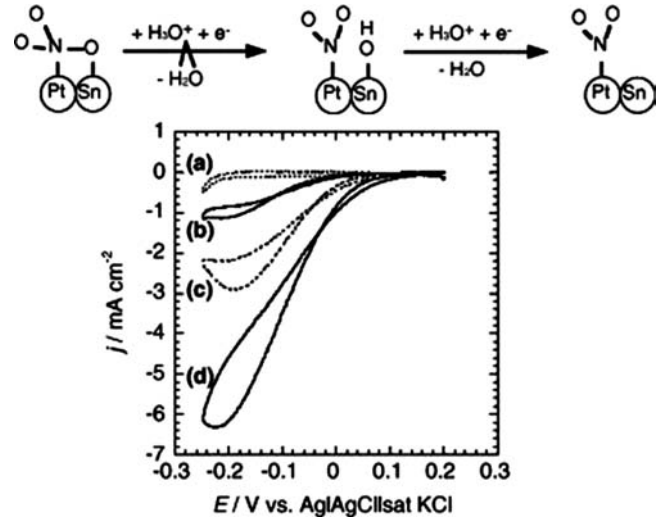

Figure 27. The reduction of nitrate on Sn/Pt electrodes. Sn-coverages: (a) 0; (b) 0.08; (c) 0.21; (d) 0.36. Electrolyte solution = 0.01 M $NaNO_3$ + 0.1 M $HClO_4$. Sweep rate = 0.010 V s^{-1}. The cartoon above shows the suggested rate-determining step reaction together with the subsequent step. Reproduced with permission from ref 330. Copyright 2005 Elsevier.

acid. The maximum activity is reached at a Sn coverage of ca. 0.35−0.4 monolayer. At these Sn coverages, the product distribution, as determined from prolonged electrolysis, is 62% ammonia, 30% N_2, and 8% N_2O. From the Tafel slope, Shimazu et al. conclude that the first electron transfer step is rate determining. They suggest that the role of tin in catalyzing this step is to provide a site to which one of the oxygens of the nitrate ion can coordinate, on the basis of the higher oxophylicity of Sn. A cartoon of this reaction is also shown in Figure 27. It is still unclear how the formation of N_2 is favored in the further reduction of nitrite. In three other papers, Shimazu et al.[331−333] studied the reduction of nitrate on gold electrodes modified with tin and palladium or platinum in order to decrease the overall loading of the noble-metal component. On the Au/Pt/Sn electrodes, a high electrocatalytic activity for nitrate reduction was observed, but the final product was 97% ammonia. On the Au/Pd/Sn electrodes also a very high catalytic performance has been observed, and more gaseous products are formed, such as N_2O and N_2, with the system reported in ref 332, giving rise to 37% N_2 formation. Prüsse et al.[15] have reported the promoting effect of indium, the nearest neighbor of tin in the periodic table, for the nitrate reduction on palladium, but to our knowledge, indium has not yet been tested as a promoter electrochemically.

Another well-known promoter for nitrate reduction on platinum is germanium. Germanium is used in the industrial process of nitrate reduction to hydroxylamine to enhance the selectivity of hydroxylamine production on palladium−platinum catalysts.[297,334] In the paper by Gootzen et al.,[297] it was suggested that the promotional effect of Ge would be similar to that suggested by Shimazu et al.[330] for tin, namely, by providing a site to which one of the oxygens of nitrate can bind favorably. However, it was recently shown by Dima et al.[298] that germanium only has an enhancing effect on the nitrate reduction in sulfuric acid and that there is essentially no increase in activity in perchloric acid, that is, without strongly adsorbing anions. Note that a similar anion effect is not observed for tin, since Figure 27 pertains to a perchloric acid solution. Moreover, from FTIR measurements it was concluded that adsorbed Ge is covered by a hydride layer in

the potential region of nitrate reduction. On the basis of this result, Dima et al. concluded that the main effect of Ge is not to directly enhance nitrate reduction but to inhibit the adsorption of specifically adsorbing anions such as sulfate. However, Ge does have a significant effect on the selectivity of the reaction. From RRDE measurements, it was found that up to 60% hydroxylamine was produced during nitrate reduction on platinum, palladium, or platinum−palladium electrodes in the presence of Ge, whereas hydroxylamine is not produced in the absence of germanium.[297,298] This selectivity effect was ascribed to a third-body effect exerted by adsorbed Ge, because the presence of Ge on the surface may inhibit the dissociation of the N−O bond in the NO intermediate by lowering the density of ensemble sites needed for N−O bond breaking (see also the discussions in sections 7.2.1 and 7.2.2). Typically, the presence of palladium seems to enhance the selectivity toward hydroxylamine, and the presence of platinum seems to promote the overall activity, because platinum is more active in reducing the NO intermediate.[334]

Safonova and Petrii have studied the effect of a number of inorganic cations (Ni^{2+}, Cd^{2+}, Co^{2+}, Ge^{4+}) in solution on the electroreduction activity of nitrate on platinum.[335] Ge was indeed found to be a good promoter, although the authors conducted their experiments only in sulfuric acid. The other three cations also promote nitrate reduction, forming ammonia as the final product. Only in the case of germanium, hydroxylamine was detected as a reaction product. These differences may point to a role of Ge that goes beyond that of a third body.

We already mentioned the modification of gold electrodes by upd Cu to catalyze nitrate reduction. Another gold modifier that has been studied for nitrate reduction is cadmium. Scherson et al. have studied this system using rotating-ring disk voltammetry and in situ FTIR spectroscopy.[327,336,337] Both techniques indicate that the only detectable product of nitrate reduction on this electrode is nitrite. On the basis of STM studies on Au(111), Shieh and Gewirth suggested that the electroactive Cd phase is a (1×1) adlattice.[338] Hsieh and Gewirth have suggested that electrocatalytic enhancement is due to the specific adsorption of nitrate to the Cd adlattice, because there is no dissolved cadmium that might interact with nitrate. Underpotential deposited layers of Ag and Pb on Au as well as mixed Ag−Pb layers on gold have also been found to enhance nitrate reduction.[339−341]

9.3. Nitrate Reduction at Platinum in Highly Acidic Solution at High Nitrate Concentration

As mentioned in the introduction to this section on nitrate reduction, at high nitrate concentrations (>1 M) in highly acidic environments (>1 M), an additional so-called indirect mechanism for nitrate reduction occurs. This indirect nitrate reduction leads to a cathodic current between 0.9−0.5 V vs NHE. In this mechanism (reactions 83−86), the reaction that takes place at the electrode is not the reduction of nitrate, since nitrate cannot be reduced on platinum at these potentials. Instead, it has been suggested that the reduction of the nitrosonium ion (NO^+) to nitric oxide takes place, in essence very similar to what happens in the reduction of nitrous acid in highly acidic solution. The nitric oxide formed in this reaction reacts with nitric acid in solution to form nitrous acid (HNO_2), which is in equilibrium with the main electroactive species NO^+. As a result, the overall reaction is the conversion of nitric acid to nitrous acid, as also illustrated in Figure 28:

$$2NO^+ + 2e^- \rightarrow 2NO \quad (83)$$

$$2NO + HNO_3 + H_2O \leftrightharpoons 3HNO_2 \quad (84)$$

$$2HNO_2 + 2H^+ \rightleftarrows 2NO^+ + 2H_2O \quad (85)$$

$$HNO_3 + 2H^+ + 2e^- \rightarrow HNO_2 + H_2O \quad \text{(overall reaction)} \quad (86)$$

The overall reaction 86 is of autocatalytic nature, since the rate of formation of the product of the reaction (HNO_2) depends on it own concentration, which is in equilibrium with the electroactive species (NO^+). Effectively more NO^+ is produced than consumed, through the formation of HNO_2, and therefore the concentration of NO^+ increases in time. As a result there is a continuous increase in reaction rate. This autocatalytic nature of the reaction is also reflected in the unusual effect of rotation.[288] If the electrode is rotated, the reaction rate decreases, because stirring limits the buildup of NO^+ near the electrode. Slow scan rates or simply waiting also lead to larger currents due to the indirect reduction mechanism.

The indirect mechanism can only occur if a small amount of NO^+ is already present in solution. This is necessary for the reaction to be initiated. In a highly acidic nitrate solution, these small amounts are always present, since nitric acid starts to decompose at concentrations above 4 M.[342,343] There are numerous reactions by which this can occur, which have been described in detail in the literature.[17,274,311] These reactions do not occur in less acidic media, and hence, the indirect reduction mechanism does not develop in these media.

The indirect reduction mechanism results not only in the formation of HNO_2 but also in the formation of NO and NO_2 as evidenced by Figure 29, which shows the results of an online DEMS experiment.[288] The gas evolution observed between 0.95 and 0.5 V is due to the indirect reduction of nitrate. The direct reduction mechanism occurs below 0.4 V in Figure 29. The buildup of NO is expected, since it takes part in the mechanism. The formation of NO_2 is presumably related to different equilibria that occur in the solution and suggests that other less volatile products such as N_2O_3 and N_2O_4 are also formed.

The autocatalytic reaction only occurs in a certain potential range (0.95−0.5 V vs SHE) and does not occur at lower potentials.[288] The reason for this is that the autocatalytic cycle is interrupted at lower potentials. The reaction responsible for the termination of the autocatalytic cycle is the further reduction of NO to N_2O (reactions 53 and 54 in section

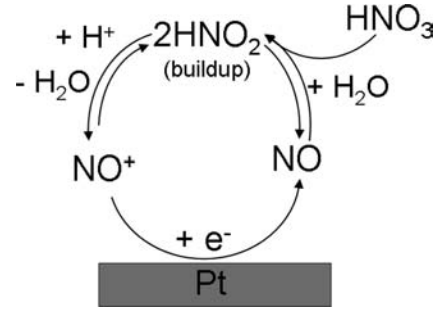

Figure 28. Schematic illustration of the indirect nitrate reduction pathway.

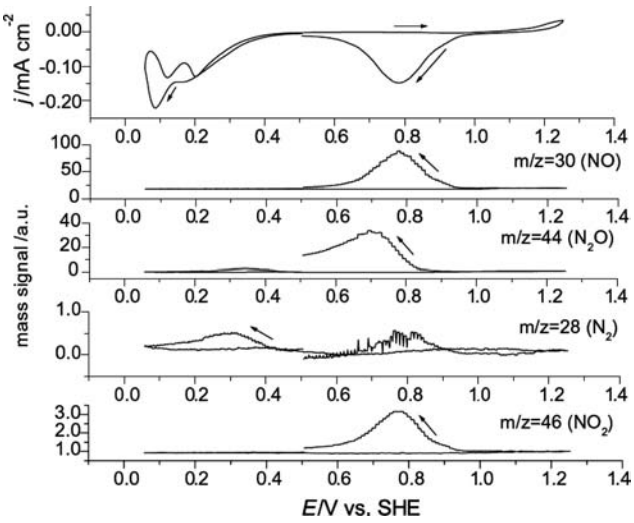

Figure 29. DEMS measurement in 4.1 M HNO_3 in 0.5 M H_2SO_4 on a platinized electrode. Scan rate = 10 mV/s. Reproduced with permission from ref 288. Copyright 2004 Elsevier.

7.2.2), which starts around 0.6 V vs SHE.[144] The formation of N_2O has also been evidenced with DEMS, as shown in Figure 28, and indeed starts at more negative potentials (0.8 V) than the formation of NO and NO_2.

The mechanism described here is not the only mechanism that has been proposed for the indirect nitrate reduction. Another mechanism involving NO_2 as the electroactive species has also been suggested.[274,344] However, we consider the mechanism described above to be the most plausible, since it provides straightforward explanations for the substantial formation of NO and the interruption of the catalytic cycle at lower potentials. Nevertheless, given the variety of nitrogen compounds present in solution in these highly acidic solutions, it is conceivable that more than one reduction mechanism occurs.

To our knowledge, there has been no systematic work on the indirect mechanism on other electrodes than platinum. Nart et al.[308] have also studied nitrate reduction in highly acidic media at high concentrations of nitrate on platinum, rhodium, and platinum−rhodium electrodes but focused only on the direct reduction mechanism. A small amount on NO and N_2O gas formation is observed in the potential region of the direct reduction mechanism, in agreement with the observations of De Groot and Koper[288] in this potential region.

9.4. Nitrate Reduction in Alkaline Media

Although there are less detailed mechanistic studies of nitrate reduction in alkaline media compared with acidic media, there seem to be some important differences with the behavior in acidic media. Part of the reason for this is the fact that some potential electrode materials for nitrate reduction are stable in alkaline media whereas they are unstable in acidic media. There is quite some interest in removing nitrate from low-level alkaline nuclear waste, which has led to some patents based on nitrate electrolysis (for an introduction into this kind of application, see the paper by Bockris and Kim[345]). We will briefly review the most pertinent mechanistic results in this section.

Horanyi and Rizmayer[252] studied the reduction of nitrate on platinum in alkaline media and observed that the reduction is significantly slower than that in acidic media (roughly by a factor of 10 compared with perchloric acid solution[290]). We believe that this difference may be due to OH^- adsorption on Pt. On the other hand, some qualitative features were very similar to acidic media: the reduction takes place in the same potential region (on the RHE scale) and the current drops rapidly in the H upd region, suggesting that adsorbed hydrogen inhibits nitrate reduction. Wasmus et al.[28] observed the formation of a small amount of N_2 during the cathodic scan in an alkaline nitrate solution and a much larger amount during the subsequent anodic scan, in exactly the potential region where ammonia is oxidized to N_2 (see section 2.1). This suggests that ammonia is the main product of nitrate reduction and that N_2 is formed from the subsequent oxidation of ammonia.

Hobbs et al.[346−348] and Bouzek et al.[349] have compared various metals in terms of their activity for nitrate reduction in (weakly) alkaline solutions. Hobbs et al. have found that in alkaline media, metals such as nickel, lead, cadmium, and zinc show a high activity for nitrate reduction. Bouzek et al. confirmed that in weakly alkaline media, platinum is not very active for nitrate reduction and that nickel and especially copper are much more active. However, ammonia is the main product on these metals (we note that ammonia is not oxidized on copper and nickel) and therefore still presents a drawback in terms of practical applications. In order to alleviate this disadvantage, Bouzek et al.[350,351] have studied copper−tin and copper−zinc alloy electrodes. Although small amounts of zinc and tin improved electrocatalytic performance, no significant improvement in N_2 yield was observed.

Palladium seems to be a better partner for copper to enhance selectivity for N_2. In addition to their studies in acidic media, as discussed in section 9.2.2, de Vooys et al.[255] also investigated the properties of Cu-modified palladium electrodes for nitrate reduction in alkaline media. Activities are lower than those in acidic media, but the selectivity for N_2 is about 50% at low Cu coverage, comparable to the situation in acidic media. The superior catalytic properties of copper−palladium for nitrate reduction in alkaline media were recently confirmed by Milhano and Pletcher.[352]

Rhodium is the most active catalyst for nitrate reduction in acidic media and also has some intriguing properties in alkaline media. Tucker et al.[353] have studied nitrate reduction on titanium-supported Rh in alkaline solution and developed an in situ electrochemical activation method to produce a high surface area catalyst with very good selectivity for N_2. The mechanistic details of this process are as yet elusive.

Pure gold is essentially inactive for nitrate reduction in acidic media. Remarkably, Ohmori et al.[354] have shown that a higher pH facilitates nitrate reduction on gold, even in mildly acidic media (pH = 2−3), although basic media are the most active. Both nitrite and ammonia are formed, with the relative amount of ammonia being higher in alkaline media. The authors ascribe the activity to the presence of alkali metal cations Na^+ and Cs^+ in solution, with Cs^+ leading to a higher relative amount of nitrite as the reduction product. Also upd Pb on gold has been shown to lead to enhanced electrocatalysis of nitrate reduction in alkaline solution, as compared with pure gold.[355] Clearly, there is a pronounced effect of metal cations, be it specifically adsorbed or on the surface as a upd layer, on the electrocatalytic activity of gold for nitrate reduction, both in acidic and in alkaline media. It is our own experience that this effect may play a role at the level of impurities, in the sense that nitrate

reduction on gold in alkaline media may be catalyzed by cationic impurities in hydroxide solutions. The exact effect of such co-adsorbed cationic layers remains to be fully understood, but the idea that solution cations may promote the reduction of oxy-anions is not new and may be explained by electrostatic effects (see, for example, ref 356).

9.5. Nitrate Reduction at Functionalized Electrodes

Nitrate reduction has primarily been studied on the same functionalized electrodes that have been used for nitrite reduction (section 8.2.3), although we should mention an older study by Tanaka et al.[357] on nitrate reduction to ammonia at a Mo−Fe cluster modified electrode. The ability of metal cyclams to electrocatalyze the reduction of nitrate, at rather negative potentials (ca. −1.4 V vs SCE), was first reported by Taniguchi et al.[271,358] using Co(III) and Ni(II) cyclams (cyclam = 1,4,8,11-tetra-azacyclotetradecane). On a mercury electrode, the main reduction product was found to be hydroxylamine. Taniguchi et al. speculated on the involvement of an adsorbed Co(I) or Ni(I) cyclam species as the effective catalyst. Li et al.[272,359] demonstrated that these Co and Ni cyclams may be incorporated into a Nafion film on gold and catalyze the reduction of nitrate to hydroxylamine in alkaline solution. Later, the same group[360] showed that direct adsorption of Co(III) cyclam onto gold also produced an active electrode surface for nitrate reduction in 3 M NaOH. Simon et al.[361] have studied the nitrate reduction by the same cyclam complexes after linking them to pyrrole and subsequently electropolymerizing them onto a gold electrode.

Metal phthalocyanine-modified electrodes have also been studied for nitrate reduction, primarily in alkaline media.[273,362] Ammonia seems to be the main product on these surfaces. Keita et al.[363] have reported the catalytic activity of Dawson-type heteropolyanions containing tungsten or molybdenum, as well as other metal cations, for the reduction of nitrate. The heteroployanions containing Cu(II) and Ni(II) proved the most efficient. More recently, Zhang et al.[364] reported the catalytic activity of multicopper-containing heteropolyoxotungstates for the electrochemical reduction of nitrate.

9.6. Nitrate Reduction by Enzymes

Nitrate reductases catalyze the reduction of nitrate to nitrite in the nitrogen cycle. Most nitrate reductases are generally large multiredox enzymes that have a molybdoptyrin (molybdenum−sulfur) complex as their active site, in addition to various other cofactors such as iron−sulfur and hemes that mediate electron transfer within the enzyme. There have been several interesting electrochemical studies of different nitrate reductases adsorbed onto graphite and gold electrodes.[365−368] It has been suggested from the extensive literature on molybdenum enzymes[369] and the above cited literature of protein film voltammetry of nitrate reductases that the molybdenum in the enzyme active site cycles between the Mo(VI) and Mo(IV) oxidation states, the latter being the oxidation state binding nitrate, returning to the Mo(VI) state after nitrite release.

10. Concluding Remarks

In this review, we have presented an extensive though incomplete account of the electrocatalytic reactions of inorganic nitrogen compounds, from ammonia oxidation to nitrate reduction. Our emphasis was focused on the various mechanisms suggested for the electrocatalysis by (modified) metal, often platinum, electrodes, with brief but we believe insightful comparisons to the way the same reactions are catalyzed by enzymes. Although it is easy to become impressed by the subtle chemistry performed by enzymes, the versatility of a single (but not simple) metal catalyst such as platinum for many of the reactions featuring in the nitrogen cycle is equally awe-inspiring.

The chemistry of the nitrogen cycle is highly complex due to the comparable stability (lability) of many of the relevant compounds. Dinitrogen is the most stable nitrogen compound and not surprisingly the most difficult one to convert into other compounds in the nitrogen cycle. Remarkably, the selective formation of dinitrogen from other relatively stable compounds, such as ammonia, nitric oxide, and nitrate, turns out to be highly complex. We believe that this remains a major challenge in the electrochemistry of nitrogen: to learn how to steer selectivity using a well-chosen catalyst for a well-chosen reaction pathway. We hope that this review will be of substantial help in prompting routes and ideas on how to establish high selectivities to, for example, dinitrogen and hydroxylamine. We have also repeatedly pointed out the importance of considering solution-phase reactions, especially in acidic media, because some of the actors in the nitrogen cycle (nitrite, hydroxylamine) tend to be highly reactive substances. There are still quite a few promising avenues to explore in this respect. The electrocatalysis of bimetallic surfaces or electrode surfaces modified by inorganic cations is still relatively unexplored and incompletely understood. Electrodes modified with metal macrocycles show some interesting reactivity (consider, for instance, the unique capability of metal cyclams to reduce nitrate to hydroxylamine) that remain relatively poorly understood. Combining such substances with more active metal substrates could also be very promising.

Finally, practical application of the catalysts discussed here may not necessarily involve electrochemical cells but rather liquid-phase heterogeneous catalysis with hydrogen or oxygen as the reducing or oxidizing agent. The equivalence of such an approach to electrochemistry has been discussed in the literature[370−372] but is still not widely embraced. Nevertheless, there has been a recent tendency in the literature to discuss the mechanisms of, for example, nitrite reduction and hydroxylamine oxidation on supported platinum catalysts in the aqueous phase also in terms of electrochemical (redox) reactions and to study them with similar spectroscopic techniques such as infrared spectroscopy.[373,374] It is hoped that the (un)equivalence of the two approaches will be further explored in the future by well-defined model approaches.

11. Acknowledgments

We gratefully acknowledge the contributions from and discussions with our colleagues Arnoud de Vooys, Guillermo Beltramo, Gabriela Dima, Maarten Merkx, Rob van Veen, and Rutger van Santen. We would also like to thank Dirk Heering for his comments on a first draft. The research described in this work was supported by grants from The Netherlands Organization for Scientific Research (NWO) and the National Research School Combination Catalysis (NRSC-C).

12. References

(1) Bothe, H., Ferguson, S., Newton, W. E., Eds.; *The Biology of the Nitrogen Cycle*; Elsevier: Amsterdam, 2006. See also a recent special issue of *Environmental Microbiology* 2008, volume *10*, edited by M. S. M. Jetten on "The microbial nitrogen cycle".
(2) Canter, L. W. *Nitrates in Groundwater*; CRC Press: Boca Raton, FL, 1997.
(3) Ferguson, S. J. *Curr. Opin. Chem. Biol.* **1998**, *2*, 182.
(4) Averill, B. A. *Chem. Rev.* **1996**, *96*, 2951.
(5) Wasser, I. M.; de Vries, S.; Moënne-Loccoz, P.; Schröder, I.; Karlin, K. D. *Chem. Rev.* **2002**, *102*, 1201.
(6) Bedioui, F.; Trevin, S.; Devynck, J. *Electroanalysis* **2005**, *8*, 1085.
(7) Moorcroft, M. J.; Davies, J.; Compton, R. G. *Talanta* **2001**, *54*, 785.
(8) Janssen, L. J. J.; Pieterse, M. M. J.; Barendrecht, E. *Electrochim. Acta* **1977**, *22*, 27.
(9) Van de Moesdijk, C. G. M. In *Catalysis of Organic Reactions in Chemical Industries*; Kosak, J. R., Ed.; Marcel Dekker: New York, 1984; vol. *18*, p 379. Van de Moesdijk, C. G. M. The Catalytic reduction of nitrate and nitric oxide to hydroxylamine: kinetics and mechanism, Ph.D. Thesis, Eindhoven University of Technology 1979.
(10) Bellusi, G.; Perego, C. *CATTECH* **2000**, *4*, 4.
(11) Gootzen, J. F. E.; Peeters, P. G. J. M.; Dukers, J. M. B.; Visscher, W.; van Veen, J. A. R. *J. Electroanal. Chem.* **1997**, *434*, 171.
(12) Oswin, H. G.; Salomon, M. *Can. J. Chem.* **1963**, *41*, 1686.
(13) Gerischer, H.; Mauerer, A. *J. Electroanal. Chem.* **1970**, *25*, 421.
(14) Hörold, S.; Vorlop, K.-D.; Tacke, T.; Sell, M. *Catal. Today* **1993**, *17*, 21.
(15) Prüsse, U.; Hähnlein, M.; Daum, J.; Vorlop, K.-D. *Catal. Today* **2000**, *55*, 79.
(16) Maloy, J. T. In *Standard Potentials in Aqueous Solutions*; Bard, A. J., Parsons, R., Jordan, J., Eds.; Marcel Dekker: New York, 1985; Chapter 7, p 127.
(17) Plieth, W. J. In *Encyclopedia of the Electrochemistry of the Elements*; Bard, A. J., Ed.; Marcel Dekker: New York, 1978; Vol. 8, p 321.
(18) Inzelt, G.; Horányi, G. In *Encyclopedia of Electrochemistry*; Pickett, C. J., Scholz, F., Eds.; Wiley-VCH: Weinheim, Germany, 2005; Vol. 7, p 241.
(19) Wynveen, R. A. *Fuel Cells* **1963**, *2*, 153.
(20) Simons, E. L.; Cairns, E. J.; Surd, D. J. *J. Electrochem. Soc.* **1969**, *116*, 556.
(21) Strickland, G. *J. Hydrogen Energy* **1984**, *9*, 759.
(22) Vitse, F.; Cooper, M.; Botte, G. G. *J. Power Sources* **2005**, *142*, 18.
(23) Marincic, L.; Leitz, F. B. *J. Appl. Electrochem.* **1978**, *8*, 333.
(24) Feng, C.; Sugiura, N.; Shimada, S.; Maekawa, T. *J. Hazard. Mater.* **2003**, *103*, 65.
(25) Pfennig, D.-M.; Deprez, J.; Kitzelmann, D. *Ber. Bunsen-Ges. Phys. Chem.* **1990**, *94*, 988.
(26) Lopez de Mishima, B. A.; Lescano, D.; Molina Holgado, T.; Mishima, H. T. *Electrochim. Acta* **1997**, *43*, 395.
(27) Halseid, R.; Wainwright, J. S.; Savinell, R. F.; Tunold, R. *J. Electrochem. Soc.* **2007**, *154*, B263.
(28) Wasmus, S.; Vasini, E. J.; Krausa, M.; Mishima, H. T.; Vielstich, W. *Electrochim. Acta* **1994**, *39*, 23.
(29) Gootzen, J. F. E.; Wonders, A.; Visscher, W.; van Santen, R. A.; van Veen, J. A. R. *Electrochim. Acta* **1998**, *43*, 1851.
(30) de Vooys, A. C. A.; Koper, M. T. M.; van Santen, R. A.; van Veen, J. A. R. *J. Electroanal. Chem.* **2001**, *506*, 127.
(31) Sexton, B. A.; Mitchell, G. E. *Surf. Sci.* **1980**, *99*, 523.
(32) Mieher, W. D.; Ho, W. *Surf. Sci.* **1995**, *322*, 151.
(33) Bradley, J. M.; Hopkinson, A.; King, D. A. *Surf. Sci.* **1997**, *371*, 255.
(34) Gohndrone, J. M.; Olsen, C. W.; Backman, A. L.; Gow, T. R.; Yagasaki, E.; Masel, R. I. *J. Vac. Sci. Technol.* **1989**, *7*, 1986.
(35) Bradley, J. M.; Hopkinson, A.; King, D. A. *J. Phys. Chem.* **1995**, *99*, 17032.
(36) Despic, A. R.; Drazic, D. M.; Rakin, P. M. *Electrochim. Acta* **1966**, *11*, 997.
(37) de Vooys, A. C. A.; Mrozek, M. F.; Koper, M. T. M.; Van Santen, R. A.; Van Veen, J. A. R.; Weaver, M. J. *Electrochem. Commun.* **2001**, *3*, 293.
(38) Vidal-Iglesias, F. J.; Solla-Gullón, J.; Perez, J. M.; Aldaz, A. *Electrochem. Commun.* **2006**, *8*, 102.
(39) Endo, K.; Katayama, Y.; Miura, T. *Electrochim. Acta* **2005**, *50*, 2181.
(40) Gao, Y.; Kita, H.; Hattori, H. *Chem. Lett.* **1994**, *11*, 2093.
(41) Vidal-Iglesias, F. J.; Garcia-Araez, N.; Montiel, V.; Feliu, J. M.; Aldaz, A. *Electrochem. Commun.* **2003**, *5*, 22.
(42) Vidal-Iglesias, F. J.; Solla-Gullon, J.; Montiel, V.; Feliu, J. M.; Aldaz, A. *J. Phys. Chem. B* **2005**, *109*, 12914.
(43) Vidal-Iglesias, F. J.; Solla-Gullón, J.; Feliu, J. M.; Baltruschat, H.; Aldaz, A. *J. Electroanal. Chem.* **2006**, *588*, 331.
(44) Vidal-Iglesias, F. J.; Solla-Gullón, J.; Rodrı´guez, P.; Herrero, E.; Montiel, V.; Feliu, J. M.; Aldaz, A. *Electrochem. Commun.* **2004**, *6*, 1080.
(45) Ahmadi, T. S.; Wang, Z. L.; Green, T. C.; Henglein, A.; El-Sayed, M. A. *Science* **1996**, *272*, 1924.
(46) Rosca, V.; Koper, M. T. M. *Phys. Chem. Chem. Phys.* **2006**, *8*, 2513.
(47) Novell-Leruth, G.; Valcarel, A.; Clotet, A.; Ricart, J. M.; Pérez-Ramı´rez, J. *J. Phys. Chem. B* **2005**, *109*, 18061.
(48) Offermans, W. K.; Jansen, A. P. J.; van Santen, R. A.; Novell-Leruth, G.; Ricart, J. M.; Pérez-Ramı´rez, J. *J. Phys. Chem. C* **2007**, *111*, 17551.
(49) Scheibe, U.; Lins, A.; Imbihl, R. *Surf. Sci.* **2005**, *577*, 1.
(50) López de Mishima, B. A.; Lescano, D.; Molina Holgado, T.; Mishima, H. T. *Electrochim. Acta* **1998**, *43*, 395.
(51) Endo, K.; Katayama, Y.; Miura, Y. *Electrochim. Acta* **2004**, *49*, 1635.
(52) Endo, K.; Nakamura, K.; Katayama, Y.; Miura, Y. *Electrochim. Acta* **2004**, *49*, 2503.
(53) Vidal-Iglesias, F. J.; Solla-Gullón, J.; Montiel, V.; Feliu, J. M.; Aldaz, A. *J. Power Sources* **2007**, *117*, 448.
(54) Moran, E.; Cattaneo, C.; Mishima, H.; Lopez de Mishima, B. A.; Silvetti, S. P.; Rodrı´guez, J. L.; Pastor, E. *J. Solid State Electrochem.* **2008**, *12*, 583.
(55) Yao, K.; Cheng, Y. F. *J. Power Sources* **2007**, *173*, 96.
(56) Strous, M.; Jetten, M. S. M. *Annu. Rev. Microbiol.* **2004**, *58*, 99.
(57) Szpak, S.; Stonehart, P.; Katan, T. *Electrochim. Acta* **1965**, *10*, 563.
(58) Nesterov, B. P.; Korovin, N. V.; Yanchuk, B. N. *Elektrokhimiya* **1969**, *5*, 298.
(59) Harrison, J. A.; Khan, Z. A. *J. Electroanal. Chem.* **1970**, *28*, 131.
(60) Petek, M.; Bruckenstein, S. *J. Electroanal. Chem.* **1973**, *47*, 329.
(61) Garcia Azorero, M. D.; Marcos, M. L.; Gonzalez Velasco, J. *Electrochim. Acta* **1994**, *39*, 1909.
(62) Garcia Azorero, M. D.; Marcos, M. L.; Velasco, J. G. *Electroanalysis* **1996**, *8*, 267.
(63) Nishihara, C.; Raspini, I. A.; Kondoh, H.; Shindo, H.; Kaise, M.; Nozoye, H. *J. Electroanal. Chem.* **1992**, *338*, 299.
(64) Gomez, R.; Orts, J. M.; Rodes, A.; Feliu, J. M.; Aldaz, A. *J. Electroanal. Chem.* **1993**, *358*, 287.
(65) Alvarez-Ruiz, B.; Gomez, R.; Orts, J. M.; Feliu, J. M. *J. Electrochem. Soc.* **2002**, *149*, D35.
(66) Rosca, V.; Koper, M. T. M. *Electrochim. Acta* **2008**, *53*, 5199.
(67) Harrison, J. A.; Khan, Z. A. *J. Electroanal. Chem.* **1970**, *26*, 1.
(68) Heitbaum, J.; Vielstich, W. *Electrochim. Acta* **1973**, *18*, 501.
(69) Fukumoto, Y.; Matsunaga, T.; Hayashi, T. *Electrochim. Acta* **1981**, *26*, 631.
(70) Kodera, T.; Honda, M.; Kita, H. *Electrochim. Acta* **1985**, *30*, 669.
(71) Alberas, D. J.; Kiss, J.; Liu, Z.-M.; White, J. M. *Surf. Sci.* **1992**, *278*, 51.
(72) Korovin, N. V.; Yanchuk, B. N. *Electrochim. Acta* **1970**, *15*, 569.
(73) Korinek, K.; Koryta, J.; Musilova, M. *J. Electroanal. Chem.* **1969**, *21*, 319.
(74) Fleischmann, M.; Korinek, K.; Pletcher, D. *J. Electroanal. Chem.* **1972**, *34*, 499.
(75) Gao, G.; Guo, D.; Wang, C.; Li, H. *Electrochem. Commun.* **2007**, *9*, 1582.
(76) Kokkinidis, G.; Jannakoukadis, P. D. *J. Electroanal. Chem.* **1981**, *130*, 153.
(77) Wang, P.; Yuan, Y.; Wang, X. P.; Zhu, G. Y. *J. Electroanal. Chem.* **2000**, *493*, 130.
(78) Cataldi, T. R. I.; Benedetto, G. D.; Bianchini, A. *J. Electroanal. Chem.* **1999**, *471*, 42.
(79) Shankaran, D. R.; Narayanan, S. S. *Russ. J. Electrochem.* **2002**, *38*, 987.
(80) Salimi, A.; Abdi, K. *Talanta* **2004**, *63*, 475.
(81) Zheng, J.; Sheng, Q.; Li, L.; Shen, Y. *J. Electroanal. Chem.* **2007**, *611*, 155.
(82) Zagal, J. H.; Lira, S.; Ureta-Zañartu, S. *J. Electroanal. Chem.* **1986**, *210*, 95.
(83) Geraldo, D.; Linares, C.; Chen., Y.-Y.; Ureta-Zañartu, S.; Zagal, J. H. *Electrochem. Commun.* **2002**, *4*, 182.
(84) Dantas, L. M. F.; dos Reis, A. P.; Tanaka, S. M. C. N.; Zagal, J. H.; Chen, Y.-Y.; Tanaka, A. A. *J. Braz. Chem. Soc.* **2008**, *19*, 720.
(85) Pang, D.-W.; Deng, B.-H.; Wang, Z.-L. *Electrochim. Acta* **1994**, *39*, 847.
(86) Bennett, J. E.; Malinski, T. *Chem. Mater.* **1991**, *3*, 490.
(87) Zagal, J. H.; Páez, M. A. *Electrochim. Acta* **1997**, *42*, 3477.
(88) Linares, C.; Geraldo, D.; Paez, M.; Zagal, J. H. *J. Solid State Electrochem.* **2003**, *7*, 626.
(89) Chorkendorff, I; Niemantsverdriet, J. W. *Concepts of Modern Catalysis and Kinetics*; Wiley-VCH: Weinheim, Germany, 2003.
(90) Paredes-García, V.; Cárdenas-Jirón, G. I.; Venegas-Yazigi, D.; Zagal, J. H.; Paez, M.; Costamagna, C. *J. Phys. Chem. A* **2005**, *109*, 1196.
(91) Cárdenas-Jirón, G. I.; Paredes-García, V.; Venegas-Yazigi, D.; Zagal, J. H.; Paez, M.; Costamagna, C. *J. Phys. Chem. A* **2006**, *110*, 11870.

(92) Schalk, J.; Oustad, H.; Kuenen, J. G.; Jetten, M. S. M. *FEMS Microbiol. Lett.* **1998**, *158*, 61.
(93) Jetten, M. S. M. *FEMS Microbiol. Revs.* **1999**, *22*, 421.
(94) Tauszik, G. R.; Grocetta, P. *Appl. Catal.* **1985**, *17*, 1.
(95) Ritz, J.; Fuchs, H.; Perryman, H. G. Hydroxylamine. *Ulmann's Encyclopedia of Industrial Chemistry*, 6th ed.; Wiley: Chichester, U.K., 2000.
(96) Doring, C.; Gehlen, H. *Z. Anorg. Allg. Chem.* **1961**, *312*, 32.
(97) Möller, D.; Heckner, K. H. *Z. Chem.* **1971**, *11*, 157.
(98) Möller, D.; Heckner, K. H. *Z. Phys. Chem.* **1974**, *255*, 33.
(99) Möller, D.; Heckner, K. H. *Z. Chem.* **1971**, *11*, 32.
(100) Möller, D.; Heckner, K. H. *Z. Chem.* **1971**, *11*, 356.
(101) Möller, D.; Heckner, K. H. *Z. Chem.* **1970**, *10*, 477.
(102) Möller, D.; Heckner, K. H. *Z. Phys. Chem.* **1972**, *251*, 81.
(103) Karabinas, P.; Wolter, O.; Heitbaum, J. *Ber. Bunsen-Ges. Phys. Chem.* **1984**, *88*, 1191.
(104) Piela, B.; Wrona, P. K. *J. Electrochem. Soc.* **2004**, *151*, E69.
(105) Rosca, V.; Beltramo, G. L.; Koper, M. T. M. *J. Electroanal. Chem.* **2004**, *566*, 53.
(106) Rosca, V.; Beltramo, G. L.; Koper, M. T. M. *J. Phys. Chem. B* **2004**, *108*, 8294.
(107) Rosca, V.; Koper, M. T. M. *J. Phys. Chem. B* **2005**, *109*, 16750.
(108) Wonders, A. H.; Housmans, T. H. M.; Rosca, V.; Koper, M. T. M. *J. Appl. Electrochem.* **2006**, *36*, 1215.
(109) Van der Vliet, D., M.Sc. Thesis, Eindhoven University of Technology, 2005.
(110) Zagal, J.; Villar, E.; Ureta-Zanartu, S. *J. Electroanal. Chem.* **1982**, *115*, 343.
(111) Ebadi, M. *Electrochim. Acta* **2003**, *48*, 4233.
(112) Cui, X.; Hong, L.; Lin, X. *Anal. Sci.* **2002**, *18*, 543.
(113) Shi, L.; Wu, T.; He, P.; Li, D.; Sun, C.; Li, J. *Electroanalysis* **2005**, *17*, 2190.
(114) Zare, H. R.; Nasirizadeh, N. *Electroanalysis* **2006**, *18*, 507.
(115) Zare, H. R.; Sobhani, Z.; Mazloum-Ardakani, M. *Sens. Actuators B* **2007**, *126*, 641.
(116) Hooper, A. B.; Vannelli, T.; Bergmann, D. J.; Arciero, D. M. *Antonie van Leeuwenhoek* **1997**, *71*, 59.
(117) Mowat, C. G.; Chapman, S. K. *Dalton Trans.* **2005**, 3381.
(118) Hendrich, M. P.; Logan, M.; Andersson, K. K.; Arciero, D. M.; Lipscomb, J. D.; Hooper, A. B. *J. Am. Chem. Soc.* **1994**, *116*, 11961.
(119) Hendrich, M. P.; Upadhyay, A. K.; Riga, J.; Arciero, D. M.; Hooper, A. B. *Biochemistry* **2002**, *41*, 4603.
(120) Fernández, M. L.; Estrin, D. A.; Bari, S. E. *J. Inorg. Biochem.* **2008**, *102*, 1523.
(121) Chatt, J. R.; da Camara Pina, L. M.; Richards, R. L. *New Trends in the Chemistry of Nitrogen Fixation*; Academic Press: London, 1980.
(122) Postgate, J. R. *Nitrogen Fixation*; Cambrige University Press: Cambridge, U.K., 1998.
(123) Pickett, C. J. *J. Biol. Inorg. Chem.* **1996**, *1*, 601.
(124) Hidai, M. *Coord. Chem. Rev.* **1999**, *185*−*186*, 99.
(125) Becker, J. Y.; Posin, B. *J. Electroanal. Chem.* **1988**, *250*, 385.
(126) Pickett, C. J.; Talarmin, J. *Nature* **1985**, *317*, 652.
(127) Marnellos, G.; Stoukides, M. *Science* **1998**, *282*, 98.
(128) Kordali, V.; Kyriacou, G.; Lambrou, Ch. *Chem. Commun.* **2000**, 1673.
(129) Köleli, F.; Röpke, T. *Appl. Catal., B* **2006**, *62*, 306.
(130) Pospı´šil, L.; Bulı´čková, J.; Hromadová, M.; Gál, M.; Civiš, S.; Cihelka, J.; Tarábek, J. *Chem. Commun.* **2007**, 2270.
(131) Pospı´šil, L.; Hromadová, M.; Gál, M.; Bulı´čková, J.; Sokolová, R.; Fanelli, N. *Electrochim. Acta* **2008**, *53*, 7445.
(132) Ebert, H.; Parsons, R.; Ritzoulis, G.; VanderNoot, T. *J. Electroanal. Chem.* **1989**, *264*, 181.
(133) Johnson, K. E.; Sawyer, D. T. *J. Electroanal. Chem.* **1974**, *49*, 95.
(134) Ahmadi, A.; Bracey, E.; Wyn Evans, R.; Attard, G. *J. Electroanal. Chem.* **1993**, *350*, 297.
(135) Haq, S.; Hodgson, A. *Surf. Sci.* **2000**, *463*, 1.
(136) Kokalj, A. *Surf. Sci.* **2003**, *532*−*535*, 213.
(137) De Vooys, A. C. A.; Koper, M. T. M.; van Santen, R. A.; van Veen, J. A. R. *J. Catal.* **2001**, *202*, 387.
(138) Tavares, P.; Pereira, A. S.; Moura, J. J. G.; Moura, I. *J. Inorg. Biochem.* **2006**, *100*, 2087.
(139) Chen, P.; Gorelsky, S. I.; Ghosh, S.; Solomon, E. I. *Angew. Chem., Int. Ed.* **2004**, *43*, 4132.
(140) Koshland, D. E., Jr. *Science* **1992**, *258*, 1861. Culotta, E.; Koshland, D. E., Jr. *Science* **1992**, *258*, 1862.
(141) Djerassi, C. *NO*; Penguin Books: New York, 2000.
(142) Allen, B. W.; Piantadosi, C. A.; Coury, L. A., Jr. *Nitric Oxide* **2000**, *4*, 75.
(143) Gootzen, J. F. E.; van Hardeveld, R. M.; Visscher, W.; van Santen, R. A.; van Veen, J. A. R. *Recl. Trav. Chim. Pays-Bas* **1996**, *115*, 480.
(144) de Vooys, A. C. A.; Koper, M. T. M.; van Santen, R. A.; van Veen, J. A. R. *Electrochim. Acta* **2001**, *46*, 923.
(145) Masel, R. I. *Catal. Rev. Sci. Eng.* **1986**, *28*, 335.
(146) Levoguer, C. L.; Nix, R. M. *Surf. Sci.* **1996**, *365*, 672.
(147) Gorte, R. J.; Gland, J. L. *Surf. Sci.* **1981**, *102*, 34.
(148) Brown, W. A.; Sharma, R. K.; King, D. A. *J. Phys. Chem. B* **1998**, *102*, 5303.
(149) Agrawal, V. K.; Trenary, M. *Surf. Sci.* **1991**, *259*, 116.
(150) Rienks, E. D. L.; Bakker, J. W.; Baraldi, A.; Carabiniero, S. A. C.; Lizzit, S.; Weststrate, C. J.; Nieuwenhuys, B. E. *Surf. Sci.* **2002**, *516*, 109.
(151) Smirnov, M. Y.; Gorodetskii, V. V.; Cholach, A. R. In *Fundamental Aspects of Heterogeneous Catalysis Studied by Particle Beams*; Brongersma, H. H., van Santen, R. A., Eds.; Plenum Press: New York, 1991; p 249.
(152) Smirnov, M. Y.; Gorodetskii, V. V.; Block, J. H. *J. Mol. Catal. A: Chem.* **1996**, *107*, 359.
(153) Matsumoto, M.; Fukutani, K.; Okano, T.; Miyake, K.; Shigekawa, H.; Kato, H.; Okuyama, H.; Kawai, M. *Surf. Sci.* **2000**, *454*−*456*, 101.
(154) Matsumoto, M.; Tatsumi, T.; Fukutani, K.; Okano, T. *Surf. Sci.* **2002**, *513*, 485.
(155) Aizawa, H.; Morikawa, Y.; Tsuneyuki, S.; Fukutani, K.; Ohno, T. *Surf. Sci.* **2002**, *514*, 394.
(156) Gardner, P.; Tueshaus, M.; Martin, R.; Bradshaw, A. M. *Surf. Sci.* **1990**, *240*, 112.
(157) Ge, Q.; Neurock, M. *J. Am. Chem. Soc.* **2004**, *126*, 1551.
(158) Gomez, R.; Rodes, A.; Orts, J. M.; Feliu, J. M.; Perez, J. M. *Surf. Sci.* **1995**, *342*, L1104.
(159) Rodes, A; Gomez, R.; Perez, J. M.; Feliu, J. M.; Aldaz, A. *Electrochim. Acta* **1996**, *41*, 729.
(160) Alvarez, B.; Rodes, A.; Perez, J. M.; Feliu, J. M. *Langmuir* **2000**, *16*, 4695.
(161) Weaver, M. J.; Zou, S.; Tang, C. *J. Chem. Phys.* **1999**, *111*, 368.
(162) Beltramo, G. L.; Koper, M. T. M. *Langmuir* **2003**, *19*, 8907.
(163) Rodes, A.; Climent, V.; Orts, J. M.; Perez, J. M.; Aldaz, A. *Electrochim. Acta* **1998**, *44*, 1077.
(164) Rosca, V.; Beltramo, G. L.; Koper, M. T. M. *Langmuir* **2005**, *21*, 1448.
(165) Lebedeva, N. P.; Koper, M. T. M.; Herrero, E.; Feliu, J. M.; van Santen, R. A. *J. Electroanal. Chem.* **2000**, *487*, 37.
(166) Lebedeva, N. P.; Koper, M. T. M.; Feliu, J. M.; van Santen, R. A. *J. Phys. Chem. B* **2002**, *106*, 12938.
(167) Nakata, K.; Okubo, A.; Shimazu, K.; Yamakata, A.; Ye, S.; Osawa, M. *Langmuir* **2008**, *24*, 4352.
(168) Cuesta, A.; Escudero, M. *Phys. Chem. Chem. Phys.* **2008**, *10*, 3628.
(169) Rosca, V.; Koper, M. T. M. *Surf. Sci.* **2005**, *584*, 258.
(170) Koper, M. T. M. *Z. Phys. Chem.* **2003**, *217*, 547.
(171) Dutta, D.; Landolt, D. *J. Electrochem. Soc.* **1972**, *119*, 1320.
(172) Savodnik, N. N.; Shepelin, V. A.; Zalkind, T. I. *Elektrokhimiya* **1970**, *7*, 424.
(173) Janssen, L. J. J.; Pieterse, M. M. J.; Barendrecht, E. *Electrochim. Acta* **1977**, *22*, 27.
(174) Paseka, I.; Vonkova, J. *Electrochim. Acta* **1980**, *25*, 1251.
(175) Paseka, I.; Hodinar, A. *Electrochim. Acta* **1982**, *27*, 1461.
(176) Colucci, J. A.; Foral, M. J.; Langer, S. H. *Electrochim. Acta* **1985**, *30*, 521.
(177) Brown, W. A.; King, D. A. *J. Phys. Chem. B* **2000**, *104*, 2578.
(178) Zaera, F.; Gopinath, C. S. *Chem. Phys. Lett.* **2000**, *332*, 209.
(179) Hess, C.; Ozensoy, E.; Yi, C.-W.; Goodman, D. W. *J. Am. Chem. Soc.* **2006**, *128*, 2988.
(180) Foral, M. J.; Langer, S. H. *Electrochim. Acta* **1988**, *33*, 257.
(181) Foral, M. J.; Langer, S. H. *Electrochim. Acta* **1991**, *36*, 299.
(182) Gómez, R.; Rodes, A.; Pérez, J. M.; Feliu, J. M. *J. Electroanal. Chem.* **1995**, *393*, 123.
(183) Rodes, A; Gomez, R.; Perez, J. M.; Feliu, J. M.; Aldaz, A. *Electrochim. Acta* **1996**, *41*, 729.
(184) Kao, C. T.; Blackman, G. S.; Van Hove, M. A.; Somorjai, G. A.; Chan, C. *Surf. Sci.* **1989**, *224*, 77.
(185) Villarubia, J. S.; Ho, W. *J. Chem. Phys.* **1987**, *87*, 750.
(186) Zou, S.; Gomez, R.; Weaver, M. J. *J. Electroanal. Chem.* **1999**, *474*, 155.
(187) Alvarez, B.; Rodes, A.; Perez, J. M.; Feliu, J. M.; Rodriguez, J. L.; Pastor, E. *Langmuir* **2000**, *16*, 4695.
(188) Yan, Y.-G.; Huang, B.-B.; Wang, J.-Y.; Wang, H.-F.; Cai, W.-B. *J. Catal.* **2007**, *249*, 311.
(189) Hayden, B. E.; Kretzschmar, K.; Bradshaw, A. M. *Surf. Sci.* **1983**, *125*, 366.
(190) Colucci, J. A.; Foral, M. J.; Langer, S. H. *Electrochim. Acta* **1985**, *30*, 1675.
(191) De Vooys, A. C. A.; Koper, M. T. M.; van Santen, R. A.; van Veen, J. A. R. *J. Catal.* **2001**, *202*, 387.
(192) Suzuki, S.; Nakato, T.; Hattori, H.; Kita, H. *J. Electroanal. Chem.* **1995**, *396*, 143.
(193) Shibata, M.; Murase, K.; Furuya, N. *J. Appl. Electrochem.* **1998**, *28*, 1121.

(194) Park, S.-Y.; Shimizu, H.; Adachi, S.-i.; Nakagawa, A.; Tanaka, I.; Nakahara, K.; Shoun, H.; Obayashi, E.; Nakamura, H.; Iizuka, T.; Shiro, Y. *Nat. Struct. Biol.* **1997**, *4*, 827.
(195) Feng, Z. Q.; Sagara, T.; Niki, K. *Anal. Chem.* **1995**, *67*, 3564.
(196) Sagara, T.; Takagi, S.; Niki, K. *J. Electroanal. Chem.* **1993**, *349*, 159.
(197) Tao, N. J.; Cardenas, G.; Cunha, F.; Shi, Z. *Langmuir* **1995**, *11*, 4445.
(198) de Groot, M. T.; Wonders, A. H.; Merkx, M.; Koper, M. T. M. *J. Am. Chem. Soc.* **2005**, *127*, 7579.
(199) Younathan, J. N.; Wood, K. S.; Meyer, T. J. *Inorg. Chem.* **1992**, *31*, 3280.
(200) Mimica, D.; Zagal, J. H.; Bedioui, F. *J. Electroanal. Chem.* **2001**, *497*, 106.
(201) de Groot, M. T.; Merkx, M.; Koper, M. T. M. *J. Am. Chem. Soc.* **2005**, *127*, 16224.
(202) Katz, E.; Willner, I. *Langmuir* **1997**, *13*, 3364.
(203) Pilloud, D. L.; Chen, X.; Dutton, P. L.; Moser, C. C. *J. Phys. Chem. B* **2000**, *104*, 2868.
(204) de Groot, M. T.; Merkx, M.; Koper, M. T. M. *C. R. Chim.* **2007**, *10*, 414.
(205) Shigehara, K.; Anson, F. C. *J. Phys. Chem.* **1982**, *86*, 2776.
(206) Collman, J. P.; Devaraj, N. K.; Decreau, R. A.; Yang, Y.; Yan, Y.-L.; Ebina, W.; Eberspacher, T. A.; Chidsey, C. E. D. *Science* **2007**, *315*, 1565.
(207) Bedioui, F.; Trevin, S.; Albin, V.; Gomez Villegas, M. G.; Devynck, J. *Anal. Chim. Acta* **1997**, *341*, 177.
(208) Hayon, J.; Ozer, D.; Rishpon, J.; Bettelheim, A. *Chem. Commun.* **1994**, 619.
(209) Otsuka, K.; Sawada, H.; Yamanaka, I. *J. Electrochem. Soc.* **1996**, *143*, 3491.
(210) Ogura, K.; Yamasaki, S. *J. Appl. Electrochem.* **1985**, *15*, 279.
(211) Vilakazi, S. L.; Nyokong, T. *Electrochim. Acta* **2000**, *46*, 453.
(212) Pan, K.-C.; Chuang, C.-S.; Cheng, S.-H.; Su, Y. O. *J. Electroanal. Chem.* **2001**, *501*, 160.
(213) Bayachou, M.; Lin, R.; Cho, W.; Farmer, P. J. *J. Am. Chem. Soc.* **1998**, *120*, 9888.
(214) Immoos, C. E.; Chou, J.; Bayachou, M.; Blair, E.; Greaves, J.; Farmer, P. J. *J. Am. Chem. Soc.* **2004**, *126*, 4934.
(215) Mimica, D.; Zagal, J. H.; Bedioui, F. *Electrochem. Commun.* **2001**, *3*, 435.
(216) de Groot, M. T.; Merkx, M.; Koper, M. T. M. *Electrochem. Commun.* **2006**, *8*, 999.
(217) Sagara, T.; Sakai, T.; Nagatani, H. *Electrochem. Commun.* **2007**, *8*, 2018.
(218) Ye, S.; Kita, H. *J. Electroanal. Chem.* **1993**, *346*, 489.
(219) Momoi, K.; Song, M.; Ito, M. *J. Electroanal. Chem.* **1999**, *473*, 43.
(220) Casero, E.; Alonso, C.; Martin-Gago, J. A.; Borgatti, F.; Felici, R.; Renner, F.; Lee, T.; Zegenhagen, J. *Surf. Sci.* **2002**, *507−510*, 688.
(221) De Vooys, A. C. A.; Beltramo, G. L.; van Riet, B.; van Veen, J. A. R.; Koper, M. T. M. *Electrochim. Acta* **2004**, *49*, 1307.
(222) Dutta, D.; Landolt, D. *J. Electrochem. Soc.* **1972**, *119*, 1320.
(223) Trévin, S.; Bedioui, F.; Devynck, J. *J. Electroanal. Chem.* **1996**, *408*, 261.
(224) Diab, N.; Schuhmann, W. *Electrochim. Acta* **2001**, *47*, 265.
(225) Pereira-Rodrigues, N.; Albin, V.; Koudelka-Hep, M.; Auger, V.; Pailleret, A.; Bedioui, F. *Electrochem. Commun.* **2002**, *11*, 922.
(226) Vilakazi, S. L.; Nyokong, T. *Electrochim. Acta* **2000**, *46*, 453.
(227) Daiber, A.; Nauser, T.; Takaya, N.; Kudo, T.; Weber, P.; Hultschig, C.; Shoun, H.; Ullrich, V. *J. Inorg. Biochem.* **2002**, *88*, 343.
(228) Kudo, T.; Takaya, N.; Park, S.-Y.; Shiro, Y.; Shoun, H. *J. Biol. Chem.* **2001**, *276*, 5020.
(229) Obayashi, E.; Tsukamoto, K.; Adachi, S.-i.; Takahashi, S.; Nomura, M.; Iizuka, T.; Shoun, H.; Shiro, Y. *J. Am. Chem. Soc.* **1997**, *119*, 7807.
(230) Shimizu, H.; Park, S. Y.; Lee, D. S.; Shoun, H.; Shiro, Y. *J. Inorg. Biochem.* **2000**, *81*, 191.
(231) de Vries, S.; Schroeder, I. *Biochem. Soc. Trans.* **2002**, *30*, 662.
(232) Suharti; Heering, H. A.; de Vries, S. *Biochemistry* **2004**, *43*, 13487.
(233) Oshima, R.; Fushinobu, S.; Su, F.; Zhang, L.; Takaya, N.; Shoun, H. *J. Mol. Biol.* **2004**, *342*, 207.
(234) Einsle, O.; Messerschmidt, A.; Huber, R.; Kroneck, P. M. H.; Neese, F. *J. Am. Chem. Soc.* **2002**, *124*, 11737.
(235) Poock, S. R.; Leach, E. R.; Moir, J. W. B.; Cole, J. A.; Richardson, D. J. *J. Biol. Chem.* **2002**, *277*, 23664.
(236) Coyle, C. M.; Vogel, K. M.; Rush, T. S., III; Kozlowski, P. M.; Williams, R.; Spiro, T. G.; Dou, Y.; Ikeda-Saito, M.; Olson, J. S.; Zgierski, M. Z. *Biochemistry* **2003**, *42*, 4896.
(237) Hu, S.; Kincaid, J. R. *J. Am. Chem. Soc.* **1991**, *113*, 9760.
(238) Vogel, K. M.; Kozlowski, P. M.; Zgierski, M. Z.; Spiro, T. G. *J. Am. Chem. Soc.* **1999**, *121*, 9915.
(239) Gwyer, J. D.; Angove, H. C.; Richardson, D. J.; Butt, J. N. *Bioelectrochemistry* **2004**, *63*, 43.
(240) Harrison, C. C.; Malati, M. A.; Smetham, N. B. *J. Solution Chem.* **1995**, *25*, 505.
(241) Park, J.-Y.; Lee, Y.-N. *J. Phys. Chem.* **1988**, *92*, 6294.
(242) Todras, Z. V. *Organic Ion Radicals*; CRC Press: Boca Raton, FL, 2002; p 63.
(243) Gadde, R. R.; Bruckenstein, S. *J. Electroanal. Chem.* **1974**, *50*, 163.
(244) Nishimura, K.; Machida, K.; Enyo, M. *Electrochim. Acta* **1991**, *36*, 877.
(245) Bae, I. T.; Barbour, R. L.; Scherson, D. A. *Anal. Chem.* **1997**, *69*, 249.
(246) Da Cunha, M. C. P. M.; Nart, F. C. *Phys. Status Solidi a* **2001**, *187*, 25.
(247) Snider, B. G.; Johnson, D. C. *Anal. Chim. Acta* **1979**, *105*, 9.
(248) Heckner, H. N.; Schmid, G. *Electrochim. Acta* **1971**, *16*, 131.
(249) Garcia, C. T.; Calandra, A. J.; Arvia, A. J. *Electrochim. Acta* **1972**, *17*, 2181.
(250) Vanderplas, J. F.; Barendrecht, E. *Rec. Trav. Chim. Pays-Bas.* **1977**, *96*, 133.
(251) Genders, J. D.; Hartsough, D.; Hobbs, D. T. *J. Appl. Electrochem.* **1996**, *26*, 1.
(252) Horanyi, G.; Rizmayer, E. M. *J. Electroanal. Chem.* **1985**, *188*, 265.
(253) Ye, S.; Hattori, H.; Kita, H. *Ber. Bunsen-Ges. Phys. Chem.* **1992**, *96*, 1884.
(254) Brylev, O.; Sarrazin, M.; Roue, L.; Belanger, D. *Electrochim. Acta* **2007**, *52*, 6237.
(255) de Vooys, A. C. A.; van Santen, R. A.; van Veen, J. A. R. *J. Mol. Catal. A: Chem.* **2000**, *154*, 203.
(256) Bae, S. E.; Stewart, K. L.; Gewirth, A. A. *J. Am. Chem. Soc.* **2007**, *129*, 10171.
(257) Cattarin, S. *J. Appl. Electrochem.* **1992**, *22*, 1077.
(258) Denuault, G.; Milhano, C.; Pletcher, D. *Phys. Chem. Chem. Phys.* **2005**, *7*, 3545.
(259) De, D.; Englehardt, J. D.; Kalu, E. E. *J. Electrochem. Soc.* **2000**, *147*, 4224.
(260) De, D. D.; Englehardt, J. D.; Kalu, E. E. *J. Electrochem. Soc.* **2000**, *147*, 4573.
(261) De, D.; Kalu, E. E.; Tarjan, P. P.; Englehardt, J. D. *Chem. Eng. Technol.* **2004**, *27*, 56.
(262) Duca, M.; Kavvadia, V.; Rodriduez, P.; Koper, M. T. M., manuscript in preparation.
(263) Lin, R.; Bayachou, M.; Greaves, J.; Farmer, P. J. *J. Am. Chem. Soc.* **1997**, *119*, 12689.
(264) Mimica, D.; Zagal, J. H.; Bedioui, F. *J. Electroanal. Chem.* **2001**, *497*, 106.
(265) Jiang, H.-J.; Yang, H.; Akins, D. L. *J. Electroanal. Chem.* **2008**, in press.
(266) Barley, M. H.; Takeuchi, K. J.; Meyer, T. J. *J. Am. Chem. Soc.* **1986**, *108*, 5876.
(267) Barley, M. H.; Rhodes, M. R.; Meyer, T. J. *Inorg. Chem.* **1987**, *26*, 1746.
(268) Rhodes, M. R.; Barley, M. H.; Meyer, T. J. *Inorg. Chem.* **1991**, *30*, 629.
(269) Toth, J. E.; Anson, F. C. *J. Am. Chem. Soc.* **1989**, *111*, 2444.
(270) Zhang, J.; Lever, A. B. P.; Pietro, W. J. *Inorg. Chem.* **1994**, *33*, 1392.
(271) Taniguchi, I.; Nakashima, N.; Matsushita, K.; Yasukouchi, K. *J. Electroanal. Chem.* **1987**, *224*, 199.
(272) Li, H.-L.; Chambers, J. Q.; Hobbs, D. T. *J. Electroanal. Chem.* **1988**, *256*, 447.
(273) Chebotareva, N.; Nyokong, T. *J. Appl. Electrochem.* **1997**, *27*, 975.
(274) Vetter, K. J. *Z. Phys. Chem.* **1950**, *194*, 199.
(275) Tanaka, N.; Kato, K. *Bull. Chem. Soc. Jpn.* **1956**, *29*, 837.
(276) Raspi, G.; Pergola, F. *Chim. Ind. (Milan, Italy)* **1963**, 45.
(277) Guidelli, R.; Pergola, F.; Raspi, G. *Anal. Chem.* **1972**, *44*, 745.
(278) Piela, B.; Wrona, P. K. *J. Electrochem. Soc.* **2002**, *149*, E55.
(279) Piela, B.; Piela, P.; Wrona, P. K. *J. Electrochem. Soc.* **2002**, *149*, E357.
(280) Xing, X.; Scherson, D. A. *Anal. Chem.* **1988**, *60*, 1468.
(281) Tau, P.; Nyokong, T. *J. Electroanal. Chem.* **2007**, *611*, 10.
(282) Matemadombo, F.; Nyokong, T. *Electrochim. Acta* **2007**, *52*, 6856.
(283) Klotz, M. G.; Schmid, M. C.; Strous, M.; Op den Camp, H. J. M.; Jetten, M. S. M.; Hooper, A. B. *Environ. Microbiol.* **2008**, *10*, 3150.
(284) Heering, H. A.; Wiertz, F. G. M.; Dekker, C.; de Vries, S. *J. Am. Chem. Soc.* **2004**, *126*, 11103.
(285) Angove, H. C.; Cole, J. A.; Richardson, D. J.; Butt, J. N. *J. Biol. Chem.* **2002**, *277*, 23374.
(286) Gwyer, J. D.; Angove, H. C.; Richardson, D. J.; Butt, J. N. *Bioelectrochemistry* **2004**, *63*, 43.
(287) Wijma, H. J.; Jeuken, L. J. C.; Verbeet, M. Ph.; Armstrong, F. A.; Canters, G. W. *J. Am. Chem. Soc.* **2007**, *129*, 8557.
(288) de Groot, M. T.; Koper, M. T. M. *J. Electroanal. Chem.* **2004**, *562*, 81.
(289) Kinza, H.; Lohse, H. *Z. Phys. Chem.-Leipzig* **1975**, *256*, 233.
(290) Horanyi, G.; Rizmayer, E. M. *J. Electroanal. Chem.* **1982**, *140*, 347.

(291) Horanyi, G.; Rizmayer, E. M. *J. Electroanal. Chem.* **1985**, *188*, 273.
(292) Petrii, O. A.; Safonova, T. Y. *J. Electroanal. Chem.* **1992**, *331*, 897.
(293) Safonova, T. Y.; Petrii, O. A. *Russ. J. Electrochem.* **1995**, *31*, 1269.
(294) daCunha, M.; Weber, M.; Nart, F. C. *J. Electroanal. Chem.* **1996**, *414*, 163.
(295) Dima, G. E.; de Vooys, A. C. A.; Koper, M. T. M. *J. Electroanal. Chem.* **2003**, *554*, 15.
(296) Santos, A. L.; Deiner, L. J.; Varela, H. *Catal. Commun.* **2008**, *9*, 269.
(297) Gootzen, J. F. E.; Peeters, P.; Dukers, J. M. B.; Lefferts, L.; Visscher, W.; vanVeen, J. A. R. *J. Electroanal. Chem.* **1997**, *434*, 171.
(298) Dima, G. E.; Rosca, V.; Koper, M. T. M. *J. Electroanal. Chem.* **2007**, *599*, 167.
(299) Nakata, K.; Kayama, Y.; Shimazu, K.; Yamakata, A.; Ye, S.; Osawa, M. *Langmuir* **2008**, *24*, 4358.
(300) Dima, G. E.; Beltramo, G. L.; Koper, M. T. M. *Electrochim. Acta* **2005**, *50*, 4318.
(301) Taguchi, S.; Feliu, J. M. *Electrochim. Acta* **2007**, *52*, 6023.
(302) Taguchi, S.; Feliu, J. M. *Electrochim. Acta* **2008**, *53*, 3626.
(303) Vijh, A. K. *J. Catal.* **1974**, *32*, 230.
(304) Khomutov, N. E.; Stamkulov, U. S. *Elektrokhimiya* **1971**, *7*, 332.
(305) Ureta-Zanaru, S.; Yanez, C. *Electrochim. Acta* **1997**, *11*, 1725.
(306) Wasberg, M.; Horanyi, G. *Electrochim. Acta* **1995**, *40*, 615.
(307) Horanyi, G.; Wasberg, M. *Electrochim. Acta* **1997**, *42*, 261.
(308) Da Cunha, M. C. P. M.; de Souza, J. P. I.; Nart, F. C. *Langmuir* **2000**, *16*, 771.
(309) Wasberg, M.; Horanyi, G. *J. Electroanal. Chem.* **1995**, *385*, 63.
(310) Pletcher, D.; Poorabedi, Z. *Electrochim. Acta* **1979**, *24*, 1253.
(311) Schmid, G. *Z. Elektrochem.* **1959**, *63*, 1183.
(312) Reyter, D.; Chamoulaud, G.; Belanger, D.; Roue, L. *J. Electroanal. Chem.* **2006**, *596*, 13.
(313) Reyter, D.; Odziemkowski, M.; Belanger, D.; Roue, L. *J. Electrochem. Soc.* **2007**, *154*, K36.
(314) Bae, S.-E.; Gewirth, A. A. *Faraday Discuss.* **2008**, *140*, 113.
(315) Filimonov, E. V.; Shcherbakov, A. I. *Prot. Met.* **2004**, *40*, 280.
(316) Da Cunha, M. C. P. M.; Weber, M.; Nart, F. C. *J. Electroanal. Chem.* **1996**, *414*, 163.
(317) Boese, S. W.; Archer, V. S. *J. Electroanal. Chem.* **1982**, *138*, 273.
(318) Hampson, N. A.; Piercy, R. *J. Electroanal. Chem.* **1973**, *45*, 326.
(319) Davenport, R. J.; Johnson, D. C. *Anal. Chem.* **1973**, *45*, 1979.
(320) Katsounaros, I.; Ipsakis, D.; Polatides, C.; Kyriacou, G. *Electrochim. Acta* **2006**, *52*, 1329.
(321) Katsounaros, I.; Kyriacou, G. *Electrochim. Acta* **2007**, *52*, 6412.
(322) Katsounaros, I.; Kyriacou, G. *Electrochim. Acta* **2008**, *53*, 5477.
(323) Scharifker, B. R.; Mostany, J.; Serruya, A. *Electrochem. Commun.* **2000**, *2*, 448.
(324) Pronkin, S. N.; Simonov, P. A.; Zaikovskii, V. I.; Savinova, E. R. *J. Mol. Catal. A: Chem.* **2007**, *265*, 141.
(325) Kerkeni, S.; Lamy-Pitara, E.; Barbier, J. *Catal. Today* **2002**, *75*, 35.
(326) Gauthard, F.; Epron, F.; Barbier, J. *J. Catal.* **2003**, *220*, 182.
(327) Xing, X.; Scherson, D. A. *J. Electroanal. Chem.* **1989**, *270*, 273.
(328) Safonova, T. Ya; Petrii, O. A. *Russ. J. Electrochem.* **1998**, *34*, 1137.
(329) Shimazu, K.; Goto, R.; Tada, K. *Chem. Lett.* **2002**, 204.
(330) Tada, K.; Shimazu, K. *J. Electroanal. Chem.* **2005**, *577*, 303.
(331) Shimazu, K.; Kawaguchi, T.; Tada, K. *J. Electroanal. Chem.* **2002**, *529*, 20.
(332) Tada, K.; Kawaguchi, T.; Shimazu, K. *J. Electroanal. Chem.* **2004**, *572*, 93.
(333) Shimazu, K.; Goto, R.; Piao, S.; Kayama, R.; Nakata, K.; Yoshinaga, Y. *J. Electroanal. Chem.* **2007**, *601*, 161.
(334) Gootzen, J. F. E.; Lefferts, L.; van Veen, J. A. R. *Appl. Catal. A: Gen.* **1999**, *188*, 127.
(335) Safonova, T. Ya.; Petrii, O. A. *J. Electroanal. Chem.* **1988**, *448*, 211.
(336) Xing, X.; Scherson, D. A.; Mak, C. *J. Electrochem. Soc.* **1990**, *237*, 2166.
(337) Huang, H.; Zhao, M.; Xing, X.; Bae, I. T.; Scherson, D. A. *J. Electroanal. Chem.* **1990**, *293*, 279.
(338) Shieh, S.-J.; Gewirth, A. A. *Langmuir* **2000**, *16*, 9501.
(339) Garcia-Domenech, J.; Climent, M. A.; Aldaz, A.; Vazquez, J. L.; Clavilier, J. *J. Electroanal. Chem.* **1983**, *159*, 223.
(340) Mayer, C.; Jüttner, K.; Lorenz, W. J. *J. Appl. Electrochem.* **1979**, *9*, 161.
(341) Hwang, S.; Lee, J.; Kwak, J. *J. Electroanal. Chem.* **2005**, *579*, 143.
(342) Balbaud, F.; Sanchez, G.; Santarini, G.; Picard, G. *Eur. J. Inorg. Chem.* **1999**, 277.
(343) Balbaud, F.; Sanchez, G.; Santarini, G.; Picard, G. *Eur. J. Inorg. Chem.* **2000**, 665.
(344) Vetter, K. J. *Z. Elektrochem.* **1959**, *63*, 1189.
(345) Bockris, J. O'M.; Kim, J. *J. Appl. Electrochem.* **1997**, *27*, 623.
(346) Li, H.-L.; Robertson, D. H.; Chambers, J. Q.; Hobbs, D. T. *J. Electrochem. Soc.* **1988**, *135*, 1154.
(347) Li, H.-L.; Robertson, D. H.; Chambers, J. Q.; Hobbs, D. T. *J. Appl. Electrochem.* **1988**, *18*, 454.
(348) Genders, J. D.; Hartsough, D.; Hobbs, D. T. *J. Appl. Electrochem.* **1996**, *26*, 1.
(349) Bouzek, K.; Paidar, M.; Sadilkova, A.; Bergmann, H. *J. Appl. Electrochem.* **2001**, *31*, 1185.
(350) Macova, Z.; Bouzek, K. *J. Appl. Electrochem.* **2005**, *35*, 1203.
(351) Macova, Z.; Bouzek, K.; Serak, J. *J. Appl. Electrochem.* **2007**, *37*, 557.
(352) Milhano, C.; Pletcher, D. *J. Electroanal. Chem.* **2008**, *614*, 24.
(353) Tucker, P. M.; Waite, M. J.; Hayden, B. E. *J. Appl. Electrochem.* **2004**, *34*, 781.
(354) Ohmori, T.; El-Deab, M. S.; Osawa, M. *J. Electroanal. Chem.* **1999**, *470*, 46.
(355) Ling, M.; Hu-Lin, L.; Cheng-Liang, C. *Electrochim. Acta* **1993**, *18*, 2773.
(356) Ferapontova, E. E.; Fedorovich, N. V. *J. Electroanal. Chem.* **1999**, *476*, 26.
(357) Kuwabata, S.; Uezumu, S.; Tanaka, K.; Tanaka, T. *J. Chem. Soc., Chem. Commun.* **1986**, 135.
(358) Taniguchi, I.; Nakashima, N.; Yasukouchi, Y. *J. Chem. Soc., Chem. Commun.* **1986**, 1814.
(359) Ma, L.; Zhang, B.-Y.; Li, H.-L.; Chambers, J. Q. *J. Electroanal. Chem.* **1993**, *362*, 201.
(360) Ma, L.; Li, H.-L. *Electroanalysis* **1995**, *7*, 756.
(361) Simon, E.; Sablé, E.; Handel, H.; L'Her, M. *Electrochim. Acta* **1999**, *45*, 855.
(362) Li, H.-L.; Chambers, J. Q.; Hobbs, D. T. *J. Appl. Electrochem.* **1988**, *18*, 454.
(363) Keita, B.; Abdeljalil, E.; Nadjo, L.; Contant, R.; Belgiche, R. *Electrochem. Commun.* **2001**, *3*, 56.
(364) Zhang, Z.; Qi, Y.; Qin, C.; Li, Y.; Wang, E.; Wang, X.; Su, Z.; Xu, L. *Inorg. Chem.* **2007**, *46*, 8162.
(365) Anderson, L. J.; Richardson, D. J.; Butt, J. N. *Biochemistry* **2001**, *40*, 11294.
(366) Butt, J. N.; Anderson, L. J.; Rubio, L. M.; Richardson, D. J.; Flores, E.; Herrero, A. *Bioelectrochemistry* **2002**, *56*, 17.
(367) Gates, A. J.; Richardson, D. J.; Butt, J. N. *Biochem. J.* **2008**, *409*, 159.
(368) Elliot, S. J.; Hoke, K. R.; Heffron, K.; Palak, M.; Rothery, R. A.; Weiner, J. H.; Armstrong, F. A. *Biochemistry* **2004**, *43*, 799.
(369) Hille, R. *Chem. Rev.* **1996**, *96*, 2757.
(370) Horanyi, G. *Catal. Today* **1994**, *19*, 285.
(371) Horanyi, G. *J. Mol. Catal. A: Chem.* **2003**, *199*, 7.
(372) Mallat, T.; Baiker, A. *Top. Catal.* **1999**, *8*, 115.
(373) Ebbesen, S. D.; Mojet, B. L.; Lefferts, L. *Langmuir* **2008**, *24*, 869.
(374) Ebbesen, S. D.; Mojet, B. L.; Lefferts, L. *J. Catal.* **2008**, *256*, 15.

CR8003696